SUBCRITICAL CRACK GROWTH, INITIATION, AND ARREST IN COLUMNAR FRESHWATER AND SEA ICE

BRUCE LEONARD PARSONS, B.Sc.(Summa Cum Laude,) M.Eng., P.Eng

SUBCRITICAL CRACK GROWTH, INITIATION, AND ARREST IN COLUMNAR FRESHWATER AND SEA ICE

BY

© Bruce Leonard Parsons,

B. Sc.(Summa Cum Laude), M. Eng., P. Eng.

A thesis submitted to the School of Graduate Studies in partial fulfillment of the requirements for the degree of

Doctor of Philosophy

Faculty of Engineering and Applied Sciences

Memorial University of Newfoundland

May 1989

St. John's Newfoundland

SUBJECT CATEGORIES

Dissertation Abstracts International is arranged by broad, general subject categories. Choose the *one* listed below (capital letters) which most nearly describes the general content of your dissertation. If the major subject category has sub-fields under it, and *only* if it does, please choose *one* (small letters). (Ex.: ECONOMICS, Theory). Enter subject category on Item 7 of Agreement Form.

HUMANITIES

IA COMMUNICATIONS AND THE ARTS
- ARCHITECTURE
- CINEMA
- FINE ARTS
- INFORMATION SCIENCE
- JOURNALISM
- LIBRARY SCIENCE
- MASS COMMUNICATIONS
- MUSIC
- SPEECH
- THEATER

IIA EDUCATION
- EDUCATION
  - General
  - Administration
  - Adult
  - Agricultural
  - Art
  - Audiovisual
  - Business
  - Community and Social
  - Community Colleges
  - Curriculum and Instruction
  - Early Childhood
  - Elementary
  - Finance
  - Guidance and Counseling
  - Health
  - Higher
  - History
  - Home Economics
  - Industrial
  - Language and Languages
  - Mathematics
  - Middle School
  - Minorities
  - Music
  - Personality Development and Mental Hygiene
  - Philosophy
  - Physical
  - Preschool
  - Programmed Instruction
  - Psychology
  - Religion
  - Sciences
  - Secondary
  - Social Sciences
  - Special
  - Teacher Training
  - Teaching Machines
  - Tests and Measurements
  - Theory and Practice
  - Vocational

IIIA LANGUAGE, LITERATURE AND LINGUISTICS
- LANGUAGE
  - General
  - Ancient
  - Linguistics
  - Modern
- LITERATURE
  - General
  - Classical
  - Comparative
  - Medieval
  - Modern
  - American
  - Asian
  - Dutch and Scandinavian
  - English
  - Germanic
  - Latin American
  - Romance
  - Russian and East European
  - Slavic and Finno-Ugrian

IVA PHILOSOPHY, RELIGION AND THEOLOGY
- PHILOSOPHY
- RELIGION
  - General
  - Clergy
  - History
  - Music
  - Philosophy
- THEOLOGY

VA SOCIAL SCIENCES
- ACCOUNTING
- AMERICAN STUDIES
- ANTHROPOLOGY
  - Archaeology
  - Cultural
  - Physical
- BANKING
- BUSINESS ADMINISTRATION
- ECONOMICS
  - General
  - Agricultural
  - Commerce-Business
  - Finance (includes Public Finance)
  - History
  - Theory
- FOLKLORE
- HISTORY
  - General
  - Ancient
  - Medieval
  - Modern
  - Black
  - Church
  - Africa
  - Asia
  - Australia and Oceania
  - Canada
  - Europe
  - Latin America
  - United States
- HISTORY OF SCIENCE
- LAW
- MANAGEMENT
- MARKETING
- POLITICAL SCIENCE
  - General
  - International Law and Relations
  - Public Administration
- PUBLIC RELATIONS
- RECREATION
- SOCIAL GEOGRAPHY
- SOCIAL STRUCTURE
- SOCIAL WORK
- SOCIOLOGY
  - General
  - Community Organization
  - Criminology
  - Demography
  - Educational
  - Individual and Family Studies
  - Industrial
  - Labor Relations
  - Public Welfare
  - Race Relations
  - Social Problems
  - Statistics–Research Methods
  - Theory
- TRANSPORTATION
- URBAN AND REGIONAL PLANNING
- WOMEN'S STUDIES

SCIENCES

IB BIOLOGICAL SCIENCES
- AGRICULTURE
  - General
  - Animal Culture
  - Animal Pathology
  - Forestry & Wildlife
  - Plant Culture
  - Plant Pathology
  - Plant Physiology
  - Range Management
  - Wood Technology
- AGRONOMY
- ANATOMY
- BIOLOGICAL OCEANOGRAPHY
- BIOLOGY
- BIOPHYSICS
  - General
  - Medical
- BIOSTATISTICS
- BOTANY
- ECOLOGY
- ENTOMOLOGY
- GENETICS
- LIMNOLOGY
- MICROBIOLOGY
- PHYSIOLOGY
- RADIATION BIOLOGY
- VETERINARY SCIENCE
- ZOOLOGY

IIB EARTH SCIENCES
- GEOCHEMISTRY
- GEODESY
- GEOLOGY
- GEOPHYSICS
- HYDROLOGY
- MINERALOGY
- PALEOBOTANY
- PALEONTOLOGY
- PALEOZOOLOGY
- PHYSICAL GEOGRAPHY
- PHYSICAL OCEANOGRAPHY

IIIB HEALTH AND ENVIRONMENTAL SCIENCES
- ENVIRONMENTAL SCIENCES
- FOOD TECHNOLOGY
- HEALTH SCIENCES
  - General
  - Audiology
  - Chemotherapy
  - Dentistry
  - Education
  - Hospital Management
  - Human Development
  - Hygiene
  - Immunology
  - Medicine & Surgery
  - Mental Health
  - Nursing
  - Nutrition
  - Pathology
  - Pharmacy
  - Public Health
  - Radiology
  - Recreation
  - Speech Pathology
- HOME ECONOMICS
- PHARMACOLOGY

IVB PHYSICAL SCIENCES

PURE SCIENCES
- CHEMISTRY
  - General
  - Analytical
  - Biological
  - Inorganic
  - Nuclear
  - Organic
  - Pharmaceutical
  - Physical
  - Polymer
  - Radiation
  - Water
- MATHEMATICS
- PHYSICS
  - General
  - Acoustics
  - Astronomy & Astrophysics
  - Atmospheric Science
  - Atomic
  - Electronics and Electricity
  - Elementary Particles and High Energy
  - Fluid and Plasma
  - Molecular
  - Nuclear
  - Optics
  - Radiation
  - Solid State
- STATISTICS

APPLIED SCIENCES
- APPLIED MECHANICS
- ASTRONAUTICS
- COMPUTER SCIENCE
- ENGINEERING
  - General
  - Aeronautical
  - Agricultural
  - Automotive
  - Biomedical
  - Chemical (includes ceramics and fuel)
  - Civil
  - Electronics and Electrical
  - Heat and Thermodynamics
  - Hydraulic
  - Industrial
  - Marine
  - Materials Science
  - Mechanical
  - Metallurgy
  - Mining
  - Nuclear
  - Petroleum
  - Sanitary and Municipal
  - System Science
- OPERATIONS RESEARCH
- PLASTICS TECHNOLOGY
- TEXTILE TECHNOLOGY

VB PSYCHOLOGY
- PSYCHOLOGY
  - General
  - Clinical
  - Experimental
  - Industrial
  - Physiological
  - Psychobiology
  - Social

ABSTRACT

A study was conducted to determine if slow stable sub-critical crack growth may occur in ice. The Double Torsion fracture toughness geometry was used to explore this phenomena in first year large grained columnar sea ice, and fine grained freshwater columnar ice. The sea ice was tested during a field trip to Resolute NWT during April 1987, and the freshwater ice tested in the cold room at the Institute for Marine Dynamics in St. John's Nfld, from July 1987 to Jan 1988.

No sub-critical crack growth was observed in either type of ice. All crack growth was abrupt. In sea ice loading was up to one hour long, and in lab grown ice deadweight loading was applied for five days. This set the limit below which any sub-critical crack growth may have taken place as approximately 2×10^{-9} m/s. Quasi-static loading up to five minutes was also applied, as arrest was more likely after quick loading.

The fracture toughness of the sea ice was 113± 38 $kNm^{-3/2}$, for $0.06 < \dot{K} < 44$ $kNm^{-3/2}s^{-1}$, $-20^{\circ}C <$ temperature $< -14^{\circ}C$; and for the fine grained ice 124 ±38 $kNm^{-3/2}$, $0.7 < \dot{K} < 85$ $kNm^{-3/2}$, at $-20^{\circ}C$. The arrest stress intensity factor was 91 ± 28 $kNm^{-3/3}$for the sea ice and 89±14

$kNm^{-3/2}$ for the freshwater ice, rate independent, and similar to the high loading rate, or creep free fracture toughness of the two ices. The instability of all crack growth in ice was argued to be a consequence of the stability of the ice crystal structure against dislocation emission. The rate dependence of ice toughness is due to the screening of the crack tip by the dislocation mechanism of creep.

Crack length was not load rate dependent. It was suggested that the switch of failure mode in ice indentation by structures is a consequence of the rate dependent material properties of ice, possibly the modulus. A risk analysis, based on the material properties of creep crack growth, and the probability distribution function for ice strength, was shown to be inapplicable to ice. The arrest stress intensity factor was used to modify the model of indentation in ice, to accommodate this as a new crack length criterion, and to accommodate the stress relief influence of ice micro cracking.

SUBCRITICAL CRACK GROWTH, INITIATION AND ARREST IN COLUMNAR FRESHWATER AND SEA ICE

TABLE OF CONTENTS

ABSTRACT

A study was conducted to determine if slow stable sub-critical crack growth may occur in ice. The Double Torsion fracture toughness geometry was used to explore this phenomena in first year large grained columnar sea ice, and fine grained freshwater columnar ice. The sea ice was tested during a field trip to Resolute NWT during April 1987, and the freshwater ice tested in the cold room at the Institute for Marine Dynamics in St. John's Nfld, from July 1987 to Jan 1988.

No sub-critical crack growth was observed in either type of ice. All crack growth was abrupt. In sea ice loading was up to one hour long, and in lab grown ice deadweight loading was applied for five days. This set the limit below which any sub-critical crack growth may have taken place as approximately 2×10^{-9} m/s. Quasi-static loading up to five minutes was also applied, as arrest was more likely after quick loading.

The fracture toughness of the sea ice was 113± 38 $kNm^{-3/2}$, for $0.06 < \dot{K} < 44$ $kNm^{-3/2}s^{-1}$, $-20^{\circ}C <$ temperature $< -14^{\circ}C$; and for the fine grained ice 124 ±38 $kNm^{-3/2}$, $0.7 < \dot{K} < 85$ $kNm^{-3/2}$, at $-20^{\circ}C$. The arrest stress intensity factor was 91 ± 28 $kNm^{-3/3}$for the sea ice and 89±14

$kNm^{-3/2}$ for the freshwater ice, rate independent, and similar to the high loading rate, or creep free fracture toughness of the two ices. The instability of all crack growth in ice was argued to be a consequence of the stability of the ice crystal structure against dislocation emission. The rate dependence of ice toughness is due to the screening of the crack tip by the dislocation mechanism of creep.

Crack length was not load rate dependent. It was suggested that the switch of failure mode in ice indentation by structures is a consequence of the rate dependent material properties of ice, possibly the modulus. A risk analysis, based on the material properties of creep crack growth, and the probability distribution function for ice strength, was shown to be inapplicable to ice. The arrest stress intensity factor was used to modify the model of indentation in ice, to accommodate this as a new crack length criterion, and to accommodate the stress relief influence of ice micro cracking.

ACKNOWLEDGEMENTS

This work would not have been possible without the generous support and co-operation of the Polar Continental Shelf Project, the Department of Energy Mines and Resources, the Government of Canada, and all the staff at the base camp in Resolute Bay, NWT, during the field trip in April 1987. I would like to also thank the National Research Council of Canada, for the support and funding for this research.

I would like to thank my supervisors for their suggestions and guidance; D.B. Muggeridge, J.P. Nadreau, S.J. Jones and G.W. Timco.

I would like to express particular thanks to my co-worker, and ofttimes co-author, J.B. Snellen for his constant supply of energy, good humour and plain stubbornness while persevering in the conducting of experiments under the most difficult conditions imaginable. Without his reservoir of stamina and innovation in the High Arctic, we would not have accomplished nearly as much.

I would also like to thank A.G. Atkins, J. Bell, M. Booton, D. Christian, F.T. Christianson, A.C.F. Cocks, D. Cameron, S.N. Chin, B. Colbourne, J.P. Dempsey, D. Diemand, R. Donnelly, R.M.W. Frederking, B. Gagnon, L. Gold, E. Guy, P. Hackett, J. Hagerty, J. Harmon, H. Hamza, R.W. Higham, B. Hill, I.J. Jordaan, P. Kalifa, M. Lal, J.

Lever, B. Michel, E. Riemer, A. Sare, N.K. Sinha, D.S. Sodhi, A. Steel, B. Stone, D. Spencer, A.S.J. Swamidas, J. Tillotson, and F.M. Williams for their suggestions, assistance, discussions, encouragement and instruction.

Finally I would like to thank my parents for the invaluable freedom they gave me, Treva for her support and patience, and Julia for being there.

LIST OF TABLES

LIST OF FIGURES

LIST OF SYMBOLS

a	crack length, m
a_T	inverse relaxation time, s^{-1}
A	proportionality constant crack surface area, m^2
b	Burgers vector, m
B	$3w_m/Wd^3G$ in double torsion geometry, $WG/3w_m^2$ in Eq 3.25
C	elastic compliance of double torsion geometry
C^*	time dependent potential energy release rate, $Jm^{-2}s^{-1}$.
C_d	damage, cracks/cm^2
d	thickness, m grain size, m
E	modulus, Pa
F	externally applied force, N
G	shear modulus, Pa Irwin-Kies potential energy release rate, Jm^{-2}
G_c	critical potential energy release rate, Jm^{-2}
H	hardness, Pa
J	time independent non-linear potential energy release rate , Jm^{-2}
k	after shielding stress intensity factor, $kNm^{-3/2}$
K	stress intensity factor, $kNm^{-3/2}$
K_C	plane stress critical stress intensity factor, $kNm^{-3/2}$
K_{Ia}	arrest stress intensity factor from quasi static analysis, $kNm^{-3/2}$
K_{Ic}	plane strain critical stress intensity factor, $kNm^{-3/2}$
K_{th}	threshold stress intensity factor, $kNm^{-3/2}$
L	length, m
n	creep power law exponent
P	load, N

R	specific work of fracture, J/m^2
r	distance from crack tip, m
r_c	creep zone radius, m
r_p	plastic zone radius
t	time, s
u	displacement in x direction, m
v	displacement in y direction, m
V	crack growth velocity, ms^{-2}
W	length from load line to end of specimen, m
W	externally applied work, J
U_E	strain energy, J
U_S	crack surface energy, J
y	load line displacement in double torsion geometry, m
α	geometric factor of indenter
β	ratio of damage radius to contact radius
	Weibull modulus
δ	deflection at point of load application, m
ε	strain
φ	stress function
Φ	Airy stress function
γ	thermodynamic surface specific energy, Jm^{-2}
γ_e	elastic crack surface specific energy, Jm^{-2}
γ_p	plastic crack surface specific energy, Jm^{-2}
μ	shear modulus, Pa
ν	Poisson's ratio, taken as 0.3 for ice
	brine volume
θ	angle from direction of crack growth
ρ	mass density, kg/m^3
σ	stress, Pa
σ_y	yield strength, Pa
τ	shear stress, Pa
τ_e	effective shear stress, $= \lvert\nabla_i\Psi\rvert$, Pa
Λ	strain energy, J

ALLAN BAY, NORTHWEST TERRITORIES, APRIL, 1987

INTRODUCTION

1) Purpose of the Work

The purpose of this work is to determine how cracks in ice may grow, and how this growth is influenced by load rate, grain size and environment.

For a designer of icebreakers or structures in ice covered waters an understanding of crack growth in ice is essential to estimating the loads generated in the ice-structure interaction.

Cracks in other brittle materials may grow when a critical fracture criterion is exceeded, or below the critical value, ie sub-critical crack growth. Sub-critical crack growth has been characterized by the applied stress intensity factor K_I , the crack growth velocity da/dt = V, and n the power law creep exponent. The relationship between these parameters was first noted empirically by Evans (1972), and explained theoretically by Hui and Riedel (1981), in the following equation,

$$da/dt = V = AK_I^n \qquad (1.1)$$

where A and n are material properties.

The material properties n and A that characterize crack growth were first used in a reliability/risk analysis for high temperature ceramics, Paluszny (1977a,1977b). A similar analysis for loads generated during ice-structure

interactions could be done if A and n for ice were known. The ice crack growth rate as a function of applied stress intensity factor could be used to give the time to failure at any specified load level and probability. This could supply a risk analysis for ice-structure loads based on ice material properties.

The theory of Hui and Riedel (1981) on the stress/strain fields in the vicinity of a moving crack tip predicts a fundamental difference in the nature of crack growth in power law creep materials between those materials with power law creep exponent $n > 3$; and those with $n<3$. For $n > 3$, sub-critical crack growth is possible, above a threshold crack velocity. For $n < 3$, crack growth is possible only when the critical stress intensity factor is exceeded in the material. Weertman (1983) provided a review and listed values of n for ice between 1.5 and 4.5.

The present work was done to clarify whether or not sub-critical crack growth may take place in ice, and to evaluate n and A if it does.

In other materials large grains have been observed to be tougher and reduce the rate of crack growth in the material, Ritter and Cavanaugh (1976), Adams et al (1981). Large grain ice was tested in the field, and fine grain ice in the laboratory.

The rate of crack growth in many materials is

sensitive to the corrosive effects of some environments, Evans (1974), Michalske and Frieman (1987). The tests done in this study were done at the low humidity of the High arctic, and in the higher humidity of the cold room in St.John's Nfld.

Hamza and Muggeridge (1984) have used equation 1.1for load prediction in ice-structure interactions. This experiment attempts to provide the material properties of ice for equation 1.1, and determines if it is possible to use it in ice-structure interactions.

2) Scope of the Work

The Double Torsion fracture geometry was used to test large grained columnar first year sea ice in the field near Resolute Bay NWT, and fine grained columnar freshwater ice grown in the cold room at the Institute for Marine Dynamics, in St. John's Nfld.

Deadweight loading of ice was applied to determine if slow crack growth could occur in ice under constant load.

All cracks prepared in the ice specimens were similarly oriented for the two ices tested, perpendicular to the original ice surface, and propagated parallel to the original ice surface, see Figure 4.1 (page 84).

The laboratory tests were all done on ice at a temperature of -20°C, and the ice tested in the field had

temperatures that ranged from -23°C to -14°C.

The rate of load application was varied from sample to sample to determine its influence on crack growth. The length of the resulting crack was recorded, and dependence on rate determined.

3) Importance of the Work

This work quantified for the first time the nature of crack growth in ice, in particular whether or not slow crack growth, known as sub-critical or creep crack growth, is possible in ice; or if crack growth occurs only when the critical stress intensity factor has been exceeded.

This is particularly relevant to an accepted procedure for supplying reliability/risk analysis for brittle materials under load. The procedure, Paluszny (1977a,1977b) is based on the material properties that quantify creep crack growth, and the statistical parameters that quantify the Weibull probability distribution function for material strength. The final formulation supplies a minimum time to failure, or load duration, at any load and risk level.

The treatment of fracture of ice in the literature has not in the past made a distinction between the critical stress intensity factor required to initiate crack growth, and the stress intensity factor that obtains at arrest. Crack growth has been assumed to proceed with the critical

stress intensity factor in effect at the crack tip, and that it is also in effect at arrest. This work makes this distinction, which is especially necessary as toughness is rate dependent.

The answer to the question, can sub-critical crack growth occur in ice? is particularly relevant to indentation of ice. If slow stable growth can take place in ice then the radial crack in the decreasing K_I field beneath an indenter might lengthen under constant load, ultimately to a free surface and provide stress relief. Otherwise the indentation load must be increased for crack extension.

The second aspect of interest is any possible rate dependence of crack length. If crack length depends on load or displacement rate, it may determine the ice failure mode. Therefore crack length was recorded as a function of rate.

4) Definition of Crack Arrest

Crack growth in a material may stop for a number of reasons. The lengthening crack may alter the loading geometry in such a way as to lower the applied load at the crack tip, as is the case in the Double Torsion geometry, Mai and Atkins (1980). A crack may also arrest if it is growing into a decreasing K_I field, such as beneath an indenter. A crack may also arrest if all applied stress is

removed by unloading.

Which threshold applied stress intensity factor is used as arrest stress intensity factor depends on whether or not sub-critical crack growth as well as critical crack growth is possible. If sub-critical growth is possible, the threshold stress intensity factor is considerably lower than the critical value, Hui and Riedel (1981). If it is not capable of sub-critical crack growth, the arrest stress intensity factor is taken as the lower bound of all available dynamic crack initiation and arrest test data, Popelar and Kanninen (1985).

5) Brief Overview of Previous Work

Considerable work has been done on the determination of the critical stress intensity factor of ice, in the field on sea ice, freshwater ice and glacier ice; and in the laboratory on fine grain columnar and random ice, and large grain random ice. A summary is supplied in Appendix 1.

The fracture toughness of ice has been measured with the following fracture geometries; Single Edge Notch, Notched Right Circular Cylinder, Compact Tension, Cracked Ring Tensile, Tapered Double Cantilever Beam Specimen, Wedge Loaded Compact Tension Specimen and Vickers Indenter. There is no ASTM test geometry specifically for the determination of ice fracture toughness. With the exception of the last

three specimens the geometry is such that the crack, once it has begun to grow, will continue to do so dynamically, Mai and Atkins (1980). The Tapered Double Cantilevered Beam, and Wedge Loaded Compact Tension Specimen are both more stable than the Double Torsion geometry used in these experiments, but Bentley et al (1988), Dempsey et al (1989b) report no crack arrest.

Gold (1963) calculated the arrest stress intensity factor that obtained at the tip of cracks in ice resulting from thermal shock. Two pieces of ice of different temperature were brought together and the resulting cracking observed. From the thermal gradient and resulting stress Gold (1963) calculated that the stress intensity factor at the crack tip was between 50 and 160 $kNm^{-3/2}$, depending on orientation to the c-axis of the crystal.

Liu and Miller (1979), using a double cantilever beam geometry that was wedged open, reported two arrests at each of -4°C and -12°C and one at -9°C in the range of 134 to 152 $kNm^{-3/2}$ for the same orientation as was used in these tests. They were unable to obtain arrest below -12° C.

Neither of the last two experiments mentioned was designed to explore sub-critical crack growth.

6) General Applicability to Ice Engineering

Hamza and Muggeridge (1984) used equation 1.1 to

predict resulting crack length in ice-structure interaction. The results obtained in the present work may be used to further refine their model, supplying an arrest criteria and the value of n for ice.

Other authors have attempted to predict resulting crack length using the critical stress intensity factor, and these models may also be refined with the arrest stress intensity factor, Smith (1976), Evans et al (1984), Palmer et al (1983), Bhat (1988, 1989). The switching in dominance of different failure modes, such as those reported in lab studies with freshwater ice by Timco (1987a) for example, may depend on the rate dependence of crack length.

The arrest stress intensity factor may also be used to modify the elastic/plastic model of indentation of Hill (1950) to make it applicable to ice. In the immediate contact area beneath an indentation in ice, the ice is intensely microcracked, or damaged, but a predominant crack has been observed to extend beyond the damage zone, Parsons (1989). Previous models of the ice structure interaction have assumed a prior knowledge of the length of a pre-existing crack in the ice. This is not realistic and the method proposed in Parsons (1989) does not require such assumptions, and uses the arrest stress intensity factor as the criterion for crack length beneath an indenter.

7) Small Scale Yielding, Small Scale Creep, and the Discrete Lattice

The experiments done in this study are long term loading, in the case of the sea ice loading was for over an hour in some cases before the crack grew. In such cases the requirement of Linear Elastic Fracture Mechanic that both the size of the yield zone and creep zone remain small with respect to specimen size must be dealt with.

As the yield strength of ice remains to date undefined the ssy criterion is difficult to evaluate. However it is possible to calculate the size of the creep zone from a commonly used theoretically obtained algorithm, from Riedel and Rice (1980), and for almost every test done, it states that LEFM is not applicable. The usual procedure is then to procede with an evaluation of the fracture criterion for such cases of time dependent non-linear crack growth. This is done by obtaining load and displacement records while the crack extends in a slow stable manner due to creep crack growth, and evaluating the C^* integral.

In these experiments, however, no such crack growth could be promoted in ice, and such load and displacement records were not obtained, and thus C^* could not be evaluated. It is clear that even though the algorithm of Riedel and Rice (1980) predicts a large creep zone, and that

this creep is assumed to be the mediating mechanism of creep crack growth, that in ice this is not sufficient to explain the absence of creep crack growth. For this reason another theory has been introduced very early in the thesis. This is the formulation of fracture in terms of the discrete lattice as presented by Thomson (1987).

The successes of this view in explaining the effects of corrosion on crack growth, and the behaviour of aged cracks take it beyond the purely continuum approach of Riedel and Rice (1980), and supply a mechanistic insight to the predictions of Hui and Riedel (1981). This latter paper is based entirely on an analysis of the strength of the mathematical singularities at the crack tip, and supplies an explanation for the observed behaviour of ice; the creep power exponent of ice must be no greater than 3. Thomson supplies a physical interpretation of this, the source of the creep quantified by the creep power exponent is dislocations, and a cloud of dislocations surrounding a crack serves to shield or screen it from the remotely applied stress. At the crack tip an elastic fracture criterion, the Griffith criterion, must still be exceeded for crack extension to occur.

In Chapter 2 a review of fracture mechanics, including both the continuum approach as presented by Rice (1968), Riedel and Rice (1980), and Hui and Riedel (1981);

and the discrete lattice interpretation of Thomson (1987) is supplied. Interpretation of critical points is supplied though both points of view. In the end it is seen that the discrete lattice formulation is necessary for a physical understanding of the observed fracture behaviour of ice.

CHAPTER 2

BACKGROUND INFORMATION

2A General

1) The G Versus the K Approach.

A crack can be loaded in three distinct modes:opening, sliding and tearing. We shall concern ourselves here only with the opening or tensile mode of loading.

The study of fracture mechanics began with Griffith (1921). He considered the energy balance within a cracked material under load and postulated that an existing crack will propagate if it lowers the total energy of the system.

The externally applied work W_L must be balanced by strain energy potential U_E and the crack surface energy U_S;

$$W_L = U_E + U_S \tag{2.1}$$

Griffith (1921) used a stress analysis of Inglis (1913) for the strain energy density per unit thickness due to the presence of the crack,

$$U_E = \pi\sigma^2 a^2/E, \tag{2.2}$$

where σ is the stress remote from the crack, 2a is the crack length, and E is the modulus of the material.

The crack surface energy U_S is given as,

$$U_S = 4a\gamma, \tag{2.3}$$

where γ is the material specific elastic crack surface energy.

The Griffith criterion is that at equilibrium;

$$d/da(W_L) = d/da(-\pi\sigma^2a^2/E + 4a\gamma) = 0.$$

The energy of the system is maximum at this equilibrium point. This yields;

$$\sigma = (2E\gamma/\pi a)^{1/2}, \qquad (2.4)$$

which gives the theoretical strength of brittle materials, and the fracture strength dependence on defect size.

Equation 2.1 may be rewritten as;

$$Fdu = d\Lambda + + GdA, \qquad (2.5)$$

where F is the externally applied force, du is the change in displacement at the point of load application, $d\Lambda$ is the change in strain energy, G is the specific energy of crack surface area, and dA is the change in crack surface area.

In a linear system;

$d\Lambda = d(Fu/2)$, and this may be used to obtain;

$$F^2 = 2G/(d/dA(u/F)) \qquad (2.6)$$

This gives a single valued relationship between F, u, and A for constant G in a linear elastic cracked material. For quasi-static cracking the critical value of G is just balanced by the work of fracture. If the work of fracture is greater than the material critical value, unstable crack growth ensues, if it is less there is no fracture.

Also, $$G = -\partial/\partial A(Fu/2)_{u=u_c} \qquad (2.7)$$

which will be used to show the equivalence of the K and G approaches at equilibrium.

Irwin and Kies (1952, 1954), Irwin (1957), and independently Orowan (1945) recognized that there must be an other mechanism involved to account for the discrepancy between the theoretical and observed strength of ductile materials, where the energy of crack creation is insignificant compared with the plastic work. They redefined the material property G as the total energy absorbed during cracking ;

$$G = \gamma_e + \gamma_p \quad ; \qquad (2.8)$$

where γ_e and γ_p are the elastic and plastic crack energies.

The thermodynamic crack surface energy for ice is the Gibbs free energy, or surface tension, measured by Ketcham and Hobbs (1969) to be .109 J/m^2 for the ice/water-vapour interface, 0.065 J/m^2 for the ice/water interface, 0.033 J/m^2 for the ice/ice (grain boundary) interface.

Theoretical work by Thomson et al (1971), Hsieh and Thomson (1973), Thomson (1978,1986,1987), Thomson and Fuller(1982), Lin and Thomson (1986), and experimental work by Mickalske and Frieman (1987) show that the fracture energy may be larger than the thermodynamic surface energy as measured by Ketcham and Hobbs (1969) for ice, if the crack is in a potential well between lattice sites, ie lattice trapping.This is distinct from the plastic fracture energy, γ_p.

The intractability of the energy approach in important problems, such as the subject of this study,

sub-critical crack growth, led Irwin (1957) to develop the stress intensity approach.

A brief outline will be given.

To solve any plane elastic problem the equilibrium equations of stresses and the compatibility equations of strain must be obeyed. Airy proposed a function $\Phi(x,y)$ which fulfills the equilibrium equations for stresses:

$$\sigma_x = \frac{\partial^2\Phi}{\partial y^2}, \quad \sigma_y = \frac{\partial^2\Phi}{\partial x^2}, \quad \sigma_{xy} = \frac{\partial^2\Phi}{\partial y \partial x} \tag{2.9}$$

From the compatibility equation of strains the biharmonic equation follows :

$$\nabla^4(\Phi) = \nabla^2[\nabla^2\Phi] = 0 \tag{2.10}$$

To solve this in an infinite, biaxially loaded, cracked plate, Westergaard (1939) used a complex stress function:

$$\Phi = \text{Re } \bar{\bar{\Phi}}(z) + y\text{Im } \bar{\Phi}(z), \tag{2.11}$$

where $\bar{\bar{\Phi}}$ and $\bar{\Phi}$ are first and second order integrals; and applied the Cauchy-Riemann equations to obtain the general solutions:

$$\begin{aligned} \sigma_x &= \text{Re } \Phi(z) - y\ \text{Im}\Phi'(z) \\ \sigma_y &= \text{Re } \Phi(z) + y\ \text{Im}\Phi'(z) \\ \tau_{xy} &= -y\text{Re } \Phi'(z). \end{aligned} \tag{2.12}$$

The boundary conditions are;

1) $\sigma_y = 0$ for $-a \le x \le a$, $y = 0$
2) $\sigma_y = -\sigma_\infty$ as $x \to \pm\infty$
3) $\sigma_y \to -\infty$ at $x = \pm a$

With the origin at the crack tip we obtain:

$$\sigma_x = \frac{\sigma(\pi a/2)\cos(\theta/2)(1-\sin\theta/2\ \sin3\theta/2)}{(2\pi r)^{1/2}}$$

$$\sigma_y = \frac{\sigma(\pi a/2)\cos(\theta/2)(1+\sin\theta/2\ \sin3\theta/2)}{(2\pi r)^{1/2}} \qquad (2.13)$$

$$\tau_{xy} = \frac{\sigma(\pi a/2)\sin(\theta/2)\cos\theta/2\ \sin3\theta/2)}{(2\pi r)^{1/2}}$$

All stresses tend to infinity at r = 0, ie the crack tip, with a strength of singularity of $r^{-1/2}$, and are the product of geometric position, $1/\sqrt{2\pi r}(f(\theta))$, and a scalar magnitude of the elastic stresses in the crack tip field $\sigma\sqrt{\pi a}$. The strength of this singularity will be compared to that of a crack imbedded in a plastic field, and a moving crack.

The magnitude of the elastic stress is called the stress intensity factor:

$$K_I = \sigma(\pi a)^{1/2} \qquad (2.14)$$

For a finite body the stress intensity factor at the crack tip may be calculated from the general form

$$K_I = \sigma(\pi a)^{1/2}\ f(a/w), \qquad (2.15)$$

where f(a/w) is a dimensionless parameter that depends on the geometry of the specimen, the crack length a, the specimen length W, and is usually $1 \leq f(a/w) \leq \pi$, see for example, Broek (1984,1988), Ewalds and Wanhill (1984), Atkins and Mai (1985). Handbooks have compiled f(a/w) calculated for a large number of practical loading configurations, Sih (1973), Tada et al (1973).

Irwin (1957) demonstrated that the critical value G

obtained using the Griffith energy approach is equivalent to the critical value of K_{Ic} reached at crack extension. Considering the work done in the extension of a crack, Atkins and Mai (1985), equation 2.7 yields

$$G = \lim_{\Delta A \to 0} \Delta\Lambda/\Delta A \tag{2.16}$$

$$= \lim_{\Delta a \to 0} 1/\Delta a \int_0^{\Delta a} \sigma_{yy}\, v_{yy} dr \tag{2.17}$$

where $\sigma_{yy} = K/(2\pi r)$ and the displacement

$$v_{yy} = (2\sigma_\infty \sqrt{ar/2})/E^* \tag{2.18}$$

where $E^* = E/(1-\nu^2)$ for plane strain conditions at the crack tip, or $E^* = E$ for plane stress.

The relationship between G_c and K_{Ic} is then;

$$G_c = K_{Ic}^2/E \quad \text{in plane stress, and} \tag{2.19}$$

$$G_c = K_{Ic}^2(1-\nu^2)/E \quad \text{in plane strain.} \tag{2.20}$$

The value of K_{Ic} may be obtained from the load to failure of a known geometry and crack length, and is used as the crack extension criterion. For each stress function of the same mode the geometric part $f(r,\theta)$ is the same and only the magnitude of K_I changes. The total stress field due to different loading systems is obtained by scalar addition of each K_{Ic} contribution. The stress state is characterized by the stress intensity factor K, that measures the strength of the $r^{-1/2}$ singularity at the crack tip.

A fundamental problem arose from treating fracture as a stress analysis problem in terms of continuum elasticity and plasticity. Rice (1966, 1976), in what has come to be called Rice's Theorem, pointed out that when a crack grows

in anything but a purely elastic material, all the work supplied by the external loading is absorbed by the plastic processes in the material, and none is left over for the creation of crack surface area. This is a consequence of the assumption that at the tip the stress reaches a maximum finite value, such as the plastic yield strength of the material. If the plastic zone extends right to the crack tip, no crack growth is possible. The description of crack growth at the continuum limit cannot be decoupled, in the Griffith sense, from the details of separation within the fracture process zone.

This paradox was resolved by Thomson (1978) and, independently, Weertman (1978), by considering the actual dislocation mechanisms responsible for plasticity and creep. They assumed there is a core elastic region in the immediate vicinity of the crack tip, that is surrounded by a plastic region consisting of dislocations. This was an explicit break with the previous purely continuum analysis and demonstrated the necessity of considering atomic detail. The model is supported by scanning electron microscope studies of cracks in ceramics, Lawn et al (1980), that show atomically sharp cracks surrounded by dislocations. This approach has solved several previously intractable problems, notably the influence of corrosive environments, and the behaviour of aged cracks, Thomson and Fuller (1982), Lin and Hirth (1982), Lin and Thomson (1986), Thomson (1987), Lawn,

et al (1987).

The robustness of the Griffith criterion has also shown itself in its applicability to moving cracks in power hardening materials, Hart (1981), though it was originally proposed for static cracks in pure elastic materials.

2) Plane Strain Versus Plane Stress

It is clear from Eq. 2.18 that the plane strain and plane stress relations between G and fracture toughness differ due to the strain at the crack tip in the two cases.

In a very thin edge loaded plate there is effectively no through thickness stresses, all the stress is in the plane of the plate, though out-of-plane strains may result. This is known as plane stress.

At the other extreme, in a thick section, under in plane loading; there is no through thickness displacement. This is known as plane strain.

In the intermediate case, between very thick and very thin specimens it is necessary to know which of the two idealizations best approximates the problem at hand.

The quantity G_c is a material property and from equations 2.19 and 2.20 we see that K_{Ic} will be greater in plane stress than plane strain. A distinction is made between K_c, obtained in plane stress, and the lower value K_{Ic} obtained from thicker specimens in plane strain.

The transition between the two, the intermediate

region, is marked by thickness greater than;

$$d = 1/3\pi(\frac{K_{Ic}}{\sigma_y})^2 \qquad (2.21)$$

and less than,

$$d = 2.5(\frac{K_{Ic}}{\sigma_y})^2 \qquad (2.22)$$

where t is specimen thickness, σ_y is yield strength, and K_{Ic} is the critical stress intensity factor obtained for thickness greater than given by 2.22, Anderson (1969).

The value of yield stress of ice is problematic. The failure strength of ice is rate dependent, and accompanied by micro and macro cracking. Yield is characterized by plastic rupture of the material , usually along slip lines, with no fracture present. It is not at all clear that ice may yield under any circumstances, as fracture usually intervenes. Perhaps only at very small scale where it is energetically impossible for fracture to take place may ice yield, see the chapter on scale effects in the book by Atkins and Mai (1985). Frost and Ashby (1982) indicate in their deformation mechanism map for ice that the yield strength of ice is at least 10 MPa, and may be an order of magnitude higher. Taking toughness of 1 x10^5 $Nm^{-3/2}$, and yield strength of 10 MPa, this implies that the smallest significant length of a fracture sample in ice should be greater than 0.25 mm to ensure plane strain.

In applied mechanics the terms "plane stress" and "plane strain" have very precise meanings. In fracture

mechanics they have been applied more loosely. While plane stress rigorously means that there is negligible stress perpendicular to the plane of interest; fracture mechanics it is taken to indicate thin components with in-plane loading, and the surface layer of thick components. But for a state of plane stress to obtain, the stress gradients must also be negligible. This is only approximately true of thin sections, or near the surface of a thick section, Popelar and Kanninen (1985).

3) Linear Elastic Fracture Mechanics

Linear elastic fracture mechanics (LEFM), or the K_I approach, is valid when;

1) the crack tip is sharp,

2) the plastic zone that develops at the crack tip is small compared to the relevant specimen dimensions. This is the small scale yielding criterion.

A sharp fatigue crack is usually created in fracture specimens with repeated load reversals. This has been claimed to be done by only one group of researchers, Liu and Miller (1979), and no details were given. Subsequent workers have found precracking is not possible in ice, as it is so brittle that any cracks that do form, easily propagate through the sample.

In ice sharp cracks have been formed by pressing with a sharp blade in a saw cut, or by creating a microcrack with

a loaded sharp blade. As some time may elapse before actual loading begins, the question arises as to how long this crack remains sharp.

Theoretical work by Rice and Thomson (1974) addresses crack tip blunting through the mechanism of dislocation emission. This requires the formation of a three dimensional kink pair. Rice and Thomson (1974) calculate the energy this requires, and predict which materials will spontaneously blunt. They show that for materials with;

$$\mu b/\gamma > 10, \tag{2.23}$$

where μ is the shear modulus, b the Burgers vector, and γ the crack surface energy, an atomically sharp crack is stable. This because the fracture surface energy is so low that a sharp crack is a lower energy state than a blunt crack accompanied by a dislocation. This criterion successfully predicted that face centred cubic materials spontaneously blunt, that iron is an intermediate case, and that ionic and covalent crystals do not.

For ice; $\mu = 3.8 \times 10^{9}$ Pa, $b = 4.5 \times 10^{-10}$ m, $\gamma = 0.109$ J/m^2; which yields $\mu b/\gamma = 17$.

Rice and Thomson (1974) point out that the greatest uncertainty in their theory is in the determination of γ. In their work the correct γ is derived as the energy necessary to break bonds at the crack tip. If there is no lattice trapping, Hsieh and Thomson 1973, the energy to grow a crack, heal a crack, and the thermodynamic surface energy

are all identical. This latter has been measured as 0.109 J/m^2, Ketchum and Hobbs (1969).

If, however, the ice crystal has high Peierls barriers where the discrete lattice force fields can trap a crack, the energies to grow a crack, heal it, and the intermediate thermodynamic equilibrium, may be different. The extension, or blunting, of the crack by the formation of a three dimensional kink pair across a Peierls energy barrier, will require a greater energy than the thermodynamic surface energy, Hirth and Lothe (1982).

The small difference between the fracture and thermodynamic energy of ice may be due to lattice trapping, but there is no evidence to support this. Dempsey et al (1989b), for example, and others have obtained toughness values that are very nearly exactly the thermodynamic surface energy. The thermodynamic surface energy of ice, .109 J/m^2, is thus used in the algorithm of Rice and Thomson (1974) and atomically sharp cracks in ice are theoretically predicted to be stable against dislocation emission mediated blunting. This stability is even greater for grain boundary cracks, with energy of 0.033 J/m^2.

Aside from these theoretical considerations that indicate a sharp crack in ice will stay sharp, Colbeck (1986) considered the thermodynamics of microcrack healing (ie. blunting) in ice, in an attempt to explain the observations of Cole (1986). He calculated that at 0°C a

crack of 1 cm length, aspect ratio of 10^3 will not change its diameter (and thus, its radius of curvature at the crack tip) appreciably for a day if open to the air, or for two hours if water vapour filled. The mechanism of healing is viscous flow. This explained the observations of Cole (1986). At lower temperatures the crack will be stable for longer.

It seems safe to proceed under the assumption that if tested within a few hours, a prepared sharp crack in ice open to air remain atomically sharp.

The second concern in LEFM is that the plastic zone be small compared to relevant test specimen dimensions. This is the small scale yielding condition. In a material that creeps, such as ice, the development of the zone of nonlinear deformation at the crack tip is time dependent, and this then becomes the small scale creep criterion, Rice (1968), Riedel and Rice (1980).

The calculation of the size of the plastic zone was calculated in the section dealing with plane strain and plane stress. Several workers in ice, Nixon and Schulson (1986a, 1986b), Timco and Frederking (1986) have made the assumption that when the creep zone size, not the plastic zone size, becomes one fiftieth the size of the smallest critical dimension of the test sample, plane strain has been compromised.

Riedel (1987) discusses the nature of the creep zone

and its development. The creep zone is arbitrarily defined as that region within which the creep strain is greater than the elastic strain, Riedel and Rice (1980). They give the creep zone boundary $r_{cr}(\theta,t)$ resulting from an instantaneous step function application of K_I as;

$$r_{cr}(\theta,t) = 1/2\pi\left(\frac{K_I}{E}\right)^2\left(\frac{(n+1)^2}{2n}\frac{E^n}{\alpha^{n+1}}Bt\right)^{2/n-1} F_{cr}(\theta) \qquad (2.24)$$

Hobbs (1974) gives two values for n; $n \cong 3$ for $\sigma \leq 2$ MPa, and $n \cong 5$ for $\sigma \geq 5$ MPa. For $n \cong 3$ this takes the form $r \propto 5.3t$; and for $n \cong 5$, $r \propto 2.7t^{1/2}$, Nixon and Schulson (1986a, 1986b). Note that this predicts that in the high stress region the creep zone will grow more slowly than in the lower stress region, i.e. the relaxation is greater.

The transition from small scale creep limit to steady state creep limit can be described as the spread of the creep zone across the ligament. There are two such transition calculations, one for plane strain, and one for plane stress. This determines whether the specimen is characterized by K_{Ic}, or by C^*, where C^* is the rate dependent strain energy density fracture criterion. It is assumed that when the creep zone has exceeded 1/50 the relevant size of the fracture sample LEFM no longer applies and also that creep crack growth has begun in the material. As creep is by definition time dependent it is possible to calculate when the contributions of the non-linear

deformations in the vicinity of the crack tip are no longer negligible and the LEFM fracture criterion K_{IC} is no longer geometry independent.

The transition time is calculated from;

$$t_1 = \frac{\alpha \, K_I^2 \, (1 - \nu^2)}{(n+1) \, EC^*} \qquad (2.25)$$

for plane strain, for plane stress the factor $(1 - \nu^2)$ is deleted, Riedel (1987). Practical guidelines for determining C^* were given by Landes and Begley (1976), for materials that follow power law creep; and exhibit creep crack growth. Load and displacement records are collected while the crack extends in a slow stable manner. There has as yet been no work done on the evaluation of C^* for ice, so it is not now possible to calculate when one should use it as a fracture criteria, instead of the critical stress intensity factor. If, however, no stable crack growth can be promoted, it is not possible to calculate C^*. It might also be inferred that neither is it necessary.

The size requirement for C^* testing validity is;

$$(a, W-a) > 2M\delta_t \qquad (2.26)$$

where δ_t is the crack tip opening displacement, and M is a factor that depends on specimen geometry, and desired accuracy, Riedel (1987).

4) The J and C^* Integrals

The J integral was introduced by Rice (1968) for

applications where elastic-plastic deformation accompanying fracture must be taken account of. In the linear approximation J is identical to G. In the non-linear case it is the rate of change with crack length of potential energy;

$$J = -\partial/\partial a \int P \, du \qquad (2.27)$$

where u is the load line deflection. A methodology exists for determining the J integral and using it in design with elasto-plastic materials, Kumar et al (1981). Eq. 2.22 determines when the small-scale yield assumption is violated. There is no known way to calculate transition times for violation for a growing crack.

The J integral may be simply extended, Riedel (1987), to give;

$$C^* = -\partial/\partial a \int P \, d\dot{u} \qquad (2.28)$$

Eq 2.25 determines when C^* should be used, but is beyond the scope of this study. When J, C^*, or K_{Ic} is the appropriate parameter for characterizing creep crack growth is presented in maps, Riedel (1987). If fracture toughness values are not unusually large; K_{Ic} would appear to be valid to characterize loading.

5) Crack Arrest Versus Crack Initiation

Crack arrest may occur after subcritical or critical crack growth. In subcritical crack growth Evans (1972,3,4) observed experimentally a threshold value for K_{th}, below

which no crack growth will occur. If the applied K_I falls below K_{th}, slow crack growth will arrest.

In materials that exhibit only critical crack growth, initiation occurs at K_{Ic}. In certain geometries arrest may occur, and the arrest K_{Ia}, is taken as the lower bound of all available dynamic crack initiation and crack arrest data, Popelar and Kanninen (1985). An ASTM standard for obtaining the crack arrest fracture toughness is under development and has been tentatively proposed for ferritic steels, Barker et al (1988). The geometry is crack-line wedge-loaded compact-type specimens with side grooves, to measure the ability of the ferritic steels to bring to rest a fast-running crack. The difficulty reported by Liu and Miller (1978), Dempsey et al (1988) Dempsey et al (1989b) in obtaining arrest in ice with this geometry suggests it will not be useful in ice.

6) ASTM Standards

There is no ASTM standard specifically for the determination of the fracture toughness of ice. The various geometries that have been used on ice were mentioned in the introduction. In general, sample dimensions have been increased to include a significant number of the large ice grains in the test specimen.

The Double Torsion geometry was chosen for this work because it is one of the best geometries for inducing stable

crack growth, regardless of the compliance of the test rig, Mai and Atkins (1980). This will be shown in detail in Chapter 3. This is particularly relevant for field work, where the test frame must be transported, in some cases by hand, to the ice.

2B) Subcritical Crack Growth

Subcritical crack growth first came under study when it was realized that catastrophic failure of steel and ceramics was occurring much below design loads. The most spectacular of these was the sinking of Liberty ships while at dock, under no apparent load. Time dependent crack growth can result from environmental or corrosion effects, or creep effects; or a combination of both.

In a recent review Rice (1987) states that it is now generally accepted that stable sub-critical crack growth due to creep effects takes place if and only if the criterion of Eq 2.23 is met. If the crack is stable against spontaneous dislocation emission and the crack tip blunting that results, then the mechanisms of slow crack growth, cavitation and ligament rupture, cannot be activated.

If there is an energy barrier to dislocation emission, this mechanism cannot spontaneously blunt atomically sharp crack. In the absence of an external source of dislocations, the crack will remain atomically sharp, and the Griffith criteria for critical crack growth must be

exceeded at the crack tip.

If on the other hand spontaneous dislocation emission occurs, blunting the crack tip, the dislocation plasticity provides the mechanism by which creep fracture may ultimately occur, through void growth and coalescence, or localized shear, or a combination of both. There still, however, remains an elastic core at the crack tip that is dislocation free and where the elastic K_{Ic} criterion holds.

From the continuum point of view the asymptotic stress and strain fields for a crack growing in an elastic-power-law creeping material have been provided through the analysis of Hart (1980, 1981), Hui and Riedel (1981). Hui (1983, 1986) has done a small-scale yielding analysis of steady state crack growth, and Riedel and Wagner (1981) have done an approximate analysis of non steady growth.

An explicit assumption of the continuum model is that some small characteristic distance ahead of the crack tip a critical strain must be exceeded for crack growth to take place. Neither this distance nor the value of critical strain can as yet be specified.

It must be emphasized that there does not exist at present any generally accepted fracture criterion, and this is a subject of ongoing research, Kannanin and Popelar (1985), Thomson (1986,1987).

As mentioned earlier, the approach of Thomson (1986)

is different, modeling the discrete lattice and crystal dislocations. Thomson et al (1971) first discussed the crack motion problem for crystal cracks. The first attempt to deduce a kinetic law for crack velocity was by Hsieh and Thomson (1973). Thomson (1986) employs a K-type failure criterion, a local after-shielding k at the atomically sharp crack tip, in a core elastic region, lower case k to be distinguished from the remotely applied K_I , similar to the approach of Hart (1981). A critical mechanism in this model is the shielding or screening effect of a dislocation, that is, that stress is reduced across a dislocation. Thus an atomically sharp crack in a core elastic region, surrounded by a plastic zone consisting of a cloud of shielding dislocations, is subject to a lower effective stress than that applied externally. This gives a physical interpretation of crack growth, intimately connected to dislocation creation, movement and shielding.

The analysis of Hui and Riedel (1981) was based on the HRR analysis of a stationary crack in an elasto-plastic material, Hutchinson (1968), Rice and Rosengren (1968). The elastic-nonlinear viscous materials, as they call them, are assumed to deform in tension according to the law,

$$\dot{\varepsilon} = \dot{\sigma}/E + B\sigma^n \qquad (2.29)$$

which is similar to, though not exactly the same as, that found to hold for ice, Sinha (1978). A third term is

used in ice to account for delayed elastic strain, but it may be shown this is similar to the first term of Eq. 2.29.

By assuming stable crack growth may take place, Hui Riedel (1981) find that for $n < 3$ the inverse square root stress singularity occurs, and no sub-critical crack growth is possible. (This is not a deterministic proof that only critical crack growth may take place for $n < 3$, but a contradiction of the original assumption.) This is the same as for the linear material, equation 2.15. In the model of Thomson (1986) plastic creep does not have time to fully shield an atomically sharp crack when it moves into new material, when crack velocity is greater than some critical value, and $n < 3$. A local k can be sustained at the crack tip and bond breaking stresses achieved; critical crack growth results.

However, the asymptotic stress and strain fields near a growing crack tip change abruptly at $n = 3$. For $n > 3$ a new type of singular field develops at a growing crack tip. The stress and strain have the same form,

$$(\sigma,\varepsilon) \propto r^{-1/(n-1)}, \qquad (2.30)$$

Hui and Riedel (1981), and below a minimum crack growth rate no steady state creep crack growth is possible. Above this minimum growth rate,

$$\dot{a} \propto K_I^n, \qquad (2.31)$$

under small scale yielding conditions.

The physical description of steady state crack growth supplied by Thomson (1986) is complex, involving explicit calculations of shielding due to dislocations a finite distance from the crack tip. Because of the rate dependence of dislocation generation, for n > 3 there will always be a limiting crack velocity where the required shielding at the crack tip cannot be achieved, and the crack can grow away, critically, from its shielding charge of dislocations.

This relationship between creep crack growth rate and applied stress, and the prediction of a threshold stress intensity factor, is consistent with the experimental observations of Evans (1974), Cook and Lawn (1984), Cannon and London (1983,1988), and Riedel (1987).

The asymptotic field around a moving crack, Eq. 2.30, should be contrasted with the stress and strain asymptotic fields near a stationary crack tip in an elasto-plastic material, Hutchinson (1967), Rice and Rosengren (1968),

$$\sigma \alpha r^{-1/(n+1)}$$
$$\varepsilon \alpha r^{-n/(n+1)} \qquad (2.32)$$

The singularity of the growing stress field is greater than the static, but the singularity of the strain field is less than the static case. In Thomson (1986) this is the same as saying that the static crack is shielded, and the effective k at the crack tip is less.

The continuum model of Hui and Riedel (1981) indicates for a moving crack, with a weaker strain singularity, the elastic contribution to strain is as important as the creep contribution. This can be seen when the very high strain rates that must exist near the tip of a moving crack are appreciated. This is consistent with Thomson (1986), where a local elastic k field is essential for crack growth.

The discrete lattice approach of Thomson (1987) has successfully shown that the corrosive effect of different environments on crack growth rate is related to the relative size of the corroding molecule and the room available for it to penetrate to the crack tip, Lawn et al (1987). This was seen in the stress corrosion of silica in various environments, Michalske and Frieman (1987).

Lawn et al (1987) considered aged indentation cracks in brittle materials, and found that the strength of the samples did not increase with age. They conclude instead, as proposed by Thomson (1986), that atomically sharp cracks are shielded by dislocations; blunting and thus strengthening does not occur.

The concurrence between the discrete lattice model with its elastic core imbedded in a dislocation cloud, and the experimental results on aged indentation cracks in brittle materials and the influence on crack growth rate of corrosive environments, take it beyond the continuum approach. The mechanisms of dislocation emission, movement,

and shielding; combined with the geometry of the crack tip, supply a physical basis for the theory of high temperature fracture.

Creep crack growth velocities as low as 10^{-10} m/s are common, Kannanin and Popelar (1985), and ranging up to as high as 10^{-2} m/s are possible, depending on the material. Such wide ranges are not generally found in a single material, however.

The effective creep power exponents as high as 100 have been obtained from empirical evaluations of eq 1.1. Such high values of n, in fact any value higher than n = 5, indicates that crack growth is due in significant part to corrosion effects as well as creep effects.

2C) Previous Fracture Toughness Work On Ice

A summary of work on the fracture toughness of ice is contained in Appendix 1. The results are consistent and indicate that the specific fracture energy of ice is within an order of magnitude of the thermodynamic surface energy of ice. The tests were conducted above 0.9 homologous temperature, where ice will creep at any load. The creep in ice contributes to the fracture energy, but not to the extent that it does in steel for example, where fracture energy may be 4000 times the thermodynamic energy, due to plastic flow in the vicinity of the crack tip.

1) Crack Tip Preparation

The concern that prepared crack tips be sharp enough to ensure valid results has received considerable attention in the literature.

Liu and Loop (1972) prepared a crack with a razor, avoiding microcracking, and coated the crack in silicon grease to prevent sublimation. Liu and Miller (1979) used a similar procedure, and as well tested precracked samples. No information was given on how precracking was done, but it is the only work in the literature on precracked samples, (other than samples deliberately microcracked under a sharp blade). Their results are particularly relevant, approximately 110 $kNm^{-3/2}$ at rate 1000 $kNm^{-3/2}$ s^{-1}, as they report no difference in toughness in samples prepared with the two different techniques.

Work to date falls into two approaches to crack tip preparation. Goodman and Tabor (1978), Hamza and Muggeridge (1979), Goodman (1980), Timco and Frederking (1983,1986), Azadeh-Tehrany (1983), Kusomoto et al (1985), Nixon and Schulson (1986a, 1986b), Bentley et al (1985), Dempsey et al (1988, 1989a, 1989b), Nixon (1988), Nixon et al (1989), Danilenko (1985), Shen and Lin (1986), prepared the crack with a razor, taking care to avoid microcrack creation. Kollé (1981), Andrews and Lockington (1983), Andrews et al (1984), Parsons et al (1985,1986,1988,1989), Tuhkuri (1987) deliberately created a jagged crack. Others such as Urabe

et al (1980,1981a) are not explicit about crack tip preparation techniques. In the light of the work of Liu and Miller (1979), the difference is not significant, though very blunt crack tips cause higher apparent toughness, Nixon (1989), Dempsey (1989a).

2) Sample Size

The question as to what is the adequate sample size to ensure that the small scale yield/creep criterion is met, has been addressed by almost all workers. The problem hinges on the choice of appropriate ice yield strength, depending on strain rate that is felt to be effective at the crack tip. For example Goodman (1980) calculates the strain rate in an equivalent uncracked beam, and using this to obtain a yield strength, calculates a plastic zone size and finds it small compared to specimen geometry. It can be argued, however, that this is too conservative, and that the stress concentration at the crack tip greatly increases the strain rate, and thus yield strength.

The question of adequate sample size, with respect to grain size, was addressed by Urabe et al (1981b), and their algorithm for correcting results from small samples was used by Timco and Frederking (1983) and Andrews et al (1984). This whole question is considered in detail by Dempsey et al(1989a, 1989b), and their results indicate that prepared crack length should be as large as possible, at least six

times, and preferably 34 times the grain size. Their results, however, also indicate that very long cracks also have low fracture energy, the lower limit approaching perfectly brittle cleavage along the basal plane, or grain boundaries. The specimen depth to crack length ratio should also be as high as possible.

3) Rate Dependence / Plane Strain versus Plane Stress

The reports of the rate dependence of ice fracture toughness are contradictory.

A review of work to that time by Urabe and Yoshitake(1981a) showed that for pure ice with grain size 5 - 10 mm that over the range $0.1 < \dot{K}_{Ic} < 10^5$ $kNm^{-3/2}s^{-1}$;

$$K_{Ic} = 216\ \dot{K}_I^{-0.11} \tag{2.33}$$

There was no transition from plane stress to plane strain observed.

Their own results, however, showed an apparent K_c hump at approximately 100 $kNm^{-3/2}s^{-1}$, with no rate dependence down to 1 $kNm^{-3/2}s^{-1}$. They report similar behavior in sea ice, Urabe and Yoshitake (1981b). This could indicate a transition from plane strain to plane stress.

Timco and Frederking (1986) found;

$$K_{Ic} = 188\dot{K}_I^{-0.13} \tag{2.34}$$

for $6 < \dot{K}_I < 90$ $kNm^{-3/2}s^{-1}$ in freshwater fine grained columnar ice, with no plane stress to plane strain hump.

Nixon and Schulson (1986b) observed what appears to be a plane strain to plane stress transition, and extended the rate dependent information another order of magnitude lower, to 10^{-2} $kNm^{-3/2}s^{-1}$. Pointing out that there is no standard for creep materials equivalent to the plane strain criterion for materials that display rate independent plasticity, they suggest that a creep zone greater than 1/50 specimen dimensions also violates plane strain. They calculated what they call the transition time from plane strain to plane stress from Eq 2.24. The rate they calculate for transition from plane strain to plane stress in their specimens, about 2 $kNm^{-3/2}s^{-1}$ fits their data.

If the plane strain condition is violated due to growth of the plastic zone, the J integral can be used. Only one calculation of the J integral for ice is reported in the literature, Urabe and Yoshitake (1981b) (though Dempsey et al (1989b) measured fracture energy directly instead of K_{Ic}). The same toughness of approximately 250 $kNm^{-3/2}$ at 0.5 $kNm^{-3/2}s^{-1}$ was obtained from both the J integral and LEFM. The J integral was calculated from;

$$J_{Ic} = 2U/(d(W-a)) \qquad (2.35)$$

where U is the area under the load versus load-point-displacement curve, d is sample thickness, W is specimen ligament and a is crack length. The J_{Ic} was used to calculate K_{Ic} from Eq. (2.20). That this agrees with the LEFM calculation of K_{Ic} shows that LEFM is adequate to 0.5

$kNm^{-3/2}s^{-1}$, and plane strain is not violated. This result will be discussed in greater detail in Chapter 4.

It is not clear how to explain the apparent plane stress to plane strain transitions reported in the 2 to $100kNm^{-3/2}s^{-1}$ range, but over the wider load rate regime of10^{-2} to 10^{5} $kNm^{-3/2}s^{-1}$, there is no transition apparent.

When the creep zone spreads through the sample, the C*integral should be used. No work has been done to determine when this should be done for ice. If the nonrate dependent work integral (J) is unnecessary to 0.5 $kNm^{-3/2}s^{-1}$, so is the rate dependent one, C*.

Liu and Miller (1979) explain rate dependence of ice toughness as a consequence of stress relaxation in the vicinity of the crack tip, which then requires a higher applied stress to reach the same level of fracture stress at the crack tip. This is the view that will be taken here, though Liu and Miller make no comment on the nature of this relaxation, the concept is consistent with the Thomson (1987) model, already presented, of crack tip shielding by dislocations.

4) Grain Size Influence

Nixon and Schulson (1986a,b) report a 25% decrease in toughness for grain size increase from 1.6 to 9.3 mm. This trend has not been found to extend to greater grain sizes. The results of Goodman and Tabor (1978) from single

crystals, Parsons and Snellen (1985) from large grain (5-10cm) freshwater ice at the mouth of the McKenzie river, and Parsons et al (1986) from large grain size sea ice, indicate similar toughness results as at the smaller grain size. Danilenko (1985) reports an increase in toughness in large (10 cm) monocrystals, as do Timco and Frederking (1982) in small grained columnar ice. A possible explanation for this has been proposed by Dempsey et al (1989a); that ice has an equicohesive temperature for certain types of ice, above this the toughness increases with increasing grain size, and below it it increases with decreasing grain size.

5) Fracture Toughness Anisotropy

The influence of anisotropy of ice crystals on fracture toughness has been reported by Kollé (1981), Timco and Frederking (1986) in fine grained freshwater columnar ice: and Urabe and Yoshitake (1981b), Danilenko (1985), Parsons et al (1985, 1986), Shen and Lin (1986), in large grained sea ice. Fracture along the basal plane is less tough than across it, in both ices. Urabe et al (1980) report cracks on bottom of sea ice tougher than those on top. Parsons et al (1986) report preferred c-axis orientation in ice also has influence on toughness, a vertical crack aligned perpendicular to the preferred c-axis has the lowest toughness. Also the temperature dependence

of the toughness is anisotropic.

6) Arrest Toughness

All the results of Gold (1963) were obtained from cracks that had arrested. Liu and Miller (1979) obtained five crack arrests with the wedge opening compact tension specimen, but none below -12° C. The indenter results of Goodman and Tabor (1978) were from cracks that had arrested, but the numerical value of the toughness were high, and it will be shown this is due to assumptions of the algorithm used to calculate toughness due to indentation load on a Vickers indenter that are inappropriate for a material that undergoes microcrack damaging beneath the indenter. Bentley et al (1988) were unable to obtain any crack arrests with a wedge loaded floating tapered double cantilevered beam, but Dempsey et al (1989b) report arrest with the same geometry in a test frame, thought they do not distinguish these from the apparent fracture toughness K_Q, their notation.

7) Damage

Timco and Frederking (1986) report toughness decreases with increase in ice damage, as quantified by crack density up to 7 cracks per cm^2. Nixon (1989) also showed toughness decreased with increased damage due to cracking, quantified by ice density that decreased with increased damage.

2D) Laboratory and Analytic Studies of Ice Fracturing.

The operational scenario for exploration in ice covered waters has been primarily in sea ice, so a number of physical model studies have been conducted on edge indentation of semi-infinite sheets of ice. Hirayama et al (1978), Croasdale et al (1978), Sodhi and Hamza (1977), Michel and Toussaint (1977), Michel and Blanchet (1983), Frederking and Timco (1985), and Timco (1987a) are examples of this work. These studies have shown how complicated the mechanisms of ice failure are, and how difficult brittle fracture can be to analyze in even a relatively simple and controlled geometry.

Out of these tests have arisen empirical equations for load prediction, and enough experience to tentatively classify and predict failure modes according to aspect ratio (structure width to ice thickness) and strain rate (structure width divided by interaction velocity).

Except at very low indentation rates where creep is the primary deformation mechanism, ice fails through the growth and interaction of cracks. The geometry, orientation and interaction of several types of cracks has made it possible to classify failure modes, Palmer et al (1983).

Local crushing is characterized by densely packed cracks in the immediate vicinity of contact. This is generally responsible for the generation of the greatest local and

global loads. It is associated with structures with width comparable to ice thickness.

With width greater than ice thickness local crushing may be accompanied by a number of different cracks; spalling, radial, and circumferential. As width increases, spalling accompanied by crushing appears first, then radial cracks with crushing (and no spalling), and then radial and circumferential cracks with crushing, and finally radial,circumferential cracks leading to buckling but no spalling.

Timco (1987a) in tests on thin freshwater ice in a model basin showed that such a classification did appear valid. It is not clear however, what determines which failure mode is activated. For example for aspect ratios of 4 and up, it is interaction velocity alone. Why is ice crack dynamics rate dependent?

This is important, as global and local loads vary greatly with failure mechanism. Local crushing generates very high local and global loads, on the order of the hardness of ice; whereas in buckling with no crushing one need only be concerned with much lower global loads. The appearance of spalling, radial, and circumferential cracks are all preceded by load peaks. A designer must be able to anticipate which regime a structure can be expected to operate in, and how the ice failure mode that generates the minimum loads on the structure might be promoted.

Palmer et al (1983) attempted to mathematically model radial cracks as an edge crack in a semi-infinite plate, wedged open by a transverse compressive force in the ice crushing region, determined from a Hertzian analysis of contact. They assumed that crack growth was stable, applied the solution for the stress intensity factor of a known crack length in this geometry, and calculated the loads corresponding to various crack lengths. They stated their solutions as the loads required to generate these cracks. They are however the loads necessary to cause cracks of that length to grow longer.

Hamza and Muggeridge (1984) consider the same geometry, assume that sub-critical crack growth is possible in ice, and that the rate of growth is determined by Eq(1.1). They found that the greater the applied stress or structure diameter the greater the maximum crack growth rate, and the further from the structure it occurs. No assumptions were made about crack arrest.

Bhat (1988) also considered the radial crack problem, following the analysis of Palmer et al (1983),but for a finite ice flow. He showed that crack growth will become dynamic when the crack reaches about 0.1 the flow diameter. This is similar to the crack instability shown in various fracture test specimen geometries, Atkins and Mai (1980). Thus maximum load is that required to increase the crack length to .1 the flow diameter. Finite element calculations

done under the constraint that the crack surfaces touch at the loaded edge show that the Hertzian analysis supplies a larger portion of crushing load to crack splitting, about fifty percent, than is consistent with this constraint. A value of twenty to thirty percent of crushing load as splitting force is more realistic and conservative.

Ashby et al (1986) show that contact between an indenter and a two dimensional brittle foam sheet is mediated through by a finite number of contact points. The fragmentation is a consequence of the interaction of the cracks that are generated at each of these contact points.

Timco (1987b) showed that the peak and average loads in an ice-structure interaction are reduced when the number, length or density of ice cracks is sufficiently high.

These studies indicate that crack presence, growth and interaction is intimately connected to limiting peak and average loads in ice-structure interaction. None of them, however, provide any fundamental insight into why any particular failure mode might be observed in a given geometry and strain rate range, though the work of Hamza and Muggeridge (1984) is very suggestive. More basic information is required on ice crack dynamics.

1) Time Aspects of Ice Behaviour

The strain rate dependence of ice indentation strength outlined by Michel (1978) shows that ice may display ductile

or brittle behaviour, depending on the strain rate, with a transition region found in the strain rate range of 10^{-4} to 10^{-3}. For strain rates below 10^{-4} the strength is controlled by creep and is a function of strain rate. Above strain rate of 10^{-2} strength is obtained from brittle fracture, and is independent of strain rate.

Early work on ice was conducted by Gold (1963, 1965,1967, 1977), from which Sinha (1978) proposed that the strain of ice may be partitioned into three components; the elastic ε_e, the delayed elastic ε_d, and the viscous ε_v. The elastic is the instantly recoverable strain, the delayed elastic is recoverable but time dependent, and the viscous is permanent. The total strain may be written;

$$\varepsilon_t = \varepsilon_e + \varepsilon_d + \varepsilon_v . \qquad (2.36)$$

Sinha (1979) modified this to accommodate the influence of grain size;

$$\varepsilon = \sigma/E + c_1[\frac{d}{d_1}][\frac{\sigma}{E}]^s[1 - \exp\{-(a_T t)^b\}] + \dot{\varepsilon}_{v_1} t[\frac{\sigma}{\sigma_1}]^n ; \qquad (2.37)$$

where E is Young's modulus, $\dot{\varepsilon}_v$ is the viscous strain rate for unit or reference stress σ_1, c_1 is a constant corresponding to the unit or reference grain size, d_1. b,n, and s are constants, and a_T is the inverse relaxation time. Both $\dot{\varepsilon}_v$ and a_T were shown to vary with temperature with the same activation energy.

Sinha (1982a) went on to show that the occurrence of

the first crack in uniaxially loaded compressive tests of ice is strongly correlated with a critical delayed elastic strain. This has become a widely held criterion for the initiation of first crack, though it does have shortcomings. It was pointed out by Sanderson and Child (1986) that this criterion implied an infinitely high initiation stress for infinitely fast loadings, yet cracks nucleate at high strain rates. Sunder and Ting (1985) proposed a critical tensile strain as a new crack initiation criterion. The tensile strain is developed perpendicular to the compressive stress through the lateral extension consistent with volume conservation. Both criteria are critical strain.

It should be emphasized that ice will creep at any load. For stress levels above .5 MPa cracks in ice will form when ε_d reaches a critical level, irrespective of the applied level of stress. For stress levels below .5 MPa the failure of ice is not accompanied by cracking, but is a result of plastic rupture or collapse.

The cracks that form in ice appear abruptly, are approximately .6 the grain diameter, scale linearly with grain size in the range 1.5 to 6 mm, Cole (1986), are aligned parallel to the direction of maximum compression, and do not grow longer with further increase of load. Instead more cracks appear Sinha (1982b), leading to progressive damage of the ice, that is, increased compliance, and only in the late stages with very high

density do they interact and link up along shear planes. The peak strength of ice corresponds to crack densities of approximately one per grain, Kalifa (1989).

This brief overview shows the integral part cracks in ice play in load determination, and highlight that more needs to be known about crack growth dynamics.

CHAPTER 3

EXPERIMENTAL

1) The Double Torsion Method

a) Three Test Methodologies

It is possible using the Double Torsion geometry to determine the fracture toughness/crack velocity relationship without measuring the crack length, or rate of crack growth. The K_I is independent of crack length and may be calculated from specimen thickness, width and applied load. The crack velocity may be derived from the plate compliance as follows (Evans 1972,1974, Williams and Evans 1973, Outwater et al 1974, Pletka et al 1979, Champomier 1979, Bond et al 1984).

For small deflections y in a rectangular bar (one half the DT geometry) with width W much greater than thickness d the torsional strain is;

$$\theta = y/w_m = 6Ta/Wd^3G, \qquad (3.1)$$

Timoshenko (1970), where a is the length of the bar (the crack length), T is the torsional moment = $(P/2)w_m$, P/2 is the load applied to one bar, and G is the shear modulus of the material, see Fig 4.1, pg 84. The viscoelasticity of ice will be taken into account subsequently.

Eq. 3.1 may be written as;

$$y/P = 3w_m^2a/Wd^3G = Ba. \qquad (3.2)$$

This equation was verified in glass with a compliance

calibration, McKinney and Smith (1973), Williams and Evans (1973). This gives an accurate prediction of the deflection of the loaded point as function of the crack length a over the range $.25 \leq a/W \leq .85$.

Three methods for obtaining crack growth velocity may be used with the Double Torsion geometry. Evans (1972) showed the crack velocity may be calculated when a constant displacement, or constant displacement rate is applied. Outwater (1974) measured the crack growth in glass optically with a travelling microscope.

i) Differentiating Eq. 3.2;

$$\dot{y} = \dot{P}Ba + PB\dot{a}. \tag{3.3}$$

For a fixed displacement $\dot{y} = 0$,

$$V = \dot{a} = -\dot{P}a/P. \tag{3.4}$$

The load relaxation technique is done under fixed grip conditions to measure high crack velocities. The crack velocity is calculated from the initial crack length a, the initial load P, and the rate of load relaxation $\dot{P}$ after rapid initial loading.

It is possible to obtain a range of velocities from a single specimen but the precision is reduced with load relaxation. The machine relaxation must be measured and subtracted to obtain the true material relaxation.

If we return to the Eq. 3.2 and assume that Contains a time dependent modulus we obtain;

$$\dot{y} = \dot{P}Ba + P\dot{B}a + PB\dot{a}, \text{ and} \qquad (3.5)$$

$$\dot{B} = \frac{-6w_m^2(1+\nu)\dot{E}}{Wd^3E^2} = -B\dot{E}/E \qquad (3.6)$$

where differentiation is at constant load and crack length.

Sinha (1978) states that $\dot{E}$ for ice is load independent for a finite time, that is temperature and grain size dependent. At -10° C it is 10 seconds, and at -45° C it is 2000 seconds. A load relaxation test cannot be conducted for longer times for this analysis to be valid. This will account for changing ice modulus influence on apparent crack velocity, but it does not account for how the creep mechanisms interact with crack extension mechanisms.

Returning to Eq. 3.2 with a time dependent compliance;

$$\dot{y} = \dot{P}Ba + P\dot{B}a - PB\dot{E}/E = 0 \qquad (3.7)$$

$$\dot{a} = -\dot{P}a/P + \dot{E}/E \qquad (3.8)$$

The machine relaxation must also be subtracted from this measured load relaxation.

ii) The constant displacement rate technique is used in the intermediate velocity range. Evans (1972) observed a load plateau during crack propagation, for a constant crosshead displacement rate.

From Eq. 3.2;

$$\dot{y} = \dot{P}Ba + PBV \text{ , for } \dot{P}=0,$$

$$V = \dot{y}/PB \qquad (3.9)$$

where $\dot{y}$ is the crosshead rate of the testing machine and P is the constant load developed at that cross head rate.

In the viscoelastic analysis we have;

$$\dot{y} = \dot{P}Ba + PBV - PB\dot{E}/E, \qquad (3.10)$$

and we obtain for the velocity;

$$V = \dot{y}/PB + \dot{E}/E \quad . \qquad (3.11)$$

The correction term is the same as above, applied in the opposite sense.

Lewis and Karunaratne (1981) have shown it is possible to obtain three platform loads and hence three points in the K-V diagram in the constant K region, $.25 \leq a/w \leq .85$. As a calibration of this compliance correction, the relaxation of an unnotched specimen should be measured.

iii) At very low velocities a constant load technique becomes appropriate, as the accuracy of the constant displacement rate technique also deteriorates at low rates.

A predetermined constant load corresponding to a low value of the stress intensity factor is applied and the crack velocity is determined by direct measurement of the crack tip advance during a predetermined time interval. With an optical microscope velocities of less than 10^{-7} m/s have been measured, and a scanning electron microscope has made measurements down to 10^{-10} m/s over twenty-four hours.

In all cases the corresponding K_I is calculated from the load, and specimen geometry, with no crack length

measurement necessary.

b) Double Torsion Geometry is Constant K for Constant Load

The derivation of the expression for the stress intensity factor of the double torsion geometry begins with eq.(3.1) rearranged as follows, Williams and Evans (1973), Fuller (1979);

$$y/P = 3w_m^2 a/Wd^3G = C \qquad (3.12)$$

where C is the elastic compliance.

The resistance to crack growth, R, is related to specimen compliance by,

$$R = P^2/2 \quad (dC/dA) \qquad (3.13)$$

where A is the area of the crack, Irwin and Kies (1954).

If the crack shape is independent of crack length;

$$R = P^2/2d \quad (dC/da) \qquad (3.14)$$

where d is plate thickness in the plane of the crack.

From Eq. (3.14) and (3.12) we get;

$$R = 3P^2w^2_m / 2Wd^4G \qquad (3.15)$$

From Eq. (2.19) and (2.20) we get;

$$K_I = (2GR/(1 \mp \nu)^{\pm 1})^{1/2} \qquad (3.16)$$

where the upper/lower signs refer to plane strain and plane stress respectively.

Eq (3.15) and (3.16) yield;

$$K_I = Pw_m/d^2 \left(\frac{3}{W(1 \mp \nu)^{\pm 1}}\right)^{1/2}, \qquad (3.17)$$

The choice between plane strain or plane stress is problematic. Fuller (1979) points out that this distinction is seldom made in ceramics, as has been noted earlier, Popelar and Kannanin (1985). If the minimum thickness of $2.5(K_{Ic}/\sigma_y)^2$ is appropriate for brittle materials, values of toughness reported in the literature have been mostly plane strain.

The plane strain expression has been verified with three dimensional finite element analysis Trantina (1977), Tseng and Berry (1979). They show that Eq (3.17) is valid for $0.1 \leq a/W \leq 0.8$, and recommend that the length of the specimen be at least three times the crack length, the thickness to crack length ratio be less than 0.33, and that the loading points be as close together as is practical. The stress in the thickness direction is shown to converge very rapidly to zero, being negligible for distance y from crack front,

$$y \leq 0.1(L - a), \tag{3.18}$$

where L is the sample length. This stress is very localized and does not directly decrease to zero but goes first negative. It would be zero on the free surface of an uncracked body. This approximation of plane strain, with non-zero stress gradients, corresponds to accepted practice for application of plane strain formulations in fracture, Popelar and Kannanin (1985).

The value of K_I varies slightly along the quarter

elliptical crack front, but for ratios of the minor to major axis of the quarter ellipse less than .15, the plane strain version of Eq. (3.17) is accurate to at least half the minor axis. At the full depth of crack (which does not extend through the thickness but leaves a small compression hinge) the K_I is eighty percent that at the tensile surface.

Williams and Evans (1973), assumed plane stress was applicable in the original derivation, and calibrated the compliance expression, though this does not validate the K_I expression. Lewis and Karunaratne (1981) wrongly quote Trantina (1977) as providing justification of this choice, though Trantina (1977) shows the plane strain expression is accurate. Sano (1988) readdresses the question of whether stress intensity factor is crack length independent, and concludes that it is, quotes the expression from Evans (1972). Mai and Atkins (1980) quote Evans (1973).

Pletka et al (1979) provide further guidelines for the Double Torsion test geometry. The standard size for testing ceramics is approximately that of a microscope slide, 2 x 25 x 75 mm. A groove is commonly used to guide the growing crack and maintain symmetry, but this may be accomplished with a sufficiently thin sample. The thickness should be less than one twelfth the width, and the length to width ratio should be greater than 2. A sample width sufficient to include a significant number of grains is recommended, as the constant K_I condition may be affected by interactions

of the propagating crack and the microstructure.

c) Stability of the Double Torsion Geometry

The derivation of crack growth stability conditions will follow Gurney and Hunt (1967), Gurney and Ngan (1971),Gurney and Mai (1972), Mai and Atkins (1980). Consider Eq. (2.5) for two different growth rates, $\dot{A}_1$ and $\dot{A}_2$. Eq 2.5 may be rewritten as Eq (2.6), or as;

$$u^2 = -2R/\frac{d}{dA}\ (F/u) \tag{3.18}$$

Differentiating this with respect to area we obtain;

$$\frac{2du}{ud\bar{A}} = \frac{1}{R}\ \frac{dR}{d\bar{A}} - \frac{d^2}{d\bar{A}^2}\ (\frac{F}{u})\ /\ \frac{d}{d\bar{A}}\ (\frac{F}{u}) \tag{3.19}$$

For a displacement controlled machine, du/u > 0, thus;

$$\frac{1}{R}\ \frac{dR}{d\bar{A}}\ > \frac{d^2}{d\bar{A}^2}(\frac{F}{u})\ /\ \frac{d}{d\bar{A}}\ (\frac{F}{u}). \tag{3.20}$$

This is the stability criterion for displacement controlled machines. The left hand side is a statement about the rate of energy absorption by the material during crack propagation. The right hand side is a statement about the rate of energy availability from the testing machine and test piece. This is referred to by Mai and Atkins (1980) as the geometric stability factor, and they calculated values for both hard and soft testing for twenty-four different fracture geometries. The more negative the right hand side, the more stable the test geometry. A detailed derivation for the double torsion geometry with finite test machine

compliance, tested under $du/u > 0$ conditions, will be given. The double torsion geometry is also stable for $dF/F > 0$, and this is not affected by finite compliance, as $d^2/dA^2(F/u_1)$ is the same as $d^2/dA^2(F/u)$.

Following Gurney and Hunt (1967), if the testing machine has linear elastic flexibility, k, we may write the total deflection as;

$$u_1 = u + kF \tag{3.21}$$

$$F/u_1 = (F/u)/(1 + k(F/u)) \tag{3.22}$$

After some manipulation Eq. (3.20) becomes;

$$\frac{1}{R}\frac{dR}{dA} > \frac{d^2}{dA^2}\left(\frac{F}{u}\right) \Big/ \frac{d}{dA}\left(\frac{F}{u}\right) - 2k\,\frac{d}{dA}\left(\frac{F}{u}\right) \Big/ (1 + k(F/u)) \tag{3.23}$$

As $d/dA\,(F/u)$ is negative, the stability is decreased by the flexibility of the testing frame.

The expression for F/u for the double torsion geometry is given in Eq (3.12), and applied to Eq, (3.20) first one obtains the stability criterion;

$$\frac{1}{R}\frac{dR}{dA} > -\frac{2}{ad} \tag{3.24}$$

for crack length a and thickness d. The right hand side is always negative, and any instability must be a consequence of negative dR/dA. This is possible in some materials that have a lower toughness at higher crack velocity, Mai and Atkins (1975), or if a blunt starter crack results in a similar effect, Selby and Miller (1975), Mai and Atkins

(1980). Local heating may result in an instability if the material has a higher toughness at higher temperature, Marshall et al (1974). Yamini and Young (1980) found in epoxy resins that those with low yield strength exhibit unstable slip/stick crack growth, but those with high yield strength display stable sub-critical crack growth.

Inserting Eq. (3.12) into Eq. (3.23), noting F = P;

$$\frac{1}{R}\frac{dR}{dA} > -\frac{2}{ad} + \frac{2kBd^2/a^2}{1 + kBd^3/a} \qquad (3.25)$$

where here $B = WG/3w_m^2$.

It is relevant to determine at what value of test machine compliance the double torsion geometry might become unstable under du/u > 0 testing conditions. This is done by setting the right hand side of Eq. (3.25) > 0, we get;

$$\frac{2kBd^2/a^2}{1 + kBd^3/a} > \frac{2}{ad} \qquad (3.26)$$

$$2k(2Bd^3/a - 2Bd^3/a) > 2 \qquad (3.27)$$

Eq. 3.27 shows that the double torsion geometry is stable, regardless of the compliance of the test rig. Any observed instability of crack growth in this configuration must be a consequence of material instabilities. Just what type, may be anticipated by the observation Mai and Atkins (1975) that a material that demonstrates increasing fracture toughness and decreasing modulus for decreasing crosshead, as does ice, has a fracture surface energy that

decreases for increasing crack velocity.

d) The Effect of the Remote Flow of Ice on the Stability

Atkins and Mai (1985) state that, in general, plastic flow remote from the crack tip of a specimen under load contributes to the stability of the situation, as it supplies a further energy sink for any excess strain energy stored in either the test rig and specimen. Eq. (2.1) maybe modified with the addition of a term to account for energy expended in plastic flow remote from the crack tip, and a term for residual strain energy;

$$Fdu = d\Lambda + RdA + d\Gamma + d\Lambda_r \qquad (3.28)$$

where the elastic surface energy is the specific work of fracture in the presence of extensive flow, Γ represents the energy dissipation due to remote plastic flow, and Λ_r is residual strain energy. It is to be emphasized that the remote plastic flow has nothing to do with the process of fracture as such, and that values of Γ depends on specimen geometry, shape, and levels of strain throughout the body. Eq. (3.36) thus becomes;

$$\frac{d}{da}\left(R + \left(\frac{\partial \Gamma}{\partial M}\right)u\right) > \frac{d^2}{dA^2}(\Lambda + \Lambda_r)u, \qquad (3.29)$$

for $du > 0$, cf. with the purely elastic case Eq. (3.20). As in Eq (3.20) the left hand side of Eq. (3.29) is material dependent, and the right hand side geometry dependent. In general $d\Gamma/dA$ is positive, and stability is improved.

In the event of crack growth instability, it is possible to determine the magnitude of kinetic energy invested into the ice, Gurney and Ngan (1971). For the ratio $a/w_m \cong 1$ used in these tests, and assumed macroscopic crack velocity of 20 m/s, Parsons et al (1987), the fracture surface energy may be exceeded by only two percent.

e) The Effect of Finite Test Frame Compliance on Crack Growth Length

Equation 3.27 shows that the Double Torsion geometry is stable regardless of test frame compliance. The resulting crack length is however influenced by any strain energy stored in the test frame.

Following the analysis of Virkar and Johnson (1976), the deflection at the point of loading due to a drop in load during crack growth is;

$$\delta = 2k_f (P_c - P_a) \tag{3.30}$$

where k is the compliance of the frame, P_c is the critical load at crack growth initiation, and P_a is the load at crack arrest. The total deflection is thus;

$$\delta_t = \delta_0 + 2k_f(P_c - P_a) \tag{3.31}$$

where δ_0 is the deflection of the ice sample. From Eq 3.2 the expression for the crack length is obtained;

$$a = [\delta_0 + 2k_f(P_c - P_a)] \,/\, [\frac{Wd^3G}{3Pw^2_m}] \tag{3.32}$$

f) The Double Torsion Test Apparatus

The test rig was designed to be as stiff as possible while still being transportable by manpower to a test site established on the sea ice in Allan Bay, near Resolute Bay NWT., 74° 43′ 45′′ N, 95° 04′ W. The dimensions of ice samples to be tested were restricted by considerations of how thin a double torsion sample might be prepared and handled. The sample width was chosen so as to include a approximately ten of the large grains that exist in first year columnar sea ice, and is approximately twelve times the thickness as recommended by Pletka et al (1977). No guiding grooves were machined into the ice as the samples were very fragile even without them and difficult to handle without breaking. The samples were machined to a smooth surface with a router mounted in a sliding jig, and then the sample turned over and the opposite face machined. Considerable care was used to ensure that the thickness was uniform by running the router up and down the specimen surface in the direction of crack growth after the initial smoothing was done, to further smooth the surface.

A load frame was designed to test ice samples 4 cm. thick (d = .04m), 50 cm. wide (W = .5m), and over a metre long. The vertical arms of the frame were built of a 5 x 7.6 cm steel I beam, and the horizontal of a 15.25 cm. deep by 7.6 cm wide steel box beam, see Fig. 4.2. This weighed eighty pounds, and was judged to be just at the limit of

what one person could safely move about and set up.

The load was applied by a ball screw actuator driven through a 20:1 reduction Boston gear by a controllable electric motor. The load cell was mounted in series between the actuator and the ice sample. A LVDT was placed on the surface of the ice sample as close as possible to the point of load application. The load and deflection data was collected in the field on a thermal strip chart recorder. During the lab tests with the same test rig, an analog tape recorder was also used.

The compliance of the test frame, including actuator and load cell was measured to be 2.0×10^{-7} m/N.

g) Precision of Measurement

To calculate the fracture toughness from the Double Torsion specimen, the applied load, resulting deflection of the ice, and the geometry must be measured.

A typical load and deflection record are shown in Fig.4.3. The load cell was calibrated to 257 N/volt, and the scale of the strip chart recorder was set at 0.1 V/cm. From the strip chart record the load can be determined to 0.5 mm,or approximately 1 N. Thus load had an accuracy of $\cong$ 1 N.

The LVDT used for collecting deflection was calibrated to 1.42×10^{-4} m/volt. The recorder was set typically to 2V/cm., and reading this to 0.5 mm precision gives a measure of the deflection with a precision of $\pm$ 13 μm.

The support points were 50.0 cm apart, and the load points were 5.0 cm apart.

Ice thickness was measured at least three times along the resulting crack and the standard deviation was typically ± 0.5 mm, as low as ± 0.1 mm, and at worst ± 1.5 mm.

Though the ice crack length was not required for the calculation of the fracture toughness, it was measured during a test, and after each crack growth. A metal tape measure was laid on the ice sample, zero set at the crack tip as seen from above through the ice, and as the crack grew its length estimated to the nearest centimeter.

From the plane strain version of Eq. 3.17 the accuracy of the fracture toughness measurement may be calculated.

The influence on K_{Ic} is greatest for the thickness. Following Bevington (1969) the influence on the standard deviation of the calculated fracture toughness from the load and thickness variability may be written;

$$\left(\frac{\text{Std dev } K}{K}\right)^2 = \left(\frac{\text{Std dev } P}{P}\right)^2 + \left(\frac{\text{Std dev } d}{d}\right)^2. \qquad (3.33)$$

Using d = 50 ± .5 mm, P = 500 ± 1 N, we obtain for a typical ice toughness $K = 100 \pm .1$ $kNm^{-3/2}$.

The influence of test frame compliance on resulting crack length may be estimated from Eq 3.32. From the system compliance of 2.0×10^{-7} m/N, an ice deflection of 1×10^{-4} minimum, a drop in load during crack growth of 100 N

typical, the contribution to crack length from the test frame is still an order of magnitude less than the measured values. Less than ten percent of the crack growth length is caused by the finite compliance of the test frame.

h) Design Shortcomings

As the Double Torsion specimen has previously been used on ceramics in much smaller proportions, about the size of a microscope slide, most problems arose in these tests because of the larger size of sample needed for ice. The large ice sample size was chosen because grain size in sea ice is typically 5-10 cm, and thus to ensure enough grains were included in the sample to consider it multi grain.

Machining an ice sample .05m x .55m x 1.5m to an acceptable level of uniformity of thickness is difficult, and as the above analysis shows, very important. The design of router and jig designed for this task was operationally satisfactory and reliable, and this has great, perhaps overriding, importance in the context of an expensive field trip, conducted under the harshest imaginable conditions for equipment and researchers. Further design work could conceivably result in an apparatus that would give better uniformity of specimen thickness.

Ironically perhaps, future field work might best be conducted in a cold room. The single most important variable beyond the control of the experimenter working on the frozen ocean is ice temperature. The field experiments

extended over the four weeks of the spring when the temperature is still low, and the sun shining. The temperatures change rapidly this time of year. Testing done in a portable cold room would eliminate the temperature variable, and make field results more uniform. It would also eliminate lost time due to extreme weather when it is impossible to work on the ice.

i) Laboratory Tests

The wet seed technique was used to grow ice in the cold room. A large tank of water was allowed to freeze at-20° C and form ice on the surface. Periodically this was broken and the tank mixed to ensure uniform cooling. Then the ice was broken and removed from the tank, any loose fragments skimmed off, the fans in the cold room shut off, and seeding begun. The room was filled with a fine ice fog generated with hot water sprayed through a fine nozzle. When the fine water aerosol came into contact with the cold air, small ice crystals formed and fell to the ice surface. These crystals acted as seed sites, and because they were uniformly and densely spread across the surface, prevented large frazil ice crystals from growing. From this fine grain surface layer a fine grain columnar ice grew.

The tank the ice sheets were grown in was .55m wide, producing a sample just wide enough for testing in the double torsion load frame, when it could be removed from the tank without fracture. It was possible to grow a 4-5 cm

thick sheet in a twenty-four hour period. These were then temperature saturated for at least 24 hours before testing.

The ice was freshwater, fine grained, with density of approximately 900 kg/m^3. The grain size at the bottom of the sheet was 5-8 mm.

The samples grown in the cold room were not machined with the router jig used to prepare samples in the field. A number of baffles were erected around the tank to ensure that the circulation created in the cold room by the refrigeration fans did not cause uneven ice growth. These samples proved to be as parallel sided as could be prepared with the router jig. The single largest problem in this procedure was removing the ice sample from the tank without fracturing it or subsequently dropping it, as it was initially wet. Immediately upon removal it was scraped with a flat edge to remove any slush or loose ice that might freeze to it. A redesign of the small tank, with at least one interior wall that could be moved back from the ice, would greatly reduce the labour and uncertainty of ice sample production. Some weeks all four attempts to remove the ice sample without breaking it were unsuccessful.

CHAPTER 4

LABORATORY TESTS WITH FRESHWATER ICE

1) Results

A schematic representation of the Double Torsion geometry is given in Fig. 4.1. Fig. 4.2 shows a schematic of the test set-up, and Fig. 4.3 is a sample load and deflection record.

Thirty-eight samples were successfully prepared and tested, the results for thirty-six are presented in Table 4.1. Two other samples were prepared and tested with deadweight loading, but these produced no results as they were not loaded to breaking. These were done to determine very low crack growth rates at a constant subcritical applied stress intensity factor. One was loaded at 25 $kNm^{-3/2}$, which is the lowest fracture toughness of ice reported in the literature, and a second sample was loaded at 40 $kNm^{-3/2}$. In both cases the load was left on for five days with less tham 1 mm of crack growth resulting. This placed an upper bound on any sub-critical crack growth that may have taken place at approximately 1×10^{-9} m/s.

There was no sub-critical crack growth observed in the freshwater ice tested; in every instance the crack grew in what is referred to as the slip/stick manner by Mai and Atkins (1980). A threshold had to be surpassed before crack growth took place, and the growth was abrupt. In some cases the crack arrested in the sample and it was possible

to determine the arrest stress intensity factor as well as the critical stress intensity factor from the load record. With a tape measure on the surface of the ice the resulting crack jump length was measured to the nearest centimeter. Fifty-nine fracture toughness values were obtained, and twenty-six values for the arrest stress intensity factor. The results are presented in Table 4.1, and include time to first crack growth. This was used to calculate the load rate, determined simply by dividing K_{Ic} at first crack growth by this time of loading. This was not done for subsequent initiation events that followed an arrest. The exact stress history for the material the crack has arrested in is unknown, and neither the time to failure or stress rate prior to initiation is meaningful.

All tests were done at nominally constant crosshead rate, with resulting loading rates from 0.7 to 85 $kNm^{-3/2}s^{-1}$. Fig 4.4 shows the fracture toughness, and Fig 4.5 the arrest stress intensity factors.

Photo 4.1 shows a thin section of the columnar grains seen through crossed polarized lenses, Photo 4.2 shows the top layer grain size, and Photo 4.3 shows the grain size on the bottom layer.

The results of 61 toughness measurements were;

$$K_{Ic} = 123 \pm 37 \ kNm^{-3/2}; \qquad (4.1)$$

and for 25 arrest stress intensity factor measurements;

$$K_{Ia} = 89 \pm 14 \ kNm^{-3/2}, \qquad (4.2)$$

with the histograms of the results in Fig. 4.1, 4.2.

For the thirty-six first crack events;

$$K_{Ic} = 112 \pm 0.32t;\ r^2 = .45, \text{ or} \qquad (4.3)$$

$$K_{Ic} = 130\ \dot{K}^{-0.065},\quad r^2 = .04,\quad 0.7 < \dot{K} < 85\ kNm^{-3/2}s^{-1}$$

Compare with;

$$K_{Ic} = 188\ \dot{K}^{-0.13},\quad 6.0 < \dot{K} < 100\ kNm^{-3/2}s^{-1}$$

Timco and Frederking (1986), with no correlation coefficient given; and;

$K_{Ic} = 216\ \dot{K}^{-0.11}$, $0.1 < \dot{K} < 10^5 kNm^{-3/2}s^{-1}$ Urabe and Yoshitake (1981b), (also with no correlation coefficient), for similar ice.

Timco and Frederking (1986) found;

$K_{Ic} = 97\ t^{0.16}$; compared to;

$K_{Ic} = 82\ t^{0.11}$; $r^2 = .14$, $1.8 < t < 254$ s, for this data. The linear fit presented here, Eq 4.3, is better than the exponential fit, with $r^2 = .45$, compared to .14 for the exponential fit used by previous authors.

A least squares fit to the dependence of the distance the crack grew in each event on the decrease in the stress intensity factor gives for the twenty-six points obtained from the freshwater ice;

$$\text{jump length (cm)} = 4.1\text{cm} + .85\ \Delta K_I\ ;\ r^2 = .47, \qquad (4.4)$$

where ΔK is in $kNm^{-3/2}$. Forty-seven percent of the variation in crack jump length is due to the change in applied stress intensity factor during the growth.

There was no significant correlation, less than five percent, of crack jump length with time to event.

2) Discussion

No sub critical crack growth was observed in the fine grained freshwater columnar grained ice, either under deadweight loading of five days duration, or in the load range .7 to 85 $kNm^{-3/2}s^{-1}$. Loading rates were not extended in the lower direction, except for the five day duration tests, as it was clear that arrest was more unlikely after long time to crack initiation.

Though the difference in the magnitude between the average critical and arrest stress intensity factors is not great, in every instance once a crack had arrested, the load had to be increased to cause further crack growth.

Because of the sensitivity of the fracture toughness algorithm to thickness, small increases in thickness might be suspected for the instability that precedes each crack growth event, or for arresting the crack growth. While it is true that a crack being forced into a slightly thicker region would grow unstably once it began, it seems unlikely that this could have been the case for every crack growth event observed. The influence of small thickness irregularities on arrest however, cannot be ruled out.

Because of the long time to failures in these tests the question arises as to whether LEFM is still valid at crack initiation. The two criteria that must be satisfied are that 1) the crack tip be sharp, and 2) the plastic and creep zones are small compared to relevant test specimen

dimensions.

Though this was discussed in detail in Chapter 2 it must be pointed out that, on purely theoretical grounds, some uncertainty remains, especially with respect to the small scale yielding (ssy) criterion. The sharp crack tip condition would seem to be adequately fulfilled based on the experimental results of Cole (1986), who found that cracks do not change their dimensions appreciably through healing or closure for a day, if open to the air as they are in this experiment. In the light of this and the theoretical arguments in Chapter 2 the time from crack tip creation to initiation will not compromise the sharpness of the crack.

The small scale yielding conditions given in Eq 2.21 and 2.22 require the yield strength of ice to make a calculation. There have as yet been no claims made in the literature as to what the fracture-free strength of ice is. All tests conducted at a stress greater than .75 MPa are accompanied by cracking. This indicates that the yield strength is still greater than the fracture strength, even in the high strength tests under tri-axial constraint of Jones (1982), where 24 MPa was reported under confining pressure of 35 MPa.

This is not surprising given the low fracture energy of ice. Nothing can be said with certainty about the application of the algorithms of Eq 2.21 and 2.22 to ice to determine relevant minimum fracture specimen size. Any

decision about whether or not ssy criterion is met will have to be based on other considerations, such as a comparison of the toughness obtained from these tests with other high rate, large specimen tests that appear to have fulfilled the ssy criterion.

Other authors have used the algorithm of Riedel and Rice (1980) given in Eq 2.24 to calculate a time dependent size of the creep zone. Instead of attempting to exactly evaluate Eq 2.24, as it is nonlinear and would require a numerical computation, it is instructive to look for evidence that indicates the creep zone size has grown to unacceptable size. In particular, the fracture toughness values obtained would be untypically high. The fracture criteria one should then use is the J or C^* integral.

As mentioned in Chapter 2 a single comparison of toughness obtained from J and K_{Ic} calculations was found to be identical, Urabe and Yoshitake (1981b), down to a rate of 0.5 $kNm^{-3/2}s^{-1}$. The value obtained was 250 $kNm^{-3/2}$, implying a loading time of 500 seconds. This indicates that for their sample geometry the size of the creep zone was not of significant size as to invalidate LEFM and require use of the J or C^* integrals. Their specimen size is large, 20 x 40 x 160 cm, with 8 cm prepared crack length. The smallest relevant dimensions are thus 40 - 8 = 32 cm as the ligament length and 20 as the sample thickness.

The algorithm of Riedel and Rice (1980) assume a step

function application of the loading, and in this case predicts a maximum value for the creep radius of 6 cm at the end of 500 seconds of loading when initiation occurs. This is most certainly greater than 1/50th either of the relevant specimen sizes, the maximum size empirically chosen as that permissible for LEFM to hold.

There are a number of possible interpretations of this. The first is that an exact numerical calculation of Eq 2.24 is required, as the approximation that the load is applied as a step function appears to be too conservative. This would conceivably reduce the calculated creep radius to less than 1/50 th of 20 cm.

Nixon and Schulson (1986a) showed that the algorithm is not very sensitive to n, so a choice of n = 5 for the high stress region is not critical.

It may be that the size of the creep radius, even if accurately given by Eq 2.24 is not so relevant, because what it implies is that one then must use the C^* integral to obtain a fracture criterion. The C^* must be evaluated while the crack is extending in a slow stable manner, and this is something that ice has not been observed to do. Without a value for C^* it is not possible to calculate the transition time from Eq 2.25.

The agreement of the J and K_{Ic} obtained by Urabe and Yoshitake (1981b) indicates that LEFM is fulfilled, yet the application of Eq 2.24 indicates that it is violated.

Application of Eq 2.24 to the Double Torsion geometry gives a minimum load rate of 37 $kNm^{-3/2}s^{-1}$ to ensure that the creep zone size does not exceed .04/50 m, where .04 m is the sample thickness, for toughness of 100 $kNm^{-3/2}$. Eq 2.24 predicts that any test that last longer than approximately 3 seconds will violate LEFM.

The load-displacement curves of a number of tests are shown in Fig 4.6 to 4.14. They do indeed look highly non-linear, as ice will creep at any applied load. Also there are a number of load drops in the curves that would indicate that crack extension had occurred, when none was observed. It is not at all clear what these load drops are associated with, but Dempsey (1988) observed similar behaviour and postulated it may be due to grain boundary sliding. In the cases of crack extension, however, it is possible to estimate J from the energy invested into the ice during crack extension and the approximate area of crack created. As the crack area so created is quarter elliptical only an approximate estimate may be made. The correspondence between K as calculated from the LEFM algorithm, and as calculated from J is good.

Also comparison with results of Parsons and Snellen (1985) obtained from compact tension samples of minimum dimensions 50 x 50 x 50 cm failed in less than 5 seconds indicate that Eq 2.24 may not be relevant to a material that does not exhibit creep crack growth.

It can only be concluded that although the creep zone size may be large this is not relevant as the crack does not grow due to creep effects. As for the plastic zone radius, for which the calculation of which is need the ice yield strength, it appears that in no instance is the ice yielding significantly before fracturing, thus driving up the apparent fracture toughness.

The non-zero strain fields perpendicular to the surface of the Double Torsion sample found in the finite element formulations of Trantina (1977) would tend to reduce the sample thickness. If this effect was significant the crack would be growing into a region of greater thickness, and this would tend to stabilize the crack growth. No stable crack growth was observed and there is no indication that the plane strain criteria was violated.

A detailed discussion as to whether the observed instability in each crack growth initiation was due to the prepared crack tip blunting prior to crack growth will be deferred to Chap. 6, where the fundamental reason for the slip/stick type of crack growth will be discussed.

At zero time to failure the critical stress intensity factor is 112 $kNm^{-3/2}$, slightly lower than the average stress intensity factor. In Chap. 6 it will be proposed that the arrest stress intensity factor is the creep free fracture toughness.

In previous sample geometries used on ice, only one

value of the fracture toughness was obtained from each sample. In the Double Torsion geometry a number of results were obtained over a short distance in the ice. For example, Sample 2 shows that in 20 cm the fracture toughness varied from 91 down to 75 and back up to 97 $kNm^{-3/2}$. The results in Table 4.1 show significant variation of the fracture toughness over short distances.

Though there was no statistically significant correlation between resulting crack length and time to event, the results in Table 4.1 show that any crack initiated in the freshwater ice after 72 seconds of increasing load, $\dot{K}_I$ lower than 1.4 $kNm^{-3/2}s^{-1}$, did not have sufficient sample length to arrest in. Experience showed to obtain arrest, the cross-head rate and thus loading rate should be high. This served to both reduce instability in in the material, and the amount of strain energy stored in the test frame. From Eq. 3.32 it is clear the less the drop in load during crack growth, the lower the contribution of machine stored energy to crack length in absolute terms.

A number of samples broke to the side instead of down the centre of the specimen. Though great care was invested in creating flat parallel sided samples, the smallest eccentricity could cause the crack to grow to one side. Despite this, no samples were prepared with guiding grooves milled down the centre of the sample, for the reason given previously, that these long, wide, thin sheets of slippery

ice were fragile and heavy enough that a great number were broken in preparation, without the grooves.

TABLE 4.1

FINE GRAINED COLUMNAR FRESHWATER ICE RESULTS

#	W	d	a	P_i	K_{Ic}	Time	$\dot{K}_{Ic}$	P_a	K_{Ia}	l	E
	m	m	m	N	$kNm^{-3/2}$	s	$kNm^{-3/2}s^{-1}$	N	$kNm^{-3/2}$	m	GPa
1	.51	.0507	.224	560	137	30.5	4.5	490	120	.31	-
				696	170	50	11	-	-	.63+	-
2	51	.0573	.262	475	91	33	2.7	392	75	.08	-
				401	77	34	-	376	72	.07	-
				391	75	35	-	366	70	.05	-
				510	97	43	-	-	-	.29+	-
3	.518	.0567	.260	545	107	56	1.9	432	87	.51	-
				716	141	123	-	-	-	.58+	-
4	.515	.049	.250	971	255	144	1.8	-	-	.89+	-
5	.515	.055	.255	495	103	110	.94	-	-	.71+	-
6	.515	.0584	.215	975	180	180	1.0	-	-	.84+	-
7	.515	.0486	.245	534	153	25	6.1	-	-	.80+	-

#	W m	d m	a m	P_i N	K_{Ic} $kNm^{-3/2}$	Time s	$\dot{K}_{Ic}$ $kNm^{-3/2}s^{-1}$	P_a N	K_{Ia} $kNm^{-3/2}$	l m	E GPa
8	.515	.0450	.22	319	99	19.5	5.1	263	82	.29	-
				332	103	24	-	313	97	.02	-
				401	124	30	-	-	-	.59'	-
9	.515	.0520	.021	498	116	22	5.3	420	97.8	.12	-
				423	98.5	23	-	386	89.8	.08	-
				460	107	26	-	370	86.2	.17	-
				595	139	40	-	-	-	.31'	-
10	.515	.0547	.28	794	167	101	1.65	-	-	.82'	-
11	.515	.0561	.34	672	134	49	2.7	453	90.4	.32	-
				509	102	55	-	472	93.6	?	-
				490	97	58	-	434	86.0	.20	-
				471	93	64	-	-	-	.38'	-
12	.520	.0550	.266	831	173	123	1.4	-	-	.84'	-
13	.52	.0536	.255	493	112	62	1.8	349	79.3	.23	-
				568	129	99	-	-	-	.54'	-

#	W	d	a	P_i	K_{Ic}	Time	$\dot{K}_{Ic}$	P_a	K_{Ia}	l	E
	m	m	m	N	$kNm^{-3/2}$	s	$kNm^{-3/2}s^{-1}$	N	$kNm^{-3/2}m$		GPa
14	.520	.0527	.409	797	181	254	.71	-	-	.35+	-
15	.520	.0495	.280	413	106	70	1.5	322	83	.21	-
				588	151	121	-	-	-	.59+	-
16	.520	.0472	.278	375	106	56	1.9	337	95	.08	-
				350	98.6	60	-	322	90.6	.05	-
				329	92.4	62	-	322	90.6	.02	-
				343	96.5	72	-	340	95.6	.03	-
				481	136	110	-	-	-	.53+	-
17	.520	.0582	.335	438	80.5	57	1.4	384	71	.10	-
				719	133	102	-	-	-	.69+	-
18	.520	.0485	.249	619	166	232	0.7	-	-	.45+	0.60
19	.510	.0460	.247	500	149	68	2.2	-	-	.86+	1.97
20	.510	.0560	.221	625	126	5.6	22.5	-	-	.65+	6.86
21	.510	.0583	.327	488	90	15.2	5.9	-	-	.47+	1.7

#	W	d	a	P_i	K_{Ic}	Time	$\dot{K}_{Ic}$	P_a	K_{Ia}	l	E
	m	m	m	N	$kNm^{-3/2}$	s	$kNm^{-3/2}s^{-1}$	N	$kNm^{-3/2}m$		GPa
23	.520	.0560	.291	344	69	1.8	38.3	-	-	.45'	-
24	.520	.0525	.255	519	115	29.7	3.9	-	-	.42'	11.6
25	.515	.0553	.255	525	132	15.6	8.5	-	-	.65'	-
27	.515	.537	.208	1018	222	28.4	7.8	-	-	.82'	2.86
28	.510	.0515	.32	413	98	12	8.2	375	89	.34	7.52
				406	96.5	18	-	-	-	.60'	-
29	.515	.0525	.32	638	146	21	6.9	-	-	.84'	4.35
30	.515	.0481	.291	812	221	4.25	52.0	-	-	.53'	-
31	.520	.0574	.295	356	68	0.8	85	-	-	.56'	-
32	.510	.0566	.280	537	106	75	6.8	-	-	.48'	-
33	.510	.0522	.255	500	116	44	2.1	-	-	.60'	4.3

#	W	d	a	P_i	K_{Ic}	Time	$\dot{K}_{Ic}$	P_a	K_{Ia}	l	E
	m	m	m	N	$kNm^{-3/2}$	s	$kNm^{-3/2}s^{-1}$	N	$kNm^{-3/2}m$		GPa
34	.510	.0539	.296	388	84	52	1.6	312	67.8	.23	4.0
				456	98.6	52	-	-	-	.40+	-
35	.505	.0518	.266	512	120	15	8.1	356	83.6	.42	3.3
				450	106	20	-	-	-	.19+	-
36	.520	.0497	.239	419	107	5.8	18.4	397	101.2	.09	5.4
				531	136	9.0	-	-	-	.40+	-
37	.520	.0464	.255	431	126	29	4.3	406	119	.08	7.0
				437	128	30	-	-	-	.07	-
38	.520	.0396	.330	300	120	33	3.6	-	-	.80+	-

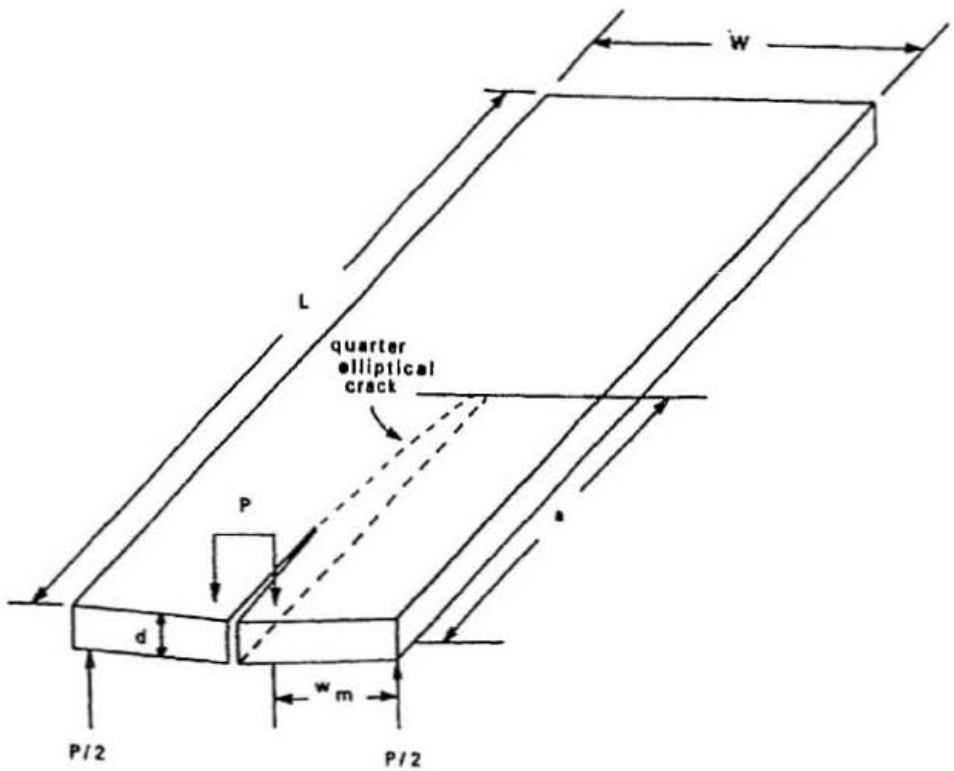

Fig 4.1 Schematic representation of the double torsion test configuration

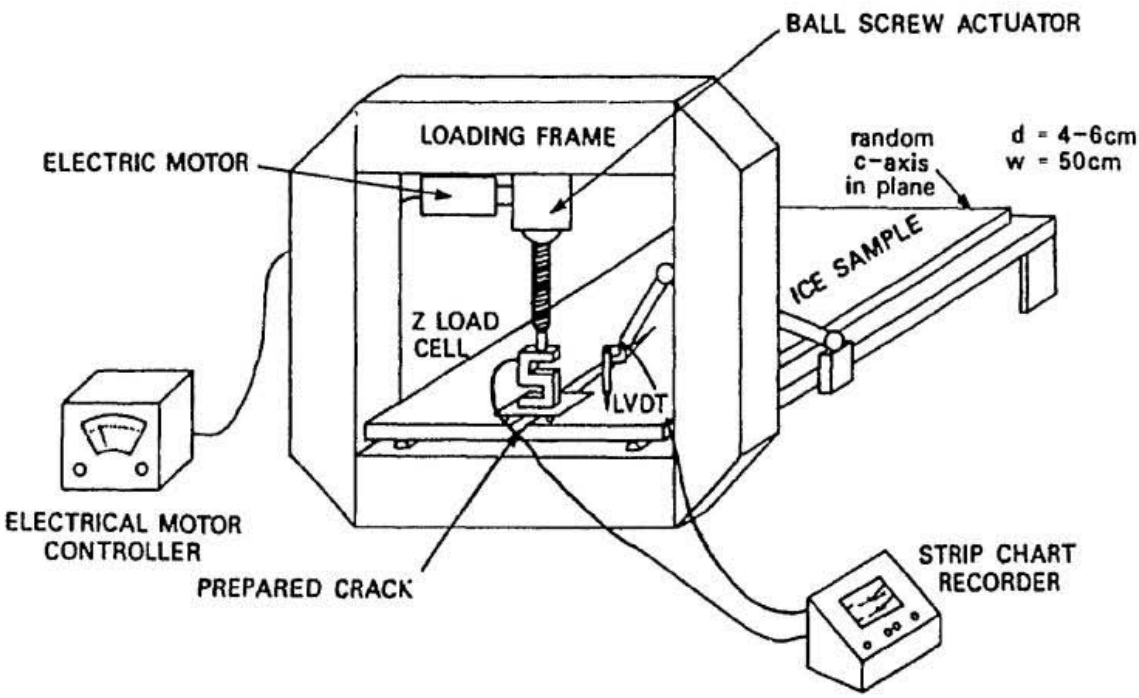

Fig 4.2 **Schematic of Test Apparatus for the Field**

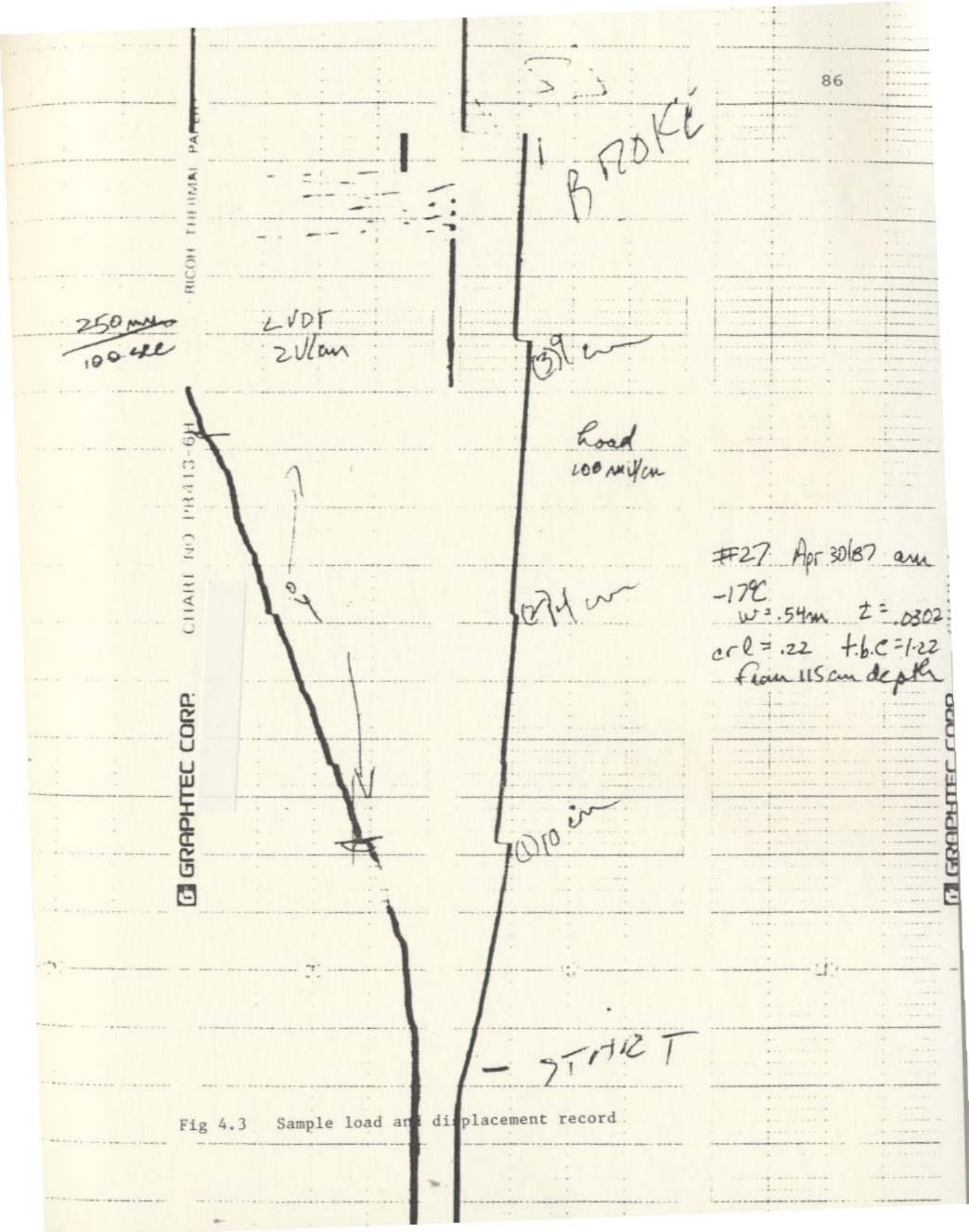

Fig 4.3 Sample load and displacement record

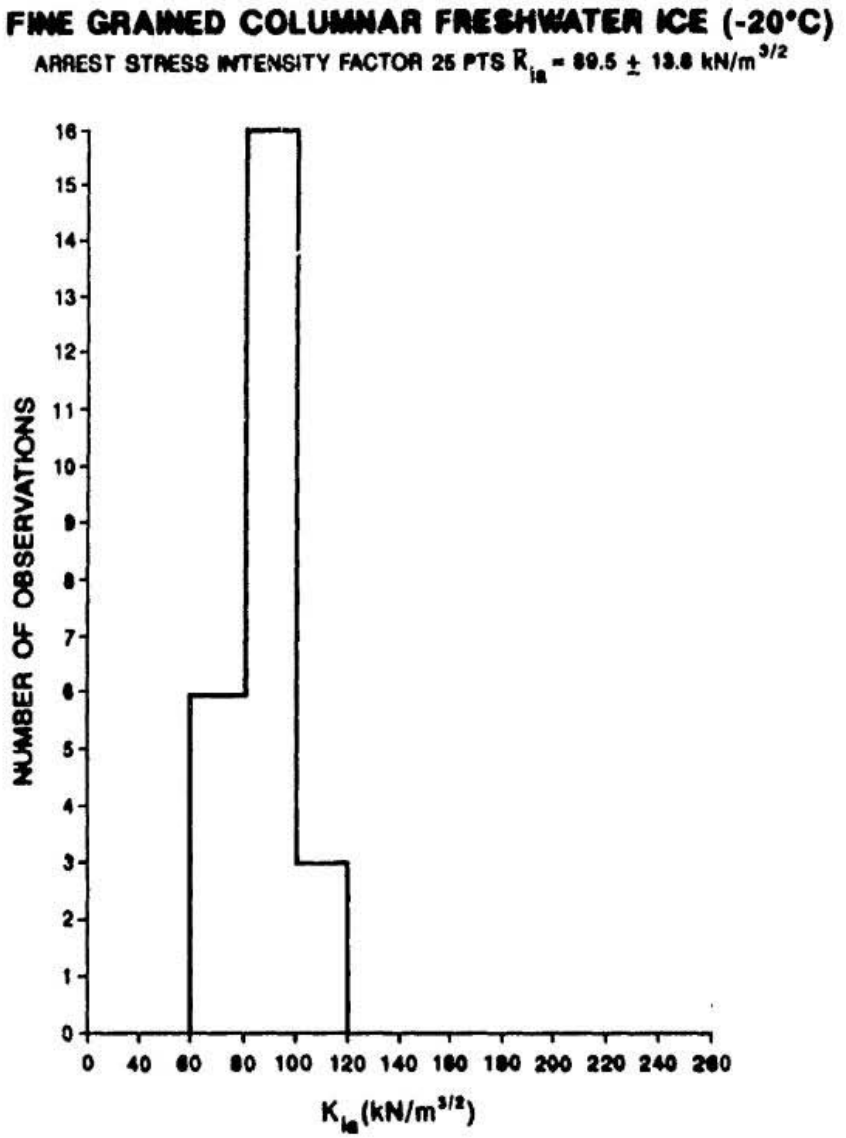
FINE GRAINED COLUMNAR FRESHWATER ICE (-20°C)
ARREST STRESS INTENSITY FACTOR 25 PTS $\bar{K}_{Ia}$ = 89.5 ± 13.8 kN/m$^{3/2}$
NUMBER OF OBSERVATIONS
0
1
2
3
4
5
6
7
8
9
10
11
12
13
14
15
16
0 40 60 80 100 120 140 160 180 200 220 240 260
K_{Ia}(kN/m$^{3/2}$)

Figure 4.4

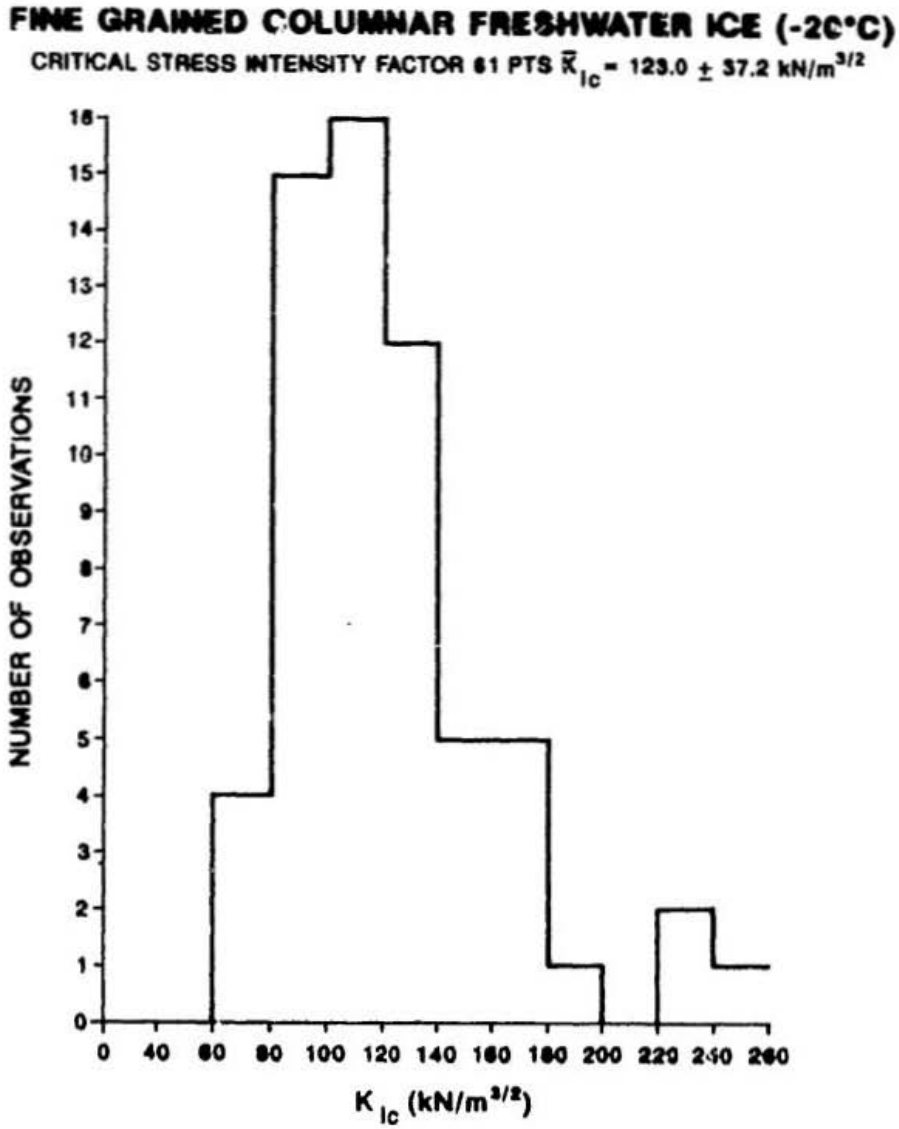
FINE GRAINED COLUMNAR FRESHWATER ICE (-20°C)
CRITICAL STRESS INTENSITY FACTOR 61 PTS $\bar{K}_{Ic}$ = 123.0 ± 37.2 kN/m$^{3/2}$
NUMBER OF OBSERVATIONS
0
1
2
3
4
5
6
7
8
9
10
11
12
13
14
15
16
0 40 60 80 100 120 140 160 180 200 220 240 260
K_{Ic} (kN/m$^{3/2}$)

Figure 4.5

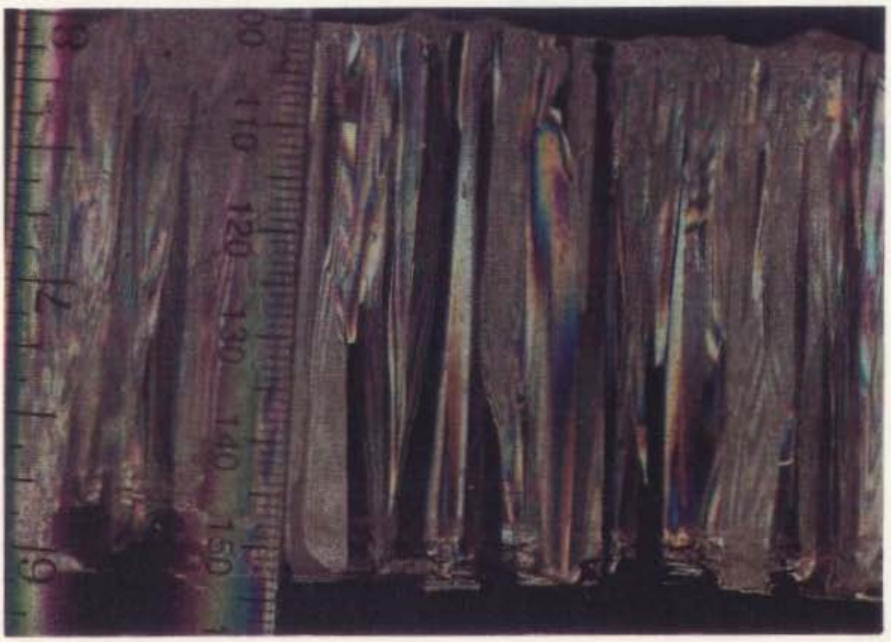


120
130
140
150
160
170

Fig. 4.6 Load Displacement Record, # 19, 68 seconds

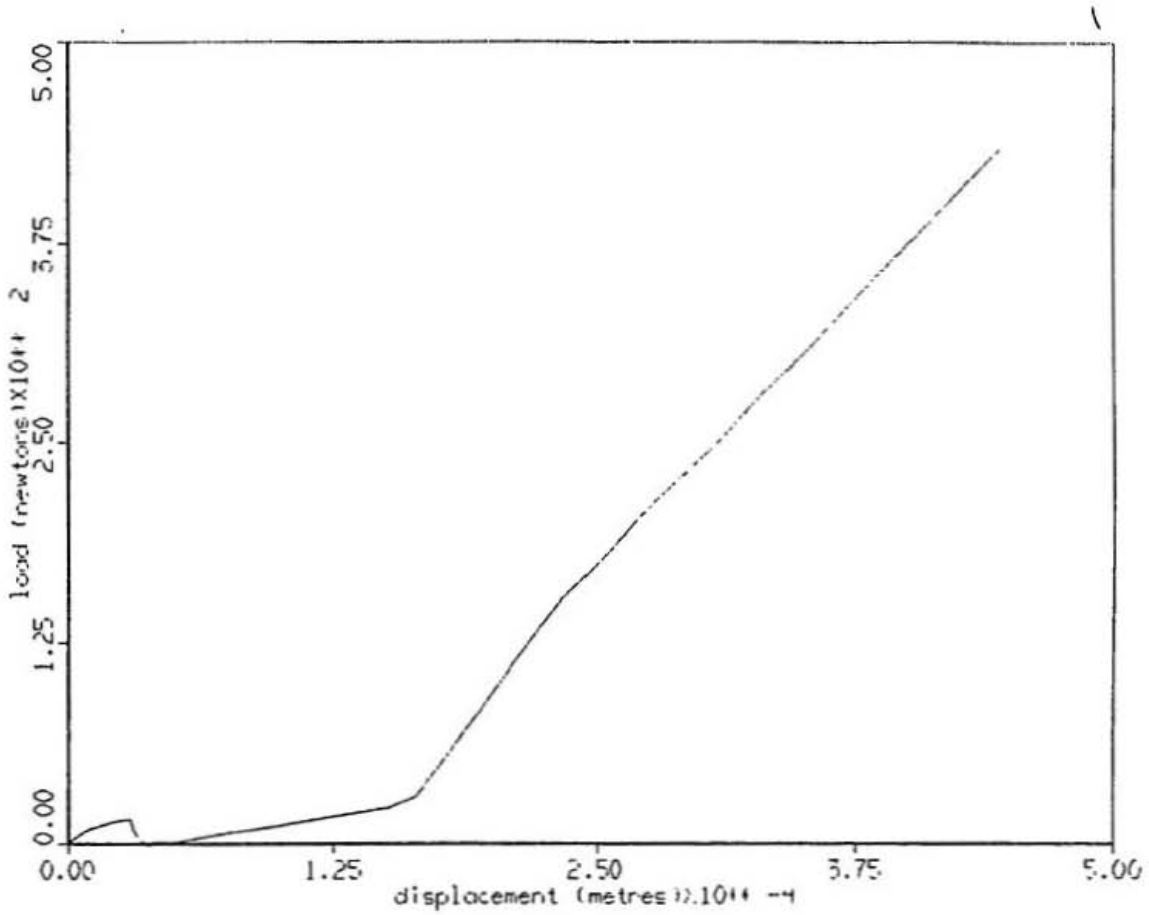

Fig. 4.7 Load Displacement Record, # 20, 5.6 seconds at peak

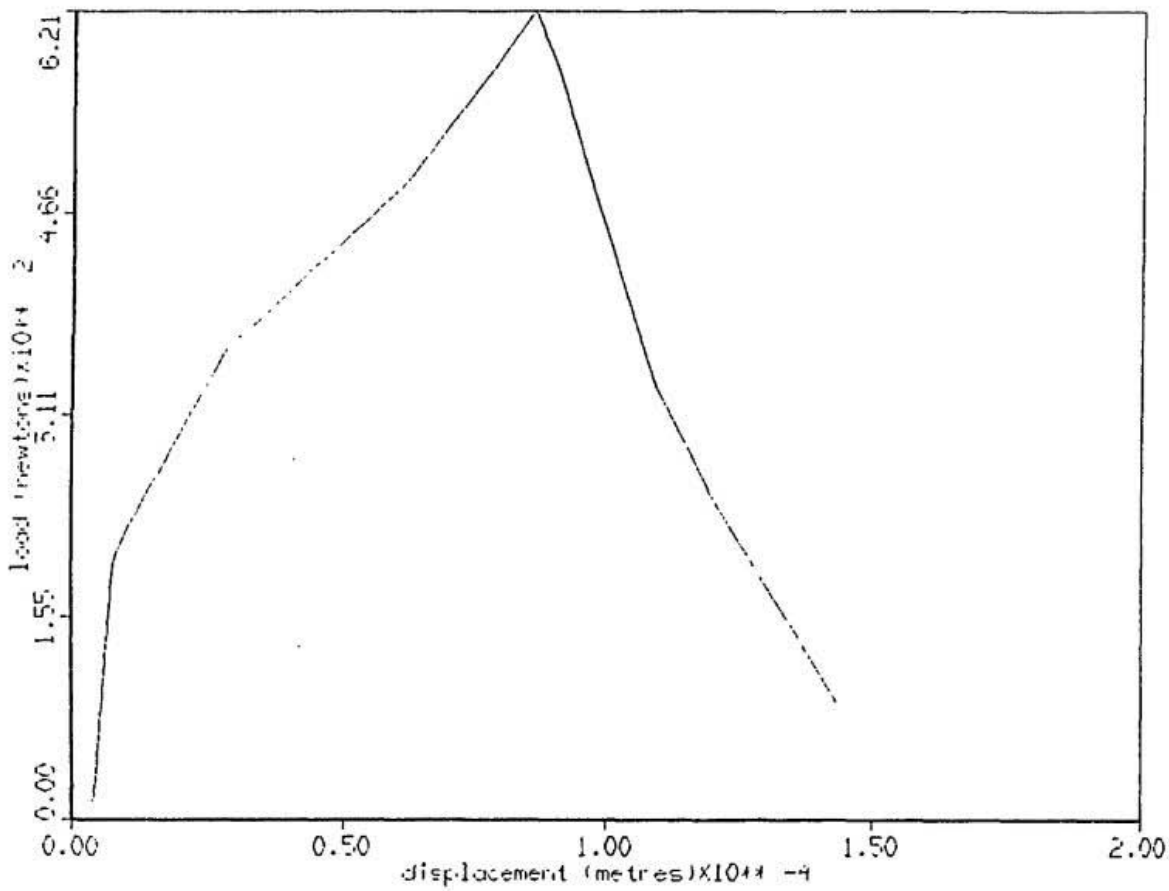

Fig. 4.8 Load Displacement Record, # 21, 15 seconds

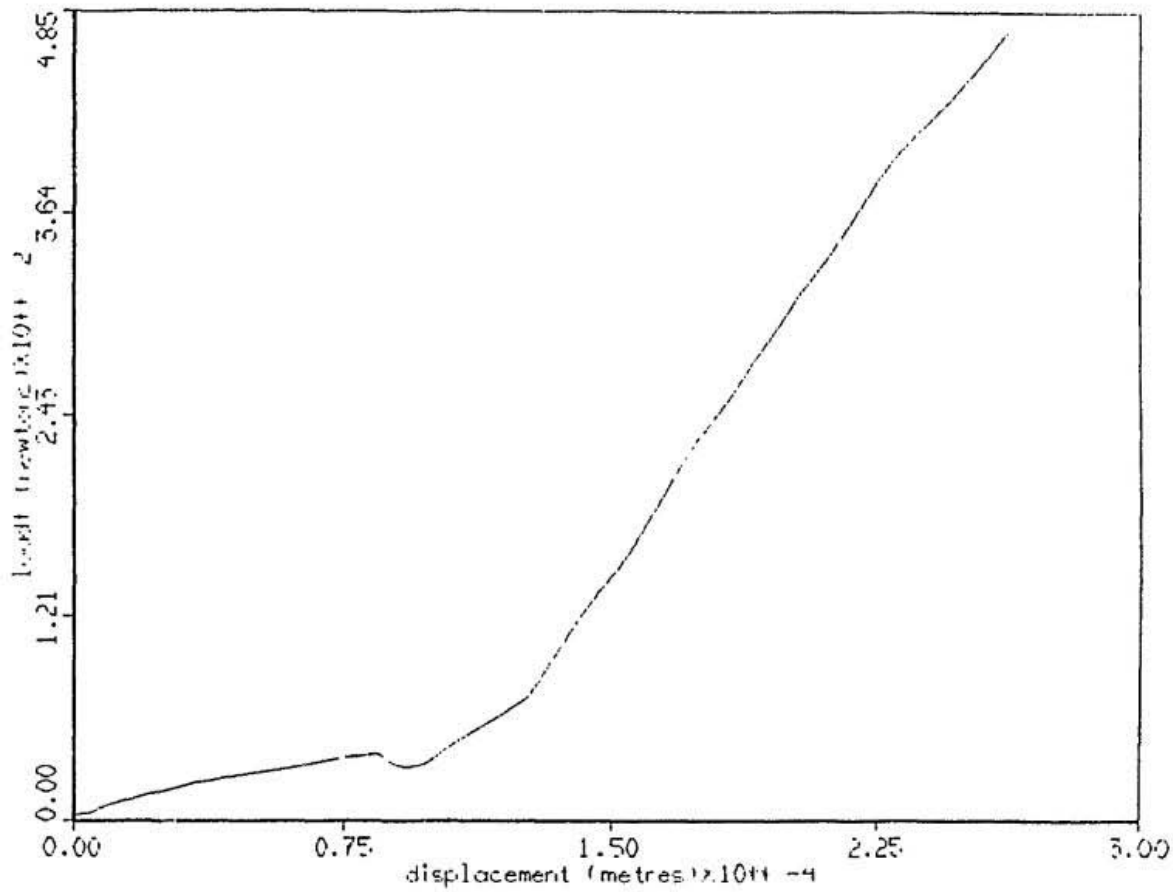

Fig. 4.9 Load Displacement Record, # 28, 18 seconds

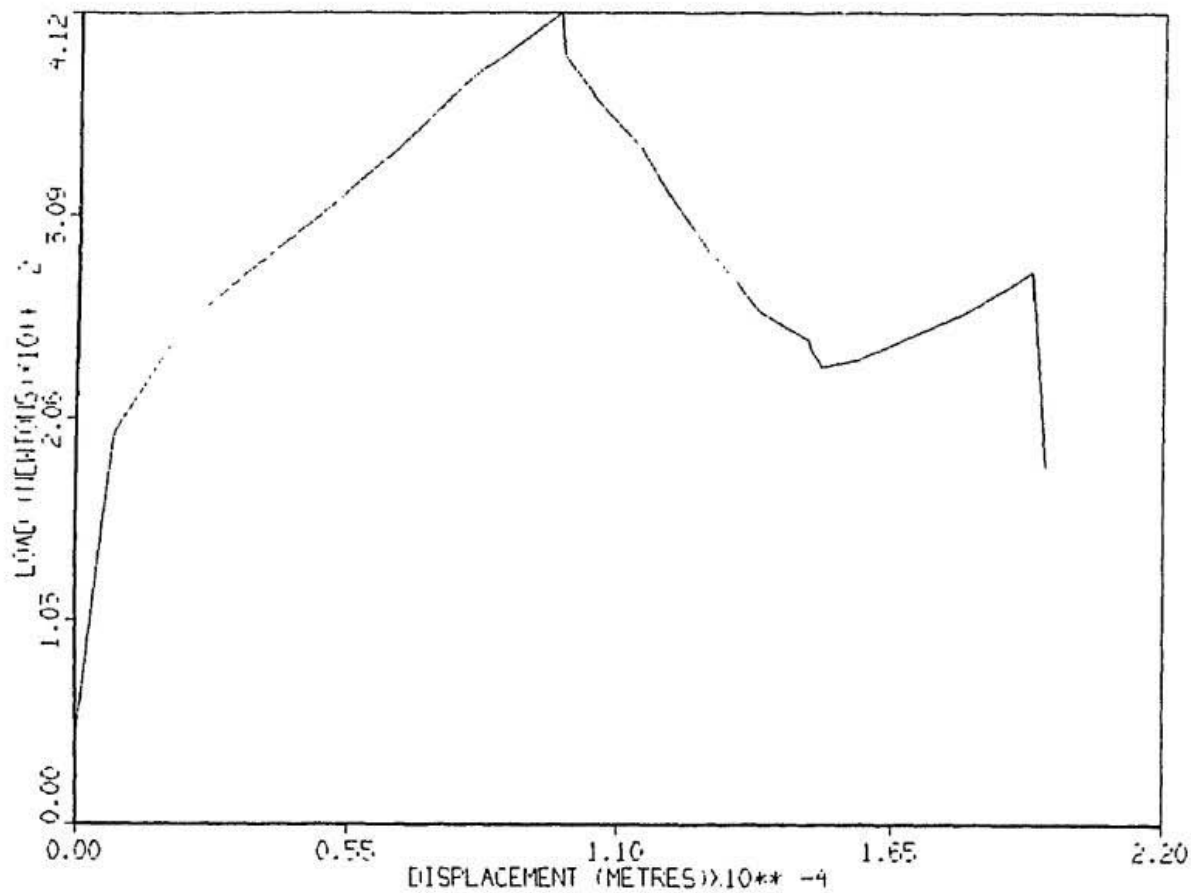

Fig. 4.10 Load Displacement Record, # 30, 4.25 seconds

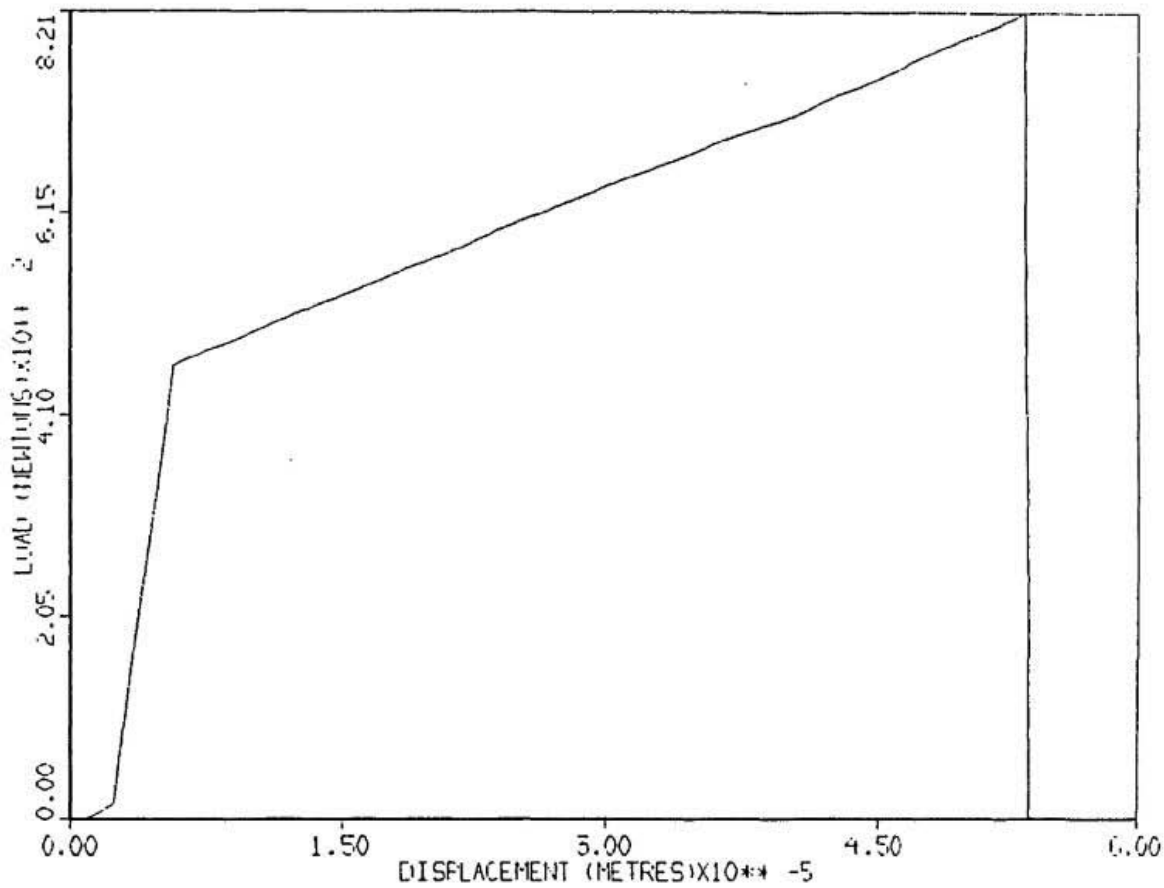

Fig. 4.11 Load Displacement Record, # 31, 0.8 seconds

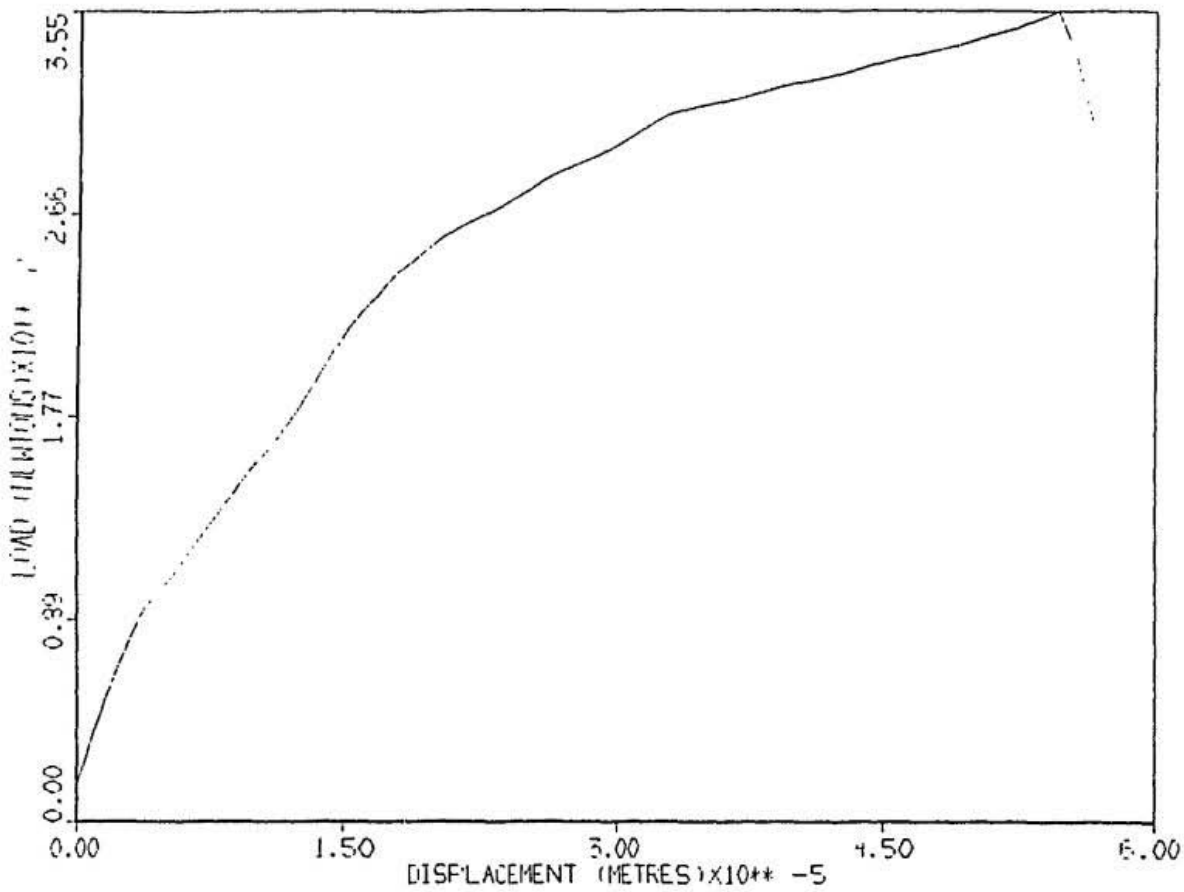

Fig. 4.12 Load Displacement Record, # 32, 75 seconds

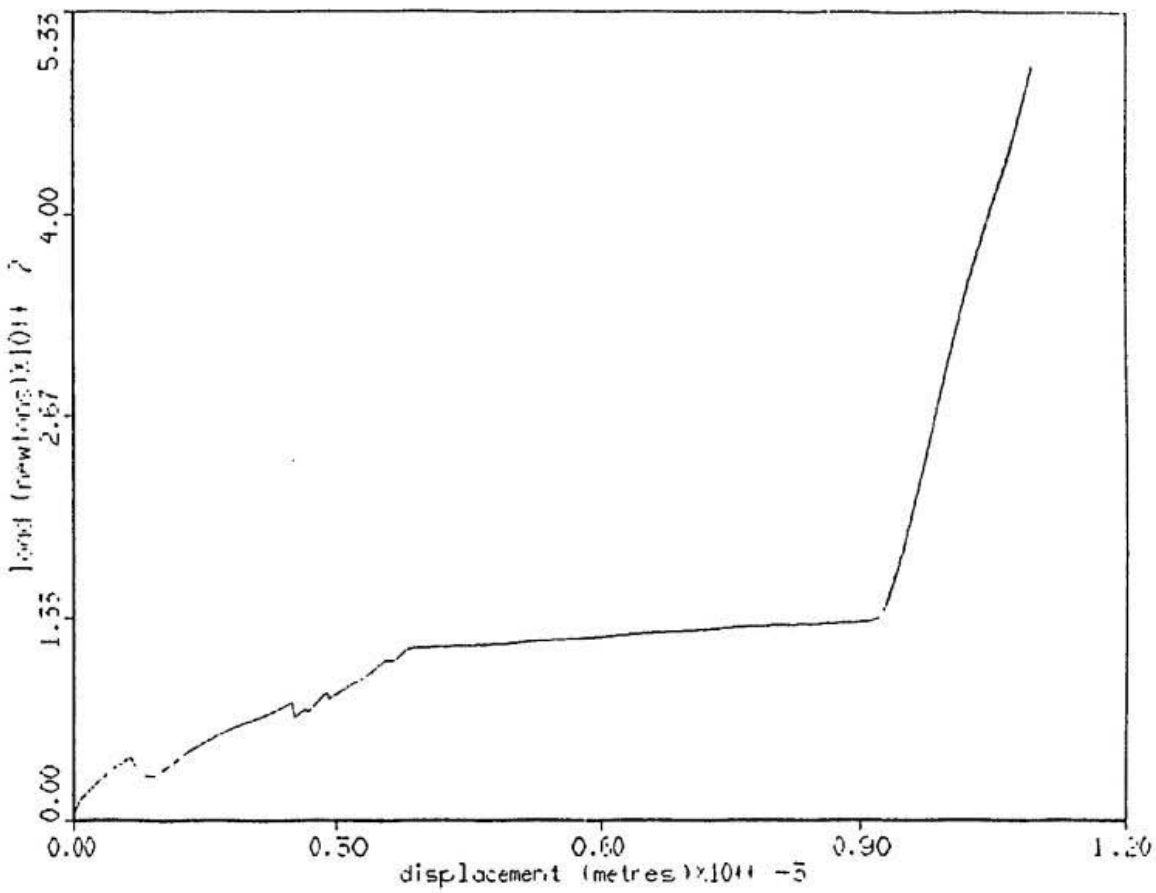

Fig. 4.13 Load Displacement Record, # 35, 20 seconds

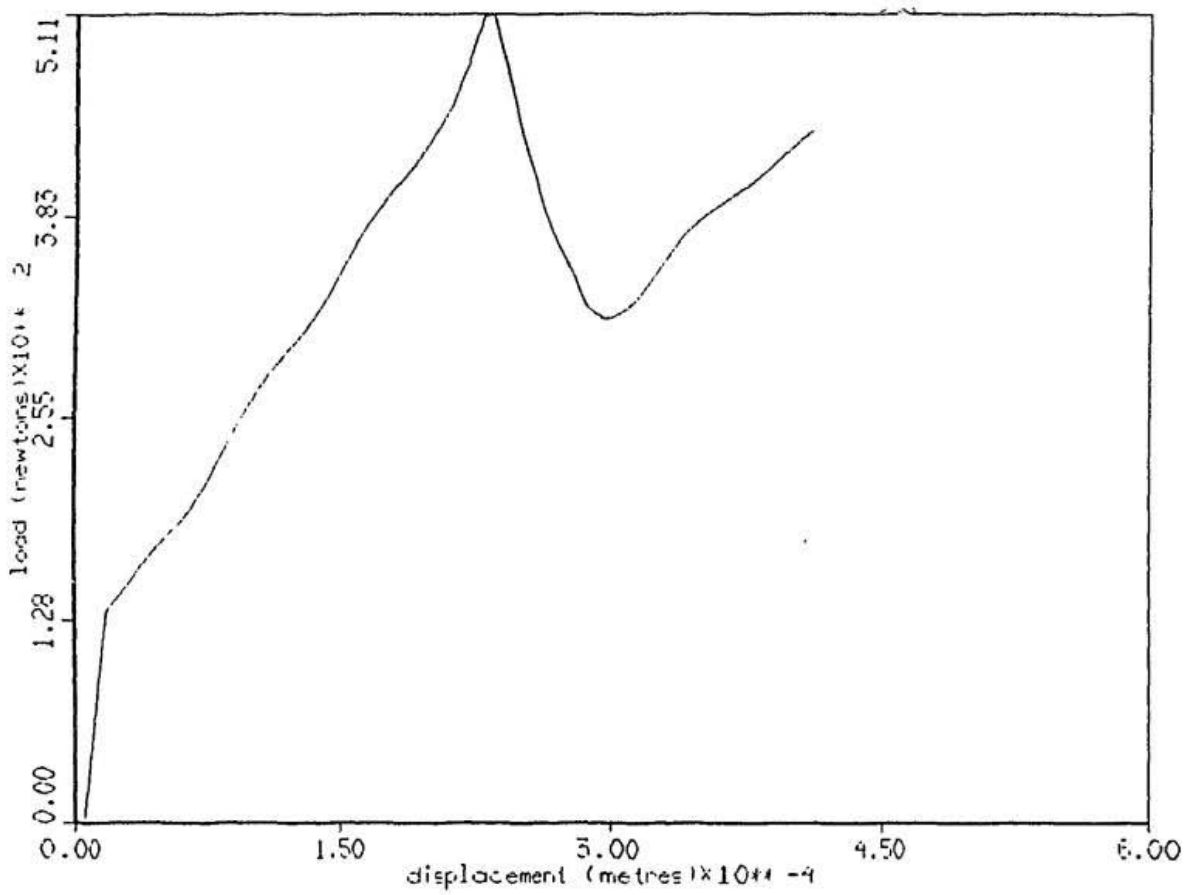

Fig. 4.14 Load Displacement Record, # 36, 9.0 seconds

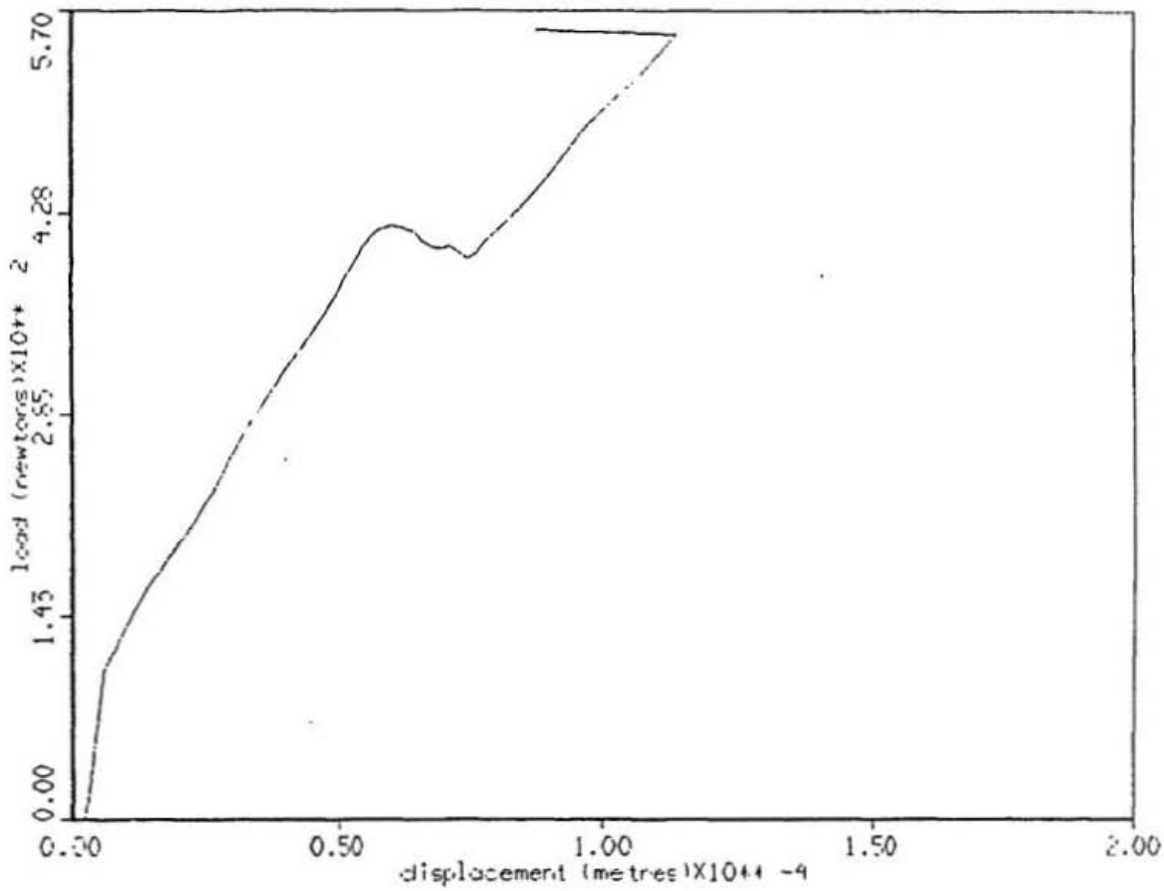

CHAPTER 5

FIELD TESTS WITH SEA ICE

1) Results

Thirty-one samples were successfully prepared from the first year sea ice found in Allan Bay NWT, (74° 43′ 45"N, 95° 04′W) near Resolute Bay. As in the laboratory tests, one was used for deadweight loading at 40 $kNm^{-3/2}$ and no subcritical, slow crack growth was observed. The larger more complicated microstructure was more likely to arrest a growing crack and thus more results were obtained, from fewer samples. Eighty measurements of the fracture toughness gave;

$$K_{Ic} = 112 \pm 37 \ kNm^{-3/2}.$$

Sixty one measurements of the arrest stress intensity factor gave;

$$K_{Ic} = 91 \pm 28 \ kNm^{-3/2}.$$

The histograms are presented in Fig 5.1, 5.2, and the data is in Table 5.1.

The time dependence of the first K_{Ic} obtained for each of the thirty samples was;

$$K_{Ic} = 89.4 + .025t; \ r^2 = .44, \text{ or}$$
$$K_{Ic} = 99.5 \dot{K}_{Ic}^{-0.095}; \ r^2 = .28, \ 0.06 < \dot{K}_{Ic} < 44$$

$kNm^{-3/2}s^{-1}$. Similarly;

$$K_{Ic} = 62.8t^{0.10}, \ r^2 = 40, \ 4 < t < 3420s.$$

Parsons et al (1986) report the toughness of sea ice from the same site two years earlier, for this crack orientation as 158 ± 26.5 $kNm^{-3/2}$, 26 < $\dot{K}_{Ic}$ < 85 $kNm^{-3/2}s^{-1}$, crack aligned perpendicular to preferred c-axis, 151.3 ± 59.7 $kNm^{-3/2}$, 2.4 < $\dot{K}_{I}$ < 69 $kNm^{-3/2}s^{-1}$, crack aligned parallel to preferred c-axis orientation, and 166.3 ± 67 $kNm^{-3/2}$, 23 < $\dot{K}_{Ic}$ < 125 $kNm^{-3/2}s^{-1}$, for crack 45° to the preferred c-axis orientation. The influence of any preferred c-axis orientation is not significant to a radial crack.

The values from the double torsion tests compare well with the lab ice, with the average toughness being slightly lower (though with the same standard deviation), as ice temperature was lower in the field tests.

The much longer loading times might be expected to create very large creep zones, or plane stress conditions, and thus larger apparent critical stress intensity factors. This has been discussed in Chapters 2, and 4 and will be reviewed again in Chapter 6, but comparison with results of Parsons et al (1985, 1986) indicate LEFM was not compromised.

The arrest stress intensity factor is approximately that of the lab grown ice, with twice the standard deviation. The toughness predicted at zero time to crack

growth is approximately the arrest stress intensity factor, with the same percent of the variability attributable to variation in time to event. This data covers 3420 seconds, compared to 72 seconds in the lab tests.

A least squares fit of the distance the crack grew in each event versus the drop in the stress intensity factor gives;

$$\text{jump length (cm)} = 8.35 + .43\ \Delta K\ ;\ r^2 = .25,$$

where ΔK is in $kNm^{-3/2}$.

A number of load deflection curves are presented in Fig 5.3 to Fig 5.18. These are for much longer loading times than the freshwater experiments and are noteworthy for a number of things. The load displacement records seen without visual observation of the prepared crack in the sample would indicate that there had been a great number of crack extension events. The load is relaxed and it would seem this could only be due to crack growth. There was however no crack growth observed.

Dempsey (1988) has suggested a possible explanation for this phenomena, which was also reported in his work. It may be that large grain boundary sliding events are responsible for the relaxation.

It is also possible that cracks are nucleated away from the prepared crack tip, and in some cases cracking was heard but no cracks could be seen anywhere. The most likely

site for such activity would be under the loading points. Comparison of the load displacement records with the data in Table 5.1 indicates where macroscopic crack growth of the prepared crack was observed and measured.

2) Sea Ice Properties

All samples were prepared from blocks of sea ice 0.75m wide, 1.3m long and 1.5m deep cut from the surface of the 2.1m thick ice and pushed into its side, Photo 5.1. From the bottom of this block sheets of ice ≅ 6 cm thick were sliced with a chain saw, Photo 5.2. These were then trimmed to a width of .55m and placed on a table designed to accept a router guide. A router then was used to prepare the sample to a uniform thickness, Photo 5.3. All samples had a similar orientation, the horizontal face parallel to the original ice surface.

The specimens had a salinity of approximately 3 ppt, typical of first year sea ice. Grain size was typically 5 to 10 cm, Photos 5.4 -7. Because of surface cracks in the 2.1 metre thick sea ice cover, all samples had to be prepared from ice taken from at least half a metre below the surface. At this depth the ice was at a higher temperature than the precipitation point of $-22.9^{\circ}C$ of $NaCl \cdot 2H_2O$. The plane below which this salt has not precipitated was clearly

visible, ice below it is quite clear, and above it cloudy, Photo 5.7. The top layer of cloudy ice was considerably cracked and it was impossible to make a sample from it, Photo 5.1. Some of these surface cracks extended deeper than half a metre and a few specimens were prepared that had large conspicuous cracks in them. During a test these cracks did not obviously interact with the growth of the prepared crack, Photo 5.8. The ice contained significant concentrations of brine drainage channels, each individual channel approximately 1mm in diameter, occurring in clusters approximately 10 cm in diameter, Photo 5.9. A sample prepared near the ice surface from the spring 1988 trip to the same area is shown in Photos 5.4 to 5.9, showing the large scale structure of the brine drainage system.

3) Discussion

As in the freshwater ice tested in the lab, no subcritical slow crack growth was observed. But unlike the lab grown ice, more than one crack extension event occurred in all specimens except one. Cracks that were loaded for as long as an hour, with monotonically increasing load, arrested in the sample after abrupt growth. This is to be contrasted with the fine grained freshwater ice, where any crack growth that occurred after 72 seconds of loading had insufficient sample length to arrest in.

The coarser, more complicated microstructure of the sea ice was more capable of arresting a growing crack than the fine grained freshwater columnar ice. Grain boundaries were not significant crack arrest structures, as most cracks appeared to arrest within a grain. It may be that unfavourably oriented grains that presented regions of greater toughness required some distance to exert their arresting influence. It was quite clear however, that brine channels were significant arrest sites, with crack growth arrested in clusters of such channels.

The temperature of the samples prepared and tested over a four week period on the sea ice in Allan Bay varied considerably. During April at this latitude the number of daylight hours changes rapidly, and daytime temperature increased from -35°C to -15°C during the course of the field trip. Future field tests might be best conducted in a portable cold room to provide constant test temperature.

The sensitivity of the Double Torsion measure of fracture toughness to small thickness variations has already been mentioned. The necessity for large samples, both to include significant number of grains, and to supply adequate sample length for arrest, impose logistical difficulty in ensuring thickness uniformity. With care and experience, however, a sample could be prepared with the router jig that

had a thickness which when measured at four points along an 80 cm crack path, had a standard deviation as low as .5mm. This implies an uncertainty of 1 $kNm^{-3/2}$in the toughness measurement; an acceptable level of precision.

Fig. 5.3 Load Displacement Record, # 3, 3744 seconds

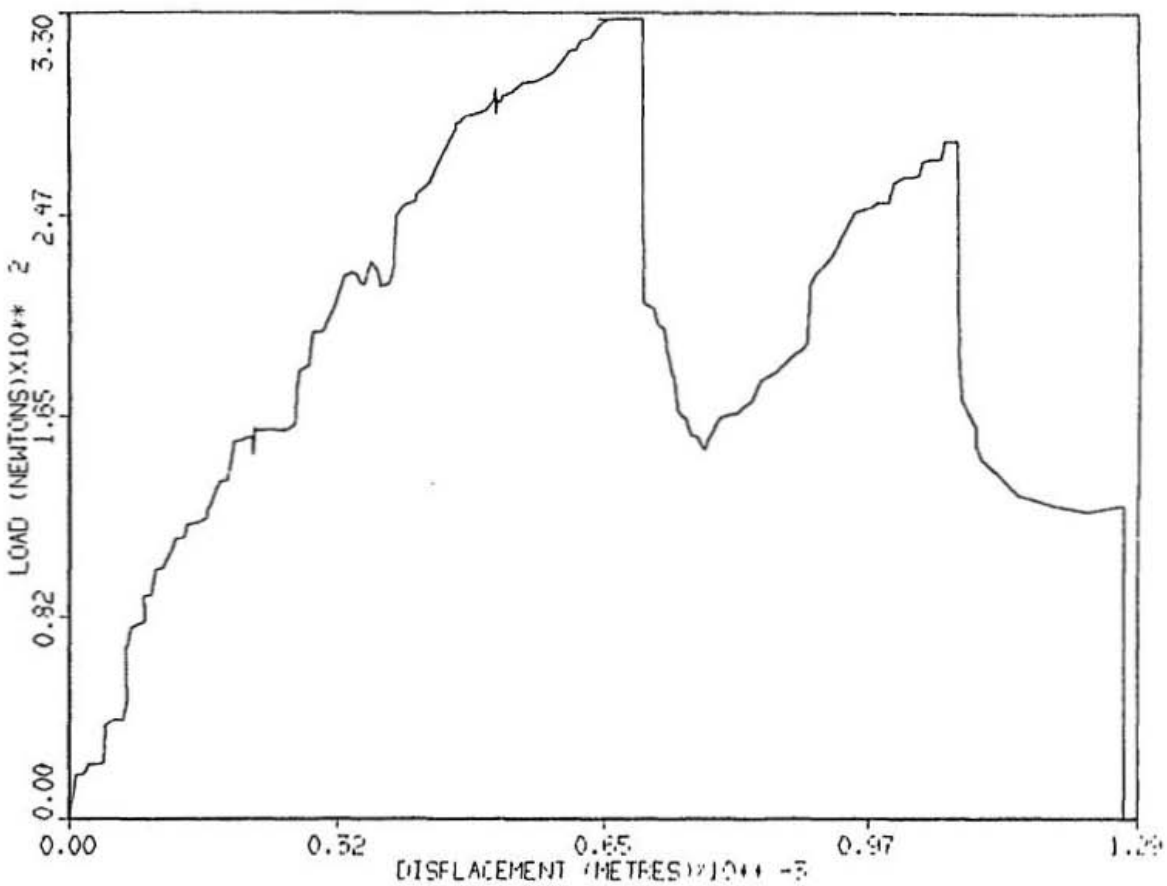

Fig. 5.4 Load Displacement Record, # 8, 2880 seconds

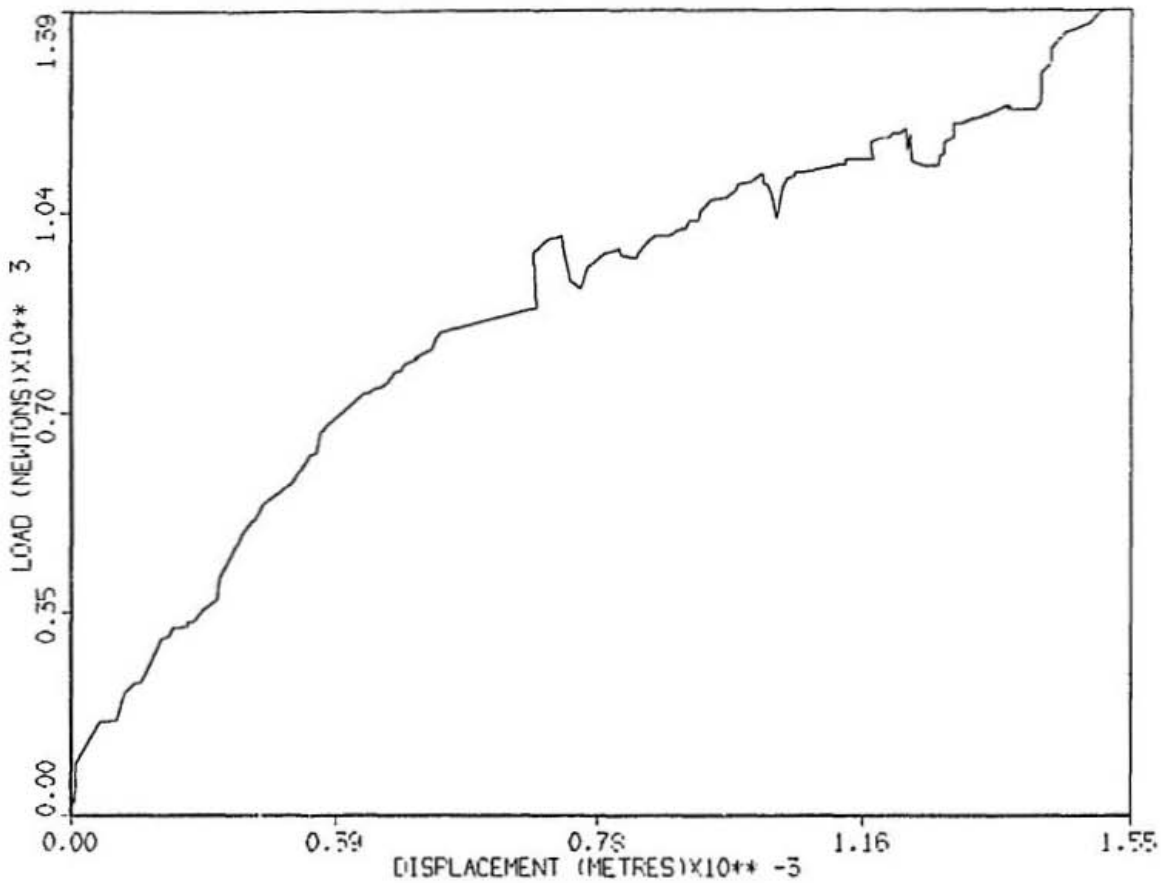

Fig. 5.5 Load Displacement Record, # 9, 2836 seconds

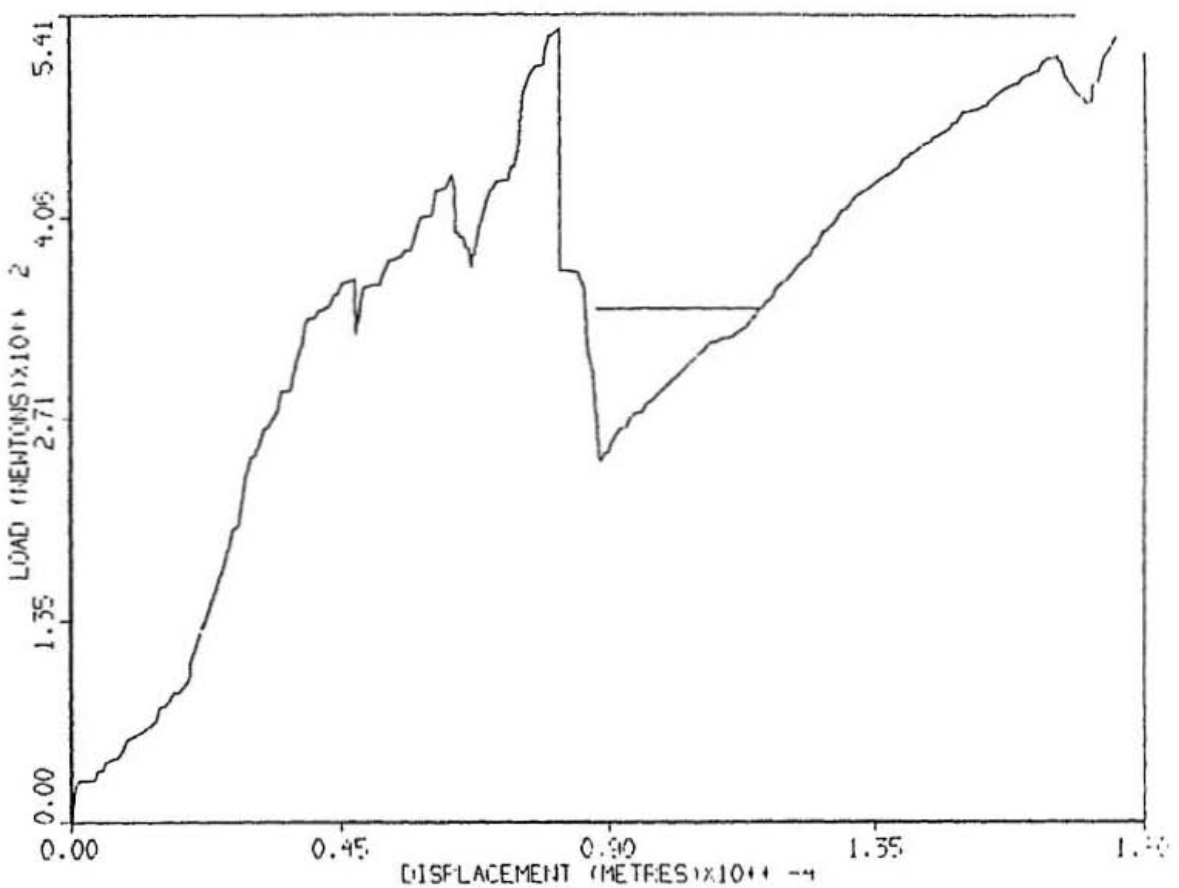

Fig. 5.6 Load Displacement Record, # 13, 800 seconds at peak, followed by load on broken sample.

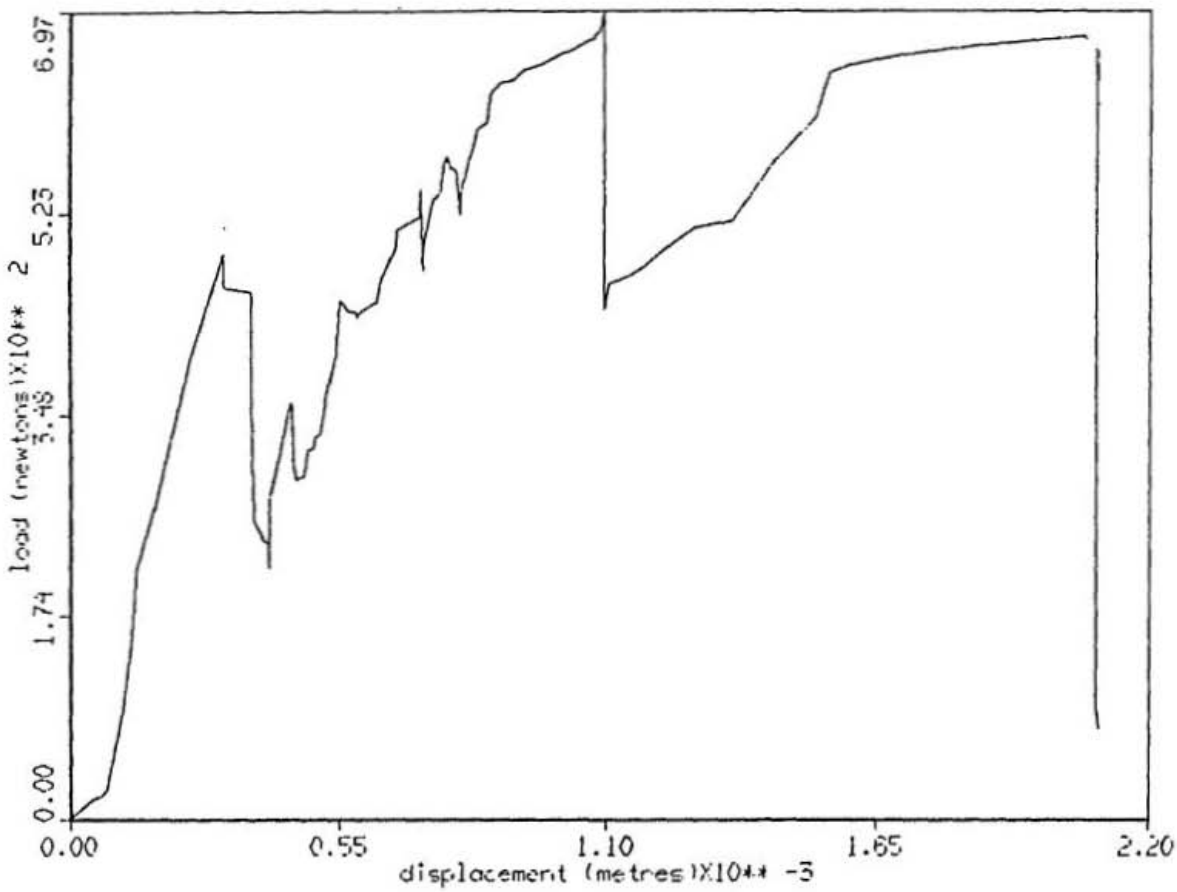

Fig. 5.7 Load Displacement Record, # 15, 548 seconds

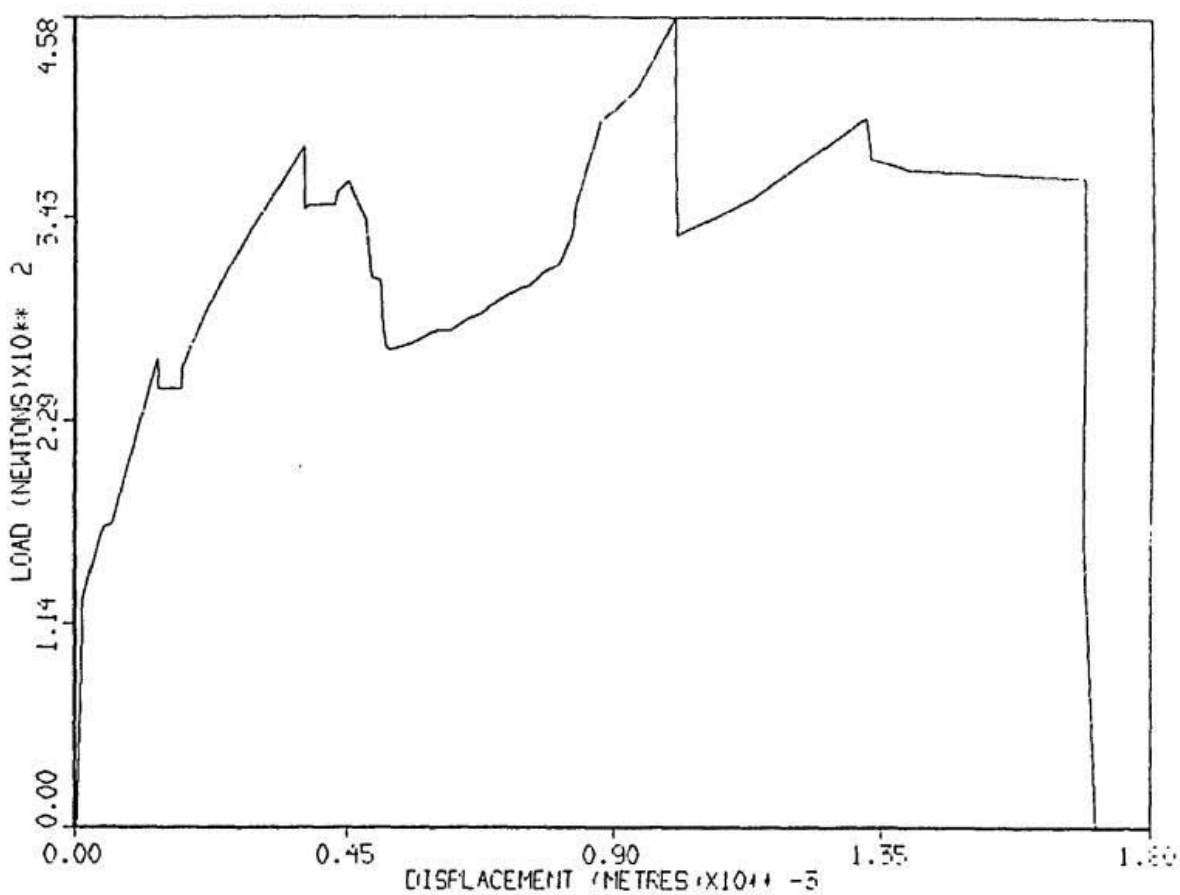

Fig. 5.8 Load Displacement Record, # 16, 478 seconds

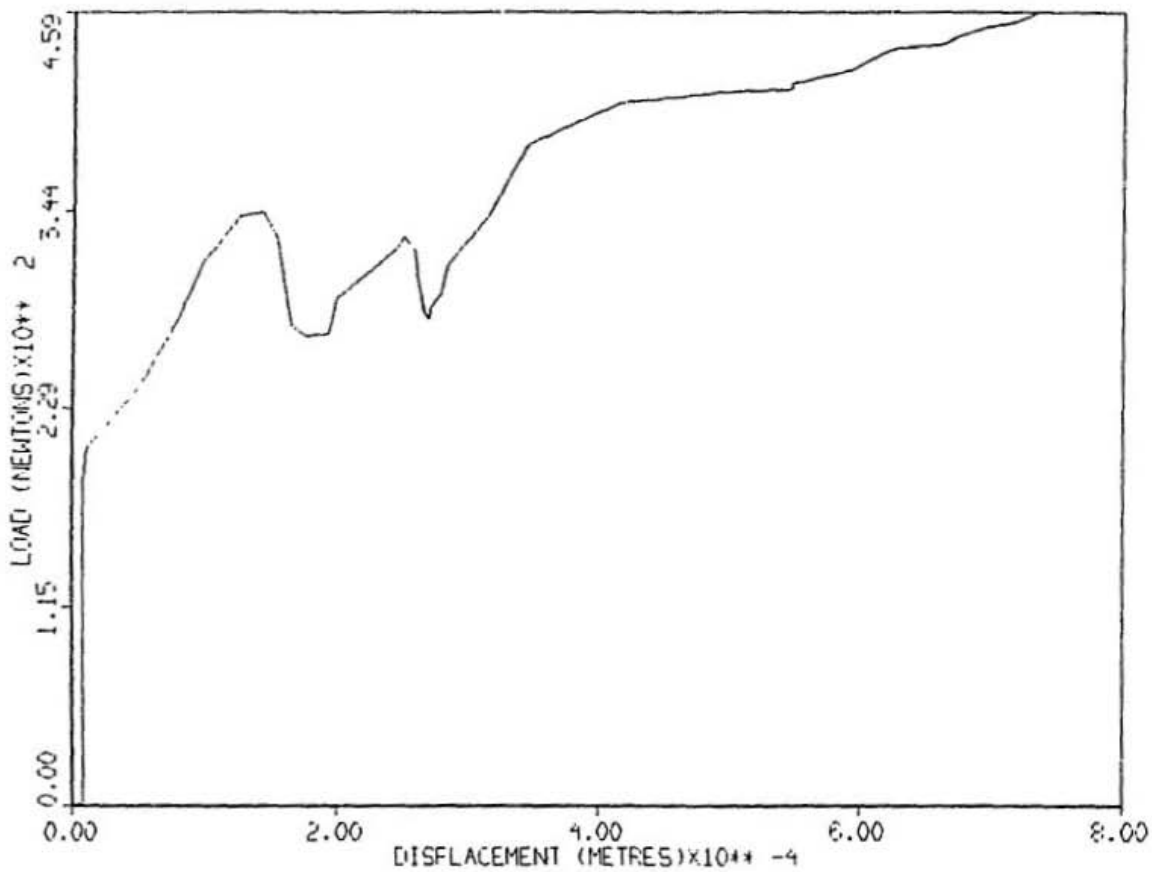

Fig. 5.9 Load Displacement Record, # 17, 143 seconds

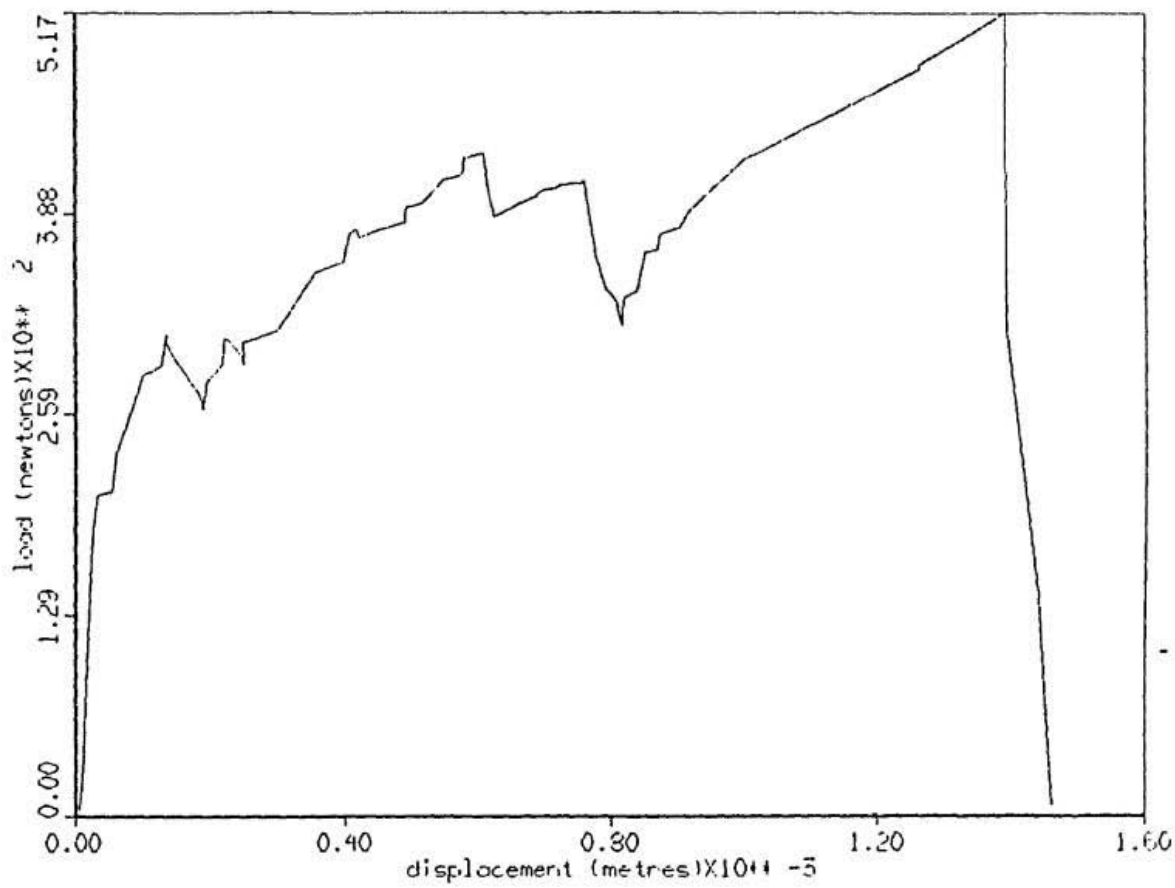

Fig. 5.10 Load Displacement Record, # 18, 807 seconds

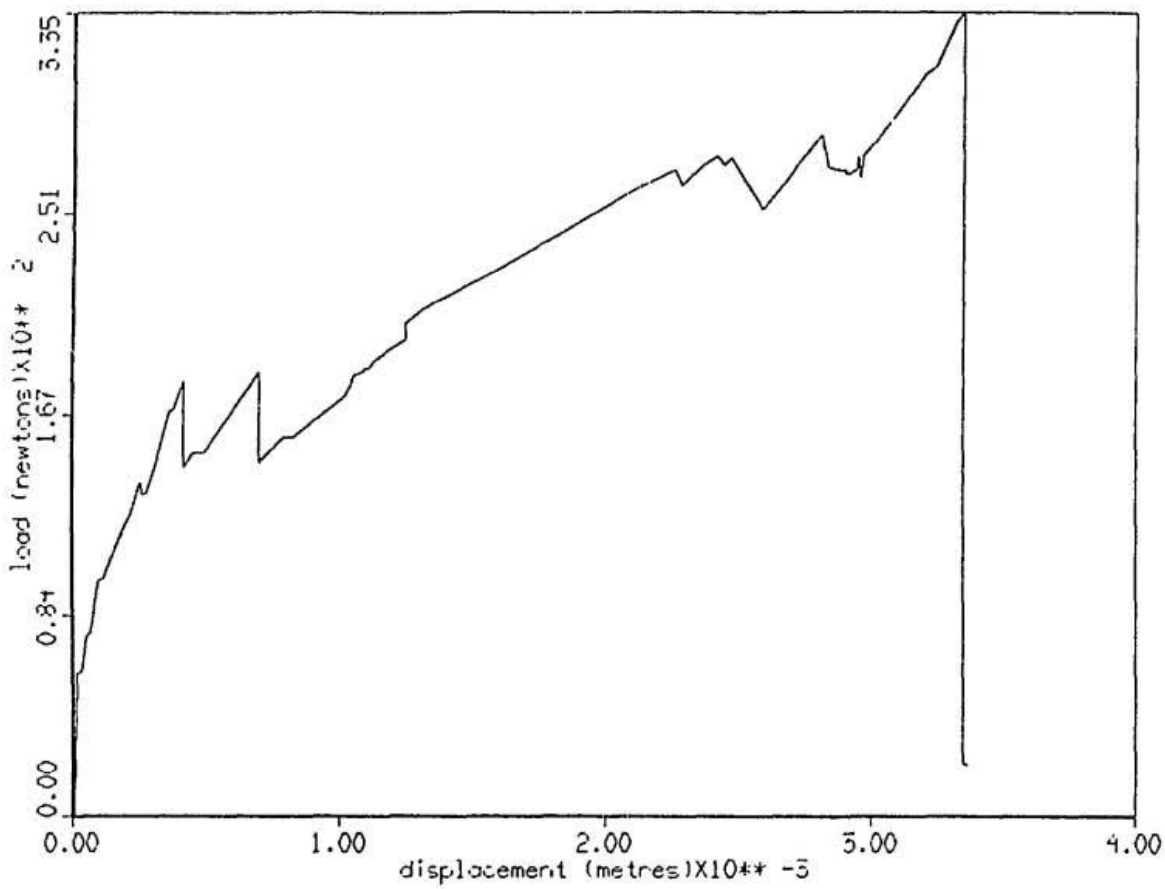

Fig. 5.11 Load Displacement Record, # 24, 80 seconds

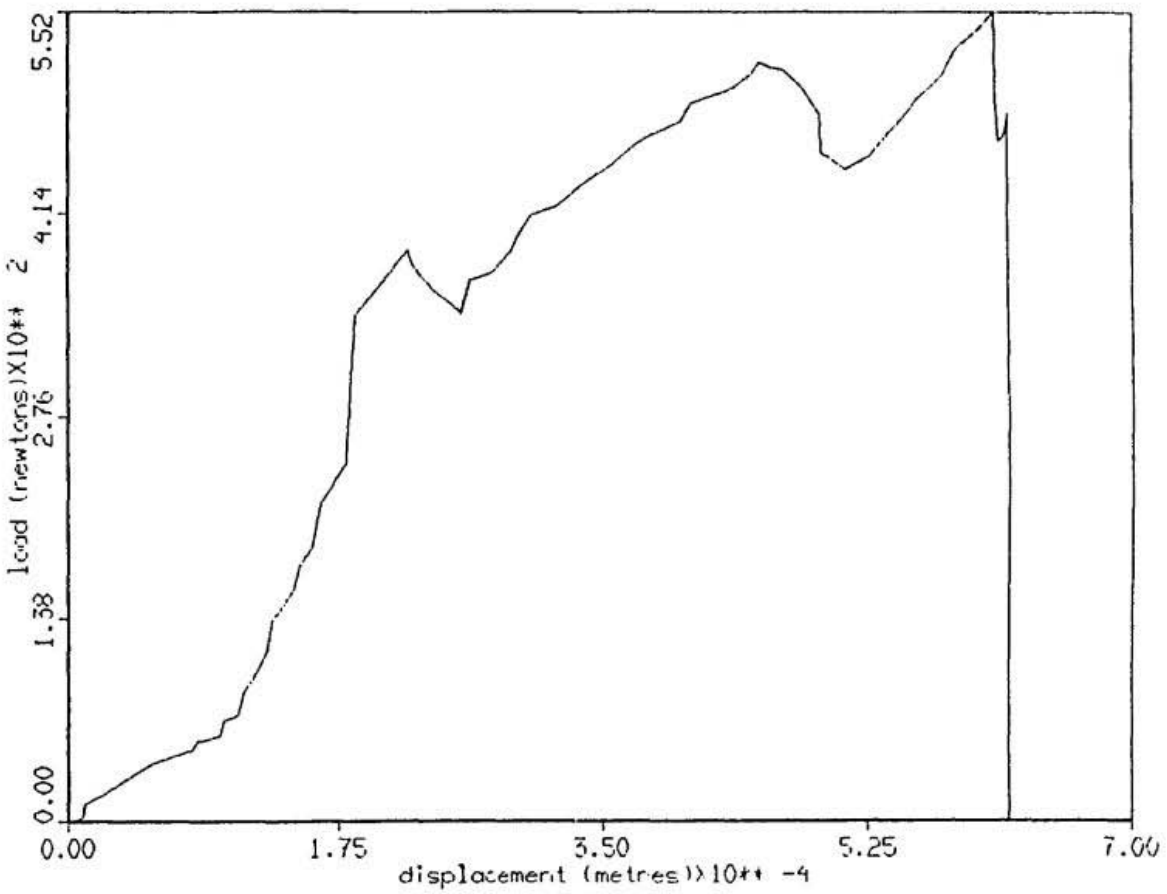

Fig. 5.12 Load Displacement Record, # 25, 70 seconds

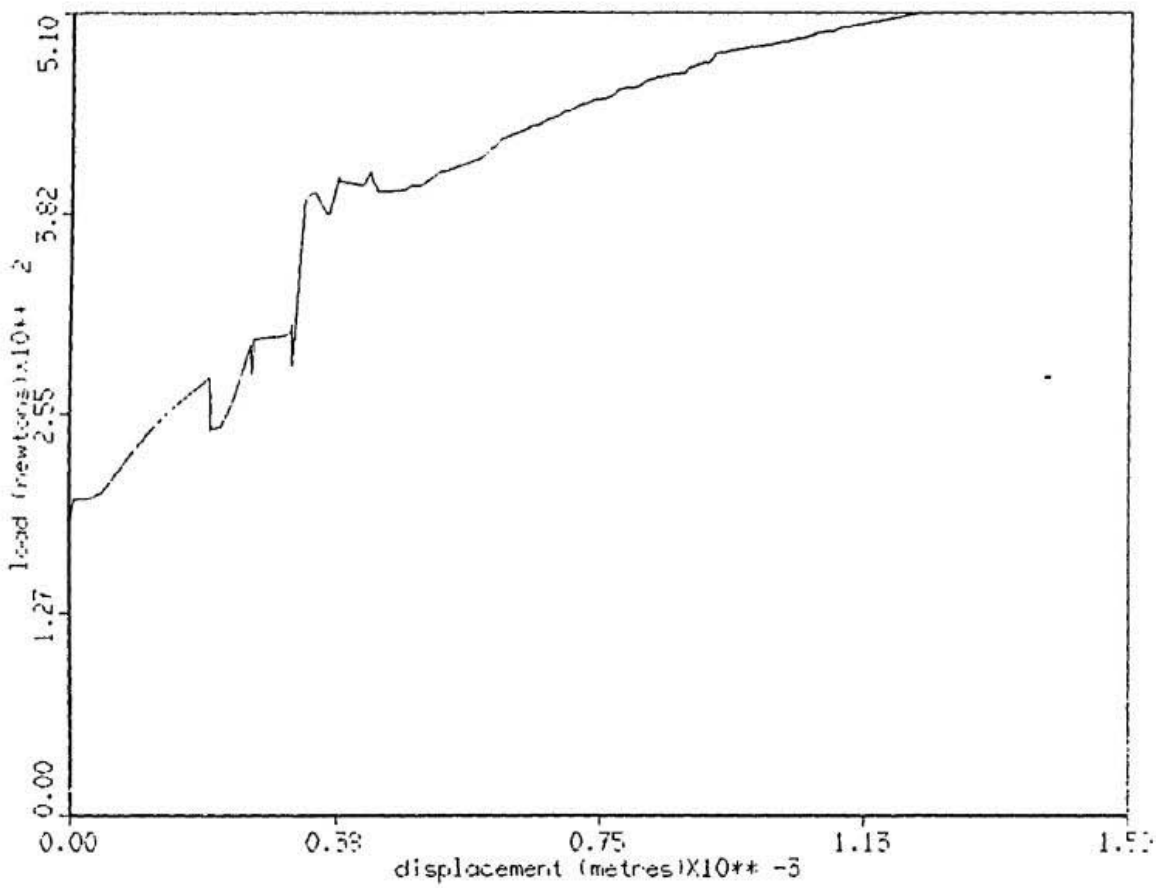

Fig. 5.13 Load Displacement Record, # 26, 127 seconds

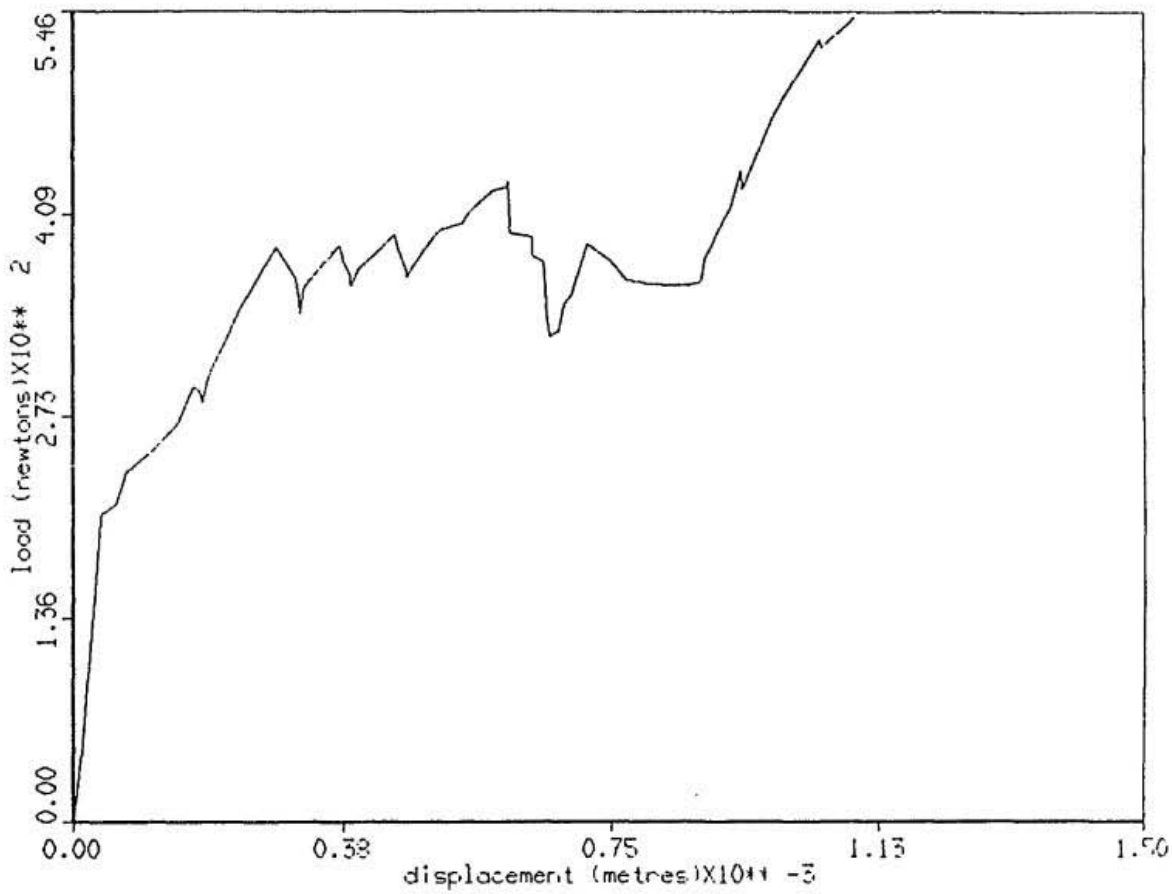

Fig. 5.14 Load Displacement Record, # 30, 10 seconds

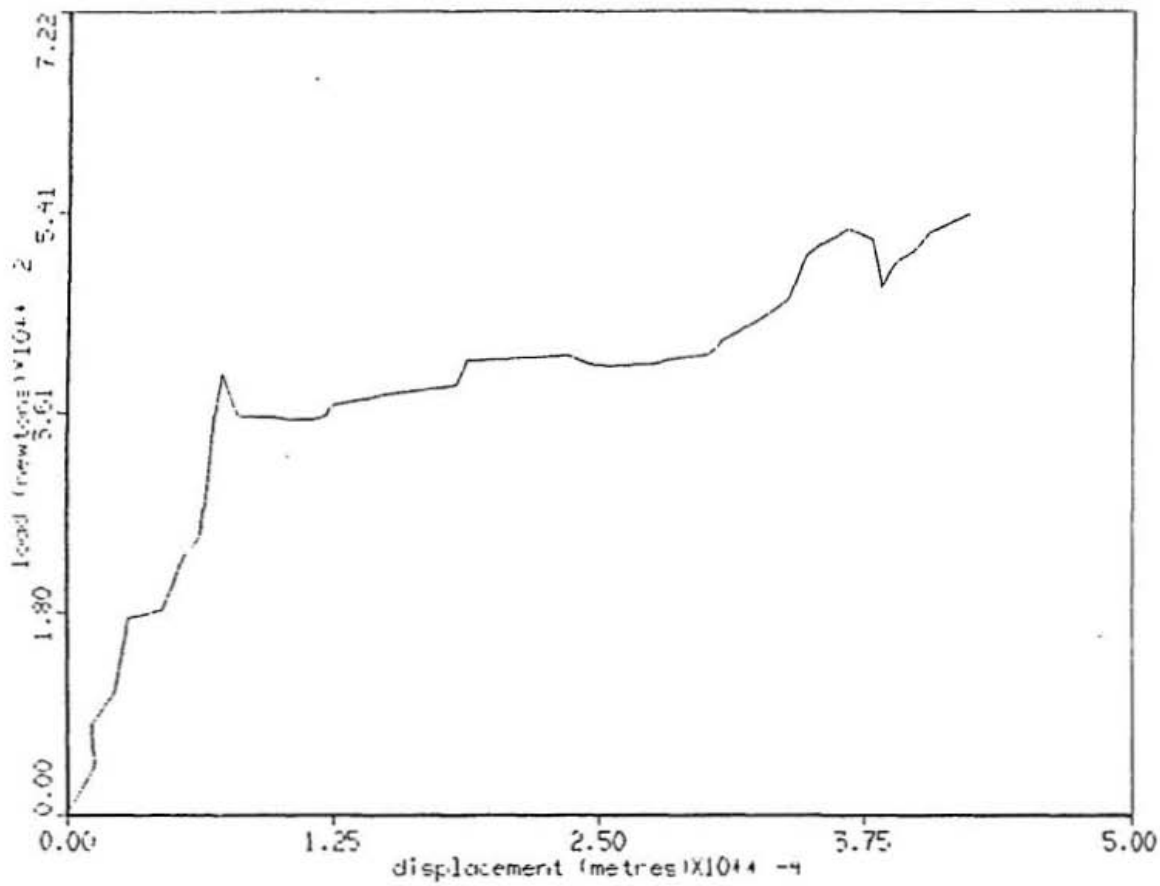

Fig. 5.14 Load Displacement Record, # 31, 22 seconds

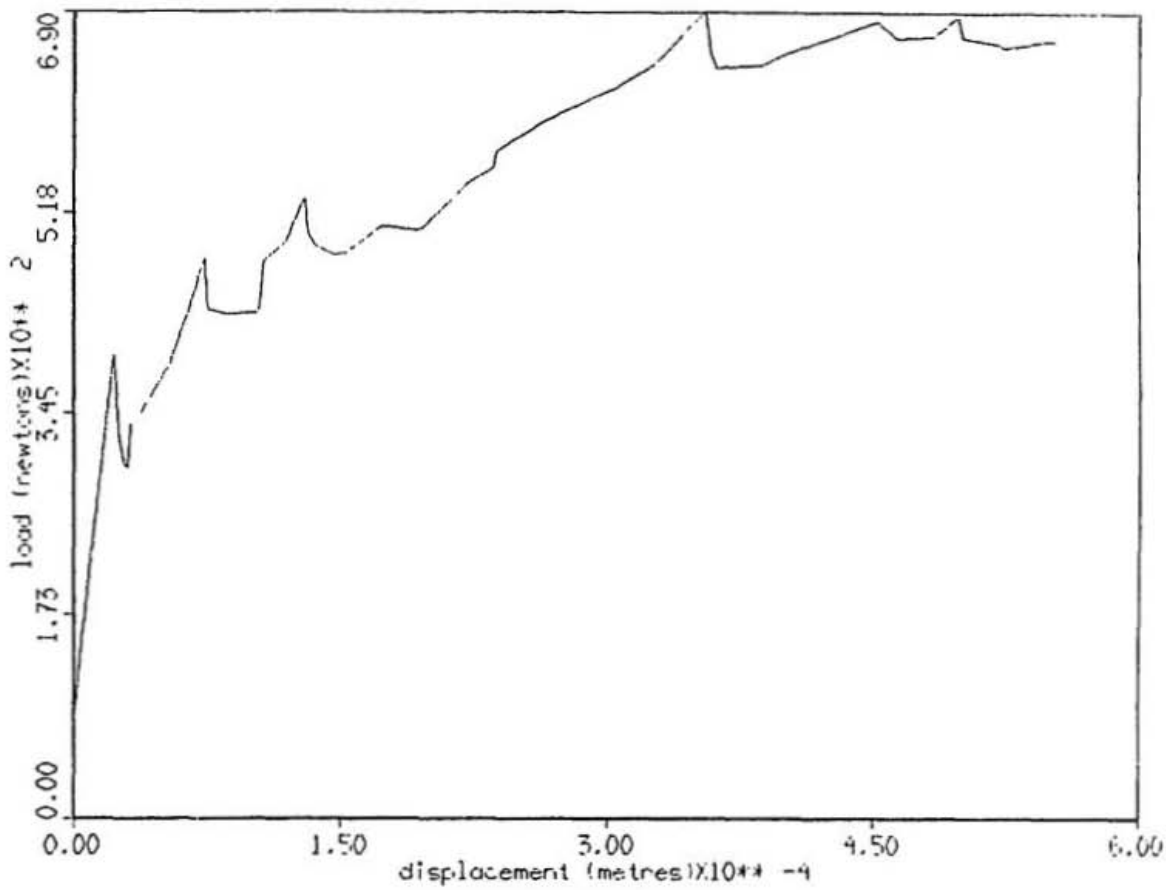

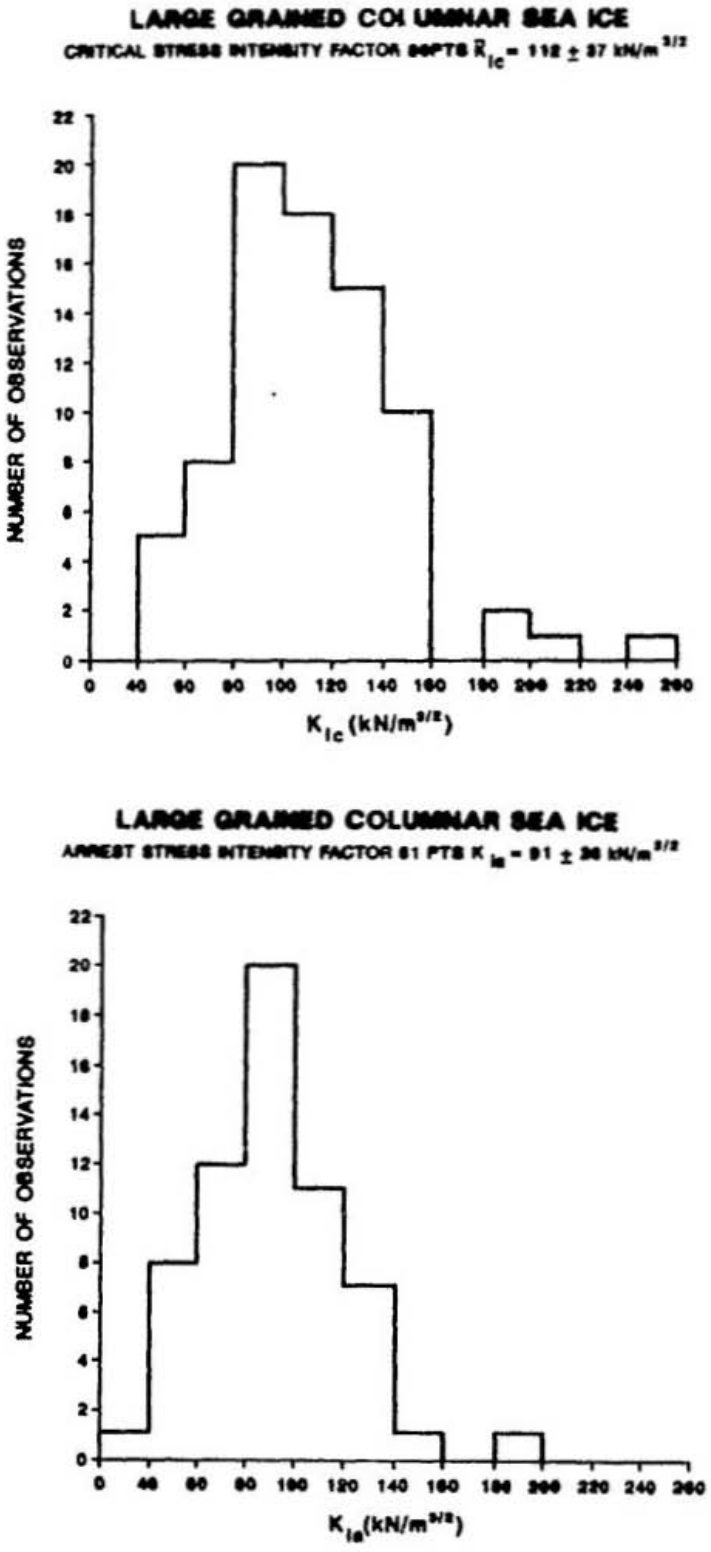
LARGE GRAINED COLUMNAR SEA ICE
CRITICAL STRESS INTENSITY FACTOR 66PTS $\bar{K}_{Ic}$ = 112 ± 37 kN/m$^{3/2}$
NUMBER OF OBSERVATIONS
0 2 4 6 8 10 12 14 16 18 20 22
0 40 60 80 100 120 140 160 180 200 220 240 260
K_{Ic}(kN/m$^{3/2}$)
LARGE GRAINED COLUMNAR SEA ICE
ARREST STRESS INTENSITY FACTOR 61 PTS K_{Ia} = 91 ± 36 kN/m$^{3/2}$
NUMBER OF OBSERVATIONS
0 2 4 6 8 10 12 14 16 18 20 22
0 40 60 80 100 120 140 160 180 200 220 240 260
K_{Ia}(kN/m$^{3/2}$)

Figure 5.16

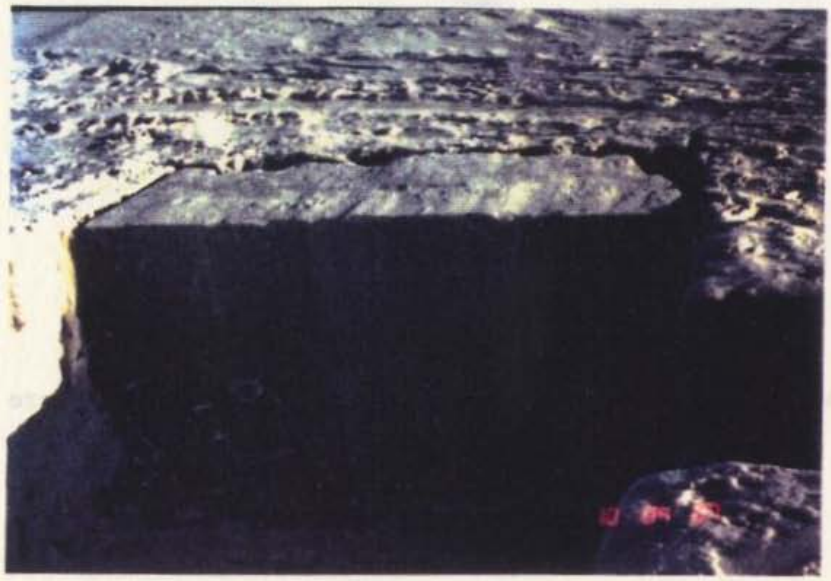


28 04 87

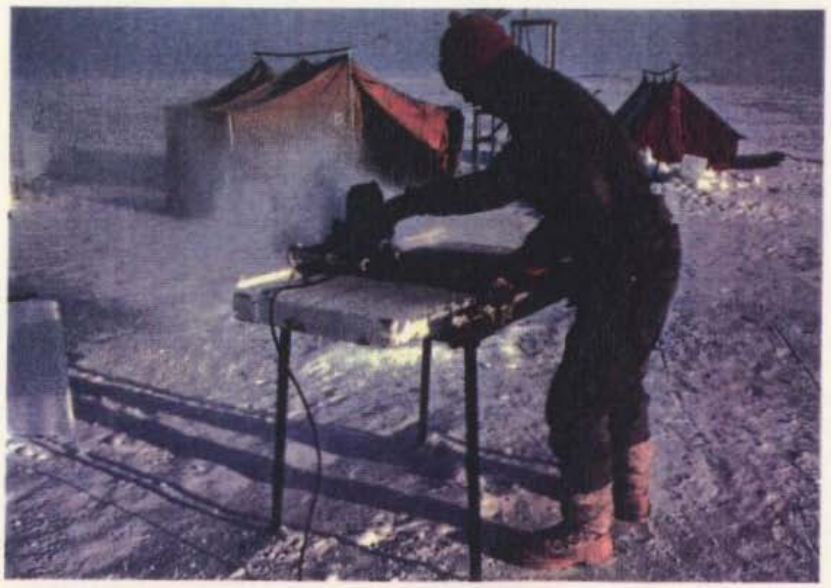

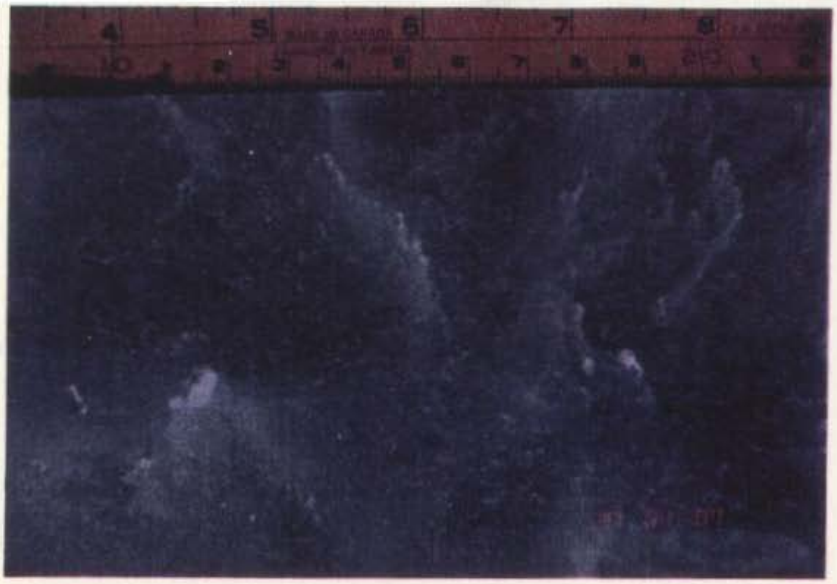

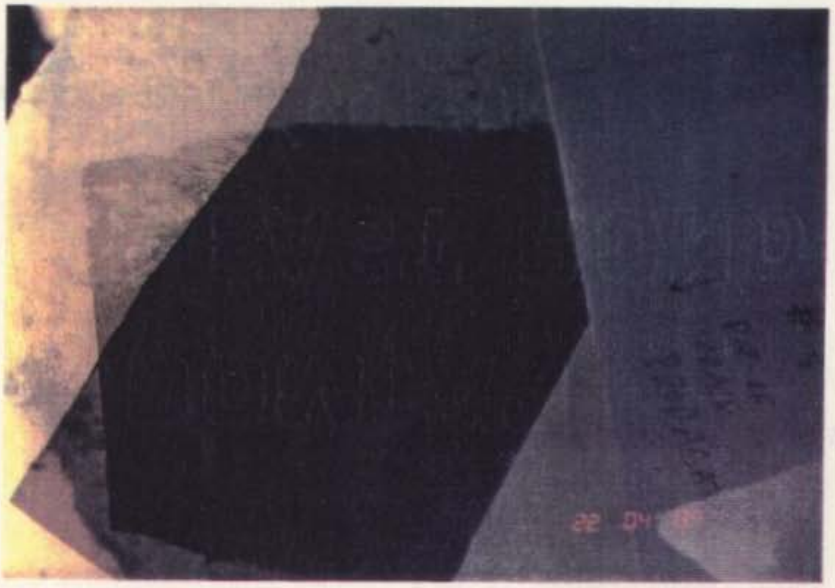

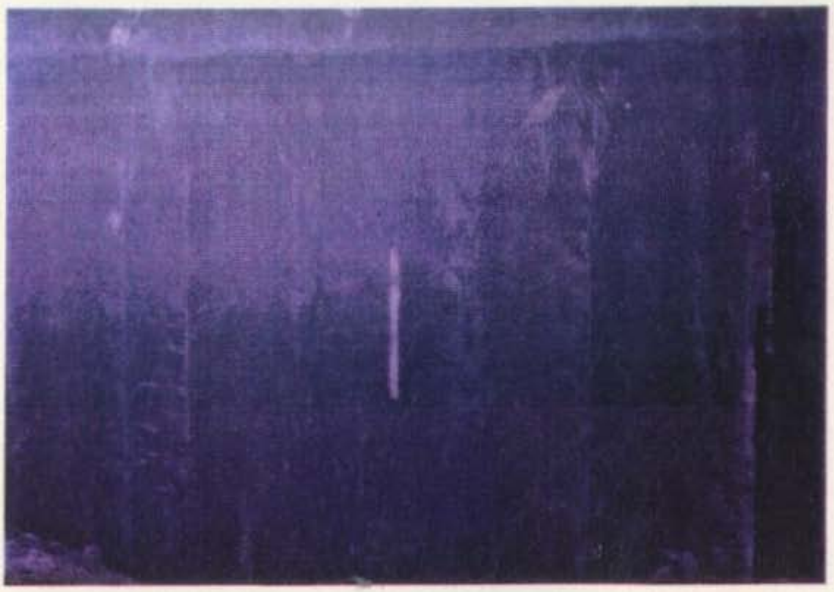

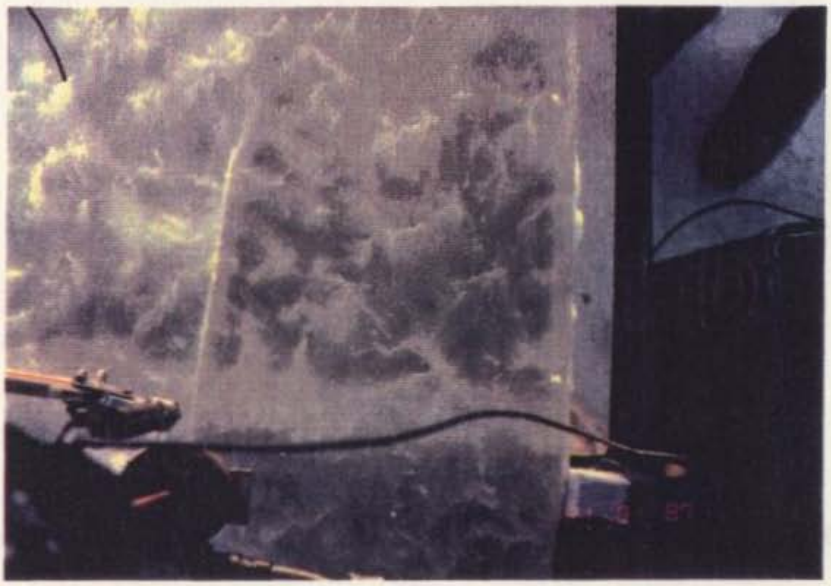

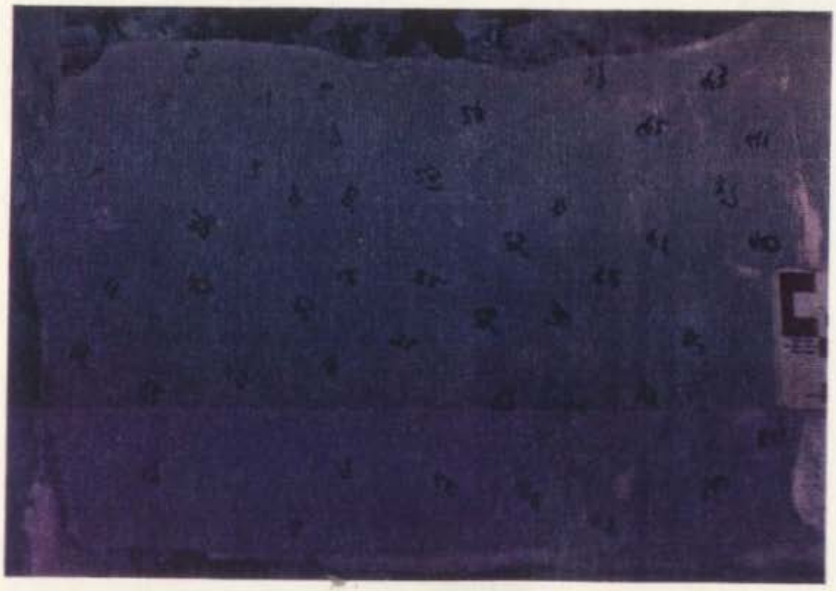

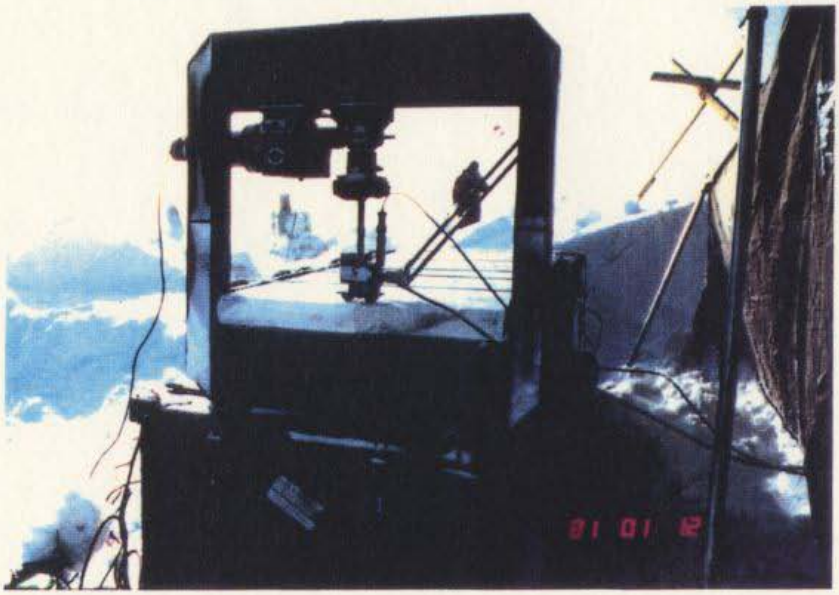
01 01 12

TABLE 5.1

LARGE GRAINED COLUMNAR SEA ICE RESULTS

#	W	d	a	P_i	K_{Ic}	Time	$\dot{K}_I$	P_a	K_{Ia}	l	E	Temp
	m	m	m	N	$kNm^{-3/2}$	s	$kNm^{-3/2}s^{-1}$	N	$kNm^{-3/2}m$		GPa	°C
1	.540	.0517	.302	670	155	1080	.14	636	147	.02	.53	-18
				600	139	1500	-	600	139	.80+	-	-
2	.530	.0505	.27	503	122	480	.25	485	118	-	.65	-16
				803	195	1808	-	-	-	.38+	-	-
3	.540	.0425	.21	326	110	2368	.5	238	80	.27	.38	-16
				291	98	3436	-	229	77	.20	-	-
				307	103	3744	-	-	-	.12+	-	-
5	.540	.0481	.206	388	103	870	.12	300	80	.20	.39	-19
				335	89	1120	-	296	78	.15	-	-
				344	91	1304	-	-	-	.32+	-	-
6	.56	.0649	.203	794	113	1910	.06	-	-	.32+	.25	-19
7	.52	.0452	.31	652	199	3420	.06	617	188	?	.5	-23
				847	258	4360	-	-	-	.49+	-	-

#	W m	d m	a m	P_i N	K_{Ic} $kNm^{-3/2}$	Time s	$\dot{K}_I$ $kNm^{-3/2}s^{-1}$	P_a N	K_{Ia} $kNm^{-3/2}$	l m	E GPa	Temp °C
8	.520	.075	.34	1129	125	1660	.08	1094	121	?	1.11	-20
				1349	149	2880	-	-	-	.71*	-	-
9	.530	.0477	.265	530	144	1650	.09	372	101	.18	.39	-18
				530	144	2836	-	-	-	.355	-	-
10	.535	.0687	.305	670	88	4	44	?	?	?	-	-19
				855	112	282	-	758	99	.41	-	-
				785	103	368	-	-	-	.50*	-	-
11	.54	.0702	.28	634	79	64	1.2	614	76	.02	.87	-16
				917	114	186	-	670	83	.40	-	-
				720	89	236	-	706	97	-	-	-
				882	109	288	-	882	109	.10	-	-
				952	118	340	-	-	-	.40*	-	-
12	.520	.0596	.275	485	85	60	1.4	459	80	?	-	-21
				617	108	120	-	590	103	?	-	-
				679	119	208	-	679	119	?	-	-
				741	130	256	-	741	130	?	-	-

#	W	d	a	P_i	K_{Ic}	Time	$\dot{K}_I$	P_a	K_{Ia}	l	E	Temp
	m	m	m	N	$kNm^{-3/2}$	s	$kNm^{-3/2}s^{-1}$	N	$kNm^{-3/2}m$		GPa	°C
13	.535	.0652	.31	485	70	228	.31	335	48	.30	.5	-21
				494	71	800	-	459	66	-	-	-
14	.520	.0407	.24	224	84	180	.47	215	81	.04	.91	-21
				358	134	466	-	307	115	.17	-	-
15	.530	.0454	.34	264	79	68	1.2	247	74	.15	.92	-21
				353	105	116	-	332	98	.07	-	-
				494	148	452	-	370	111	-	-	-
				450	135	498	-	423	127	.15	-	-
				423	127	548	-	-	-	.55+	-	-
16	.525	.0465	.27	335	96	17	5.7	273	78	.13	.92	-20
17	.535	.0441	.275	309	98	26	3.2	265	84	.12	1.96	-19
				309	98	33	-	282	89	.10	-	-
				414	131	60	-	380	120	.15	-	-
				494	156	143	-	-	-	.23+	-	-

#	W m	d m	a m	P_i N	K_{Ic} $kNm^{-3/2}$	Time s	$\dot{K}_I$ $kNm^{-3/2}s^{-1}$	P_a N	K_{Ia} $kNm^{-3/2}$	l m	E GPa	Temp °C
18	.520	.030	.23	141	98	88	1.1	137	96	-	1.37	-19
				176	123	124	-	150	105	.20	-	-
				182	127	183	-	155	109	-	-	-
				309	215	807	-	-	-	.77*	-	-
19	.52	.032	.20	256	156	148	1.02	-	-	.45*	-	-20
20	.520	.0373	.24	261	115	22	5.2	212	93	.10	-	-17
				314	138	70	-	212	93	.351	-	-
				310	136	148	-	-	-	.50*	-	-
21	.54	.0426	.255	230	78	22	3.5	194	66	.10	-	-16
				353	120	84	-	220	75	.835*	-	-
22	.52	.037	.26	176	80	34	2.4	106	48	.20	5.5	-16
				176	80	57	-	123	56	.05	-	-
				176	80	77	-	141	64	.15	-	-

#	W m	d m	a m	P_i N	K_{Ic} $kNm^{-3/2}$	Time s	$\dot{K}_I$ $kNm^{-3/2}s^{-1}$	P_a N	K_{Ia} $kNm^{-3/2}$	l m	E GPa	Temp °C
23	.520	.048	.30	273	74	9	8.2	-	-	-	-	-16
				344	93	31	-	247	67	-	-	-
				326	88	34	-	273	74	.20	1.27	-
				317	86	36	-	-	-	.15+	-	-
24	.54	.046	.265	388	112	29	3.9	335	97	.05	.65	-16
				547	158	77	-	459	132	.26+	-	-
25	.540	.044	.23	282	89	36	2.4	247	78	.08	.77	-14
26	.540	.045	.295	291	88	20	4.3	264	80	.10	3.2	-14
				370	112	30	-	317	96	.10	-	-
27	.540	.0302	.22	176	116	17	6.9	124	81	.10	1.5	-17
				194	128	32	-	176	116	.14	-	-
				229	151	51	-	185	122	.09	-	-
28	.54	.0393	.235	282	112	5.5	20.7	238	94.5	-	.99	-15
				326	129	13.8	-	273	109	-	-	-
				361	143	18.2	-	-	-	1.02+	-	-

#	W m	d m	a m	P_i N	K_{Ic} $kNm^{-3/2}$	Time s	$\dot{K}_I$ $kNm^{-3/2}s^{-1}$	P_a N	K_{Ia} $kNm^{-3/2}$	l m	E GPa	Temp °C
29	.535	.0572	.24	512	96.3	6.8	14.2	459	86.3	.25	3.0	-15
				556	104	8	-	450	86.6	.48'	-	-
30	.54	.0571	.22	397	41	2.8	14.7	352	36.5	-	-	-17
				529	55	7	-	459	43.6	.25	-	-
				706	73	-	-	-	-	.82'	-	-
31	.535	.0564	.33	388	41	4	10	388	41	?	-	-17
				476	50	13	-	446	47	.15	-	-
				511	54	15	-	458	48	.05	-	-
				653	69	22	-	600	63	.10	-	-

CHAPTER 6

DISCUSSION AND CONCLUSIONS

1) Sea Ice Versus Freshwater Ice

The fracture toughness values for the two different types of ice are not greatly different. The freshwater ice was all tested at -20°C, $0.7 < \dot{K}_I < 85$ $kNm^{-3/2}s^{-1}$, while the variable conditions in the field meant that the results were from ice in the temperature range -23°C to -14°C, with most warmer than -20°C, and $0.06 < \dot{K}_I < 44$ $kNm^{-3/2}s^{-1}$. The small difference, 124 ± 38 $kNm^{-3/2}$ for the lab ice compared to 113 ± 38 $kNm^{-3/2}$ for the sea ice maybe due to this small temperature difference, and the order of magnitude lower rate used in the sea ice, and the order of magnitude difference in grain size.

As has already been pointed out in Chapters 4 and 5, these values agree well with previous work and give confidence that the double torsion geometry is plane strain, and LEFM is adequate.

Although the very long loading in sea ice did lead to higher fracture toughness than fast loading, these values were still within the range reported in plane strain fracture tests for this type of ice. Parsons et al (1986) report the toughness of sea ice from the same site two years

earlier, for this crack orientation as 158 ±26.5 $kNm^{-3/2}$, 26 < $\dot{K}_I$ < 85 $kNm^{-3/2}s^{-1}$, crack aligned perpendicular to preferred c-axis, 151.3 ± 59.7 $kNm^{-3/2}$, 2.4 < $\dot{K}_I$ < 69 $kNm^{-3/2}s^{-1}$, crack aligned parallel to preferred c-axis orientation, and 166.3 ± 67 $kNm^{-3/2}$, 23 < $\dot{K}_I$ < 125 $kNm^{-3/2}s^{-1}$, for crack 45° to the preferred c-axis orientation. The influence of any preferred c-axis orientation is not significant to a radial crack.

The rate dependence of the fracture toughness reported in Chapter 4 and 5 agrees well with previous results, though a linear dependence of toughness on time to failure fits the data better than the exponential fit used by previous authors, Urabe and Yoshitake (1981b), Timco and Frederking (1986). There is clearly an influence of loading rate on ice fracture toughness, the slower the load rate, the tougher the ice.

The implication of the rate dependence of toughness on ice strength, through Eq. (2.14), is opposite to what has been found in other brittle materials. In the glasses and ceramics at high temperature, slow loading allows pre-existing flaws to lengthen through slow sub-critical crack growth. But slow loading of a pre-existing crack in ice, if the load is not critical, allows the crack to become tougher, instead of growing longer and weaker. Ice is

weakest when loaded fast, ceramics strongest.

Contrary to the findings on the toughness of ice with grain size less than 1 cm, there is no significant difference in the toughness of the large grained (5 to 10 cm) sea ice and the small grained (1 to 3 mm) freshwater columnar ice.

The arrest stress intensity factor for the sea ice and lab ice are approximately the same; 91 ± 28 $kNm^{-3/2}$ for the sea ice, and 89 ± 14 $kNm^{-3/2}$ for the lab ice. The larger grain size of the sea ice does not have significant influence on the value of the arrest stress intensity factor, though brine channels create greater scatter in the results. The close agreement suggests that the arrest stress intensity factor of ice is a material property, not significantly influenced by microstructure.

The magnitude of the arrest stress intensity factor is slightly lower than the average fracture toughness of ice at -20°C, 90 $kNm^{-3/2}$ compared to 120 $kNm^{-3/2}$. This difference may not seem great until one considers the important indentation loading geometry, where crack length is dependent on the square of the arrest criterion.

2) Arrest Versus Critical Stress Intensity Factor

The fundamental question is, what is the difference

between the arrest and critical stress intensity factors, or to put it another way, why aren't they the same magnitude. This is also the same as the question of why is there no slow sub-critical crack growth, why must a threshold be exceeded in every case for crack growth to take place?

The rate dependence of the critical stress intensity factor indicates that faster loading leads to lower toughness. In the sea ice the toughness predicted at zero time to loading is from Eq (5.3), 89 $kNm^{-3/2}$, compared to the arrest toughness of 91 $kNm^{-3/2}$, suggesting that the arrest stress intensity factor is the zero time to loading, or creep free, ice fracture toughness.

This is not so strongly indicated in the freshwater ice results, where the arrest stress intensity factor is 89 $kNm^{-3/2}$, and the zero time to loading toughness is 112 $kNm^{-3/2}$. It is, however, indicated by high rate toughness values reported by Hamza and Muggeridge (1979), at -20°C, 10 tests, K_{Ic} = 57 ± 5 $kNm^{-3/2}$ for 8 mm grain size, and 73 ± 13 $kNm^{-3/2}$ for 12 mm grain size, at approximately 5 x 10^{4} $kNm^{-3/2}s^{-1}$; Nixon and Schulson (1986a), from 14 tests K_{Ic} = 80.5 ± 7.5 $kNm^{-3/2}$, 10 < $\dot{K}_I$ < 10 $kNm^{-3/2}s^{-1}$, grain size .9 to 8.5 mm.

In every case a threshold had to be exceeded for crack growth to take place, and the crack growth was abrupt, the

slip/stick type of growth referred to by Mai and Atkins (1975). There is an instability, and this can arise either because of the loading geometry and test frame compliance, or because it is a material property. The discussion of the stability of the Double Torsion geometry in Chapter 3 showed that it was stable regardless of the compliance of the test frame. The slip/stick crack growth is a consequence of the ice material properties, from Eq. (3.24);

$$\frac{1}{r}\frac{dR}{dR} > -\frac{2}{a\bar{d}}; \qquad (3.24)$$

dR/dA must be < 0 for there to be an instability. There must be a lower toughness at higher crack velocity.

3) Material Properties that Could Cause Instability

a) $n \leq 3$

In the context of the work of Hui and Riedel (1981) an adequate condition to prevent sub-critical crack growth is that the power law creep exponent be no greater than three. Wertmaan (1983) shows that values from 1.5 to 5 have been reported, from tests on various types of ice under uniaxial to triaxial stress conditions. He concludes that quasi-steady-state creep rate of coarse grain and single crystal ice at moderate stress levels and relatively large strains is best described by a power creep equation with

power exponent of 3.

We will discuss first the possible causes for negative dR/dA, pointing out that the theory of Hui and Riedel (1981) is equivalent, but stated in terms of continuum elasticity and strength of the singularity in the stress and strain fields, instead of the energetics of the system.

b) Toughness Increases With Increasing Temperature.

Local heating of the loaded material in the vicinity of the crack tip may result in instability if the material has higher toughness at higher temperature, Marshall et al (1974), Mai and Atkins (1975). However as ice temperature increases, toughness decreases, ruling out this mechanism.

c) Toughness Increases With Increasing Crack Velocity

Physically, negative dR/dA is equivalent to lower toughness at higher crack velocity, Mai and Atkins (1975). This was proposed by Mai and Atkins to explain the slip/stick growth of epoxy resin Selby and Miller (1975).

Mai and Atkins (1975) show that a material that has increasing toughness and decreasing modulus for decreasing crosshead rate, as does ice, has fracture surface energy that decreases with increasing crack velocity. Their argument was applied to a material that changed modulus slightly and toughness by a factor of two during a series of

slip/stick crack growth events, under crosshead rate that varied over two orders of magnitude.

The modulus of ice is rate sensitive, Sinha (1981), falling from 9.8 GPa when measured at acoustic frequencies, to half this for an event of 10 seconds duration, to approximately 1 GPa after ten minutes. The fracture toughness does not change so greatly but does increase slightly with duration of load, as has been seen in the results obtained in these experiments, and as has been reported by other workers. The difference between ice behavior and that described by Selby and Miller (1975) (and explained by Mai and Atkins (1975)), however may be that during each crack growth event, of duration less than 0.1 s, the higher value of the ice modulus is in effect. Although creep of ice reduces the effective modulus to time of crack initiation, there is no reason to assume that during the short duration of crack growth that the modulus is not approximately 9.8 GPa. This point is relevant to the following analysis, which follows Mai and Atkins (1975), but for the double torsion geometry used here.

Eq (2.5) may be differentiated with respect to time and manipulated to obtain;

$$\frac{\dot{a}}{\dot{u}} = \frac{1}{d} = \frac{P}{(2R + u(dP/d(da))} \qquad (6.1)$$

In the double cantilever beam geometry used by Selby and Miller (1975) dP/da is zero, and Eq (6.1) reduced to a simple ratio. The ratio of crack growth rates and fracture surface energies at different crosshead rates was easily extracted. For the double torsion geometry the equivalent formulation is;

$$\frac{\dot{a}_1}{\dot{a}_2} = \frac{\dot{u}_1}{\dot{u}_2}\frac{P_1}{P_2}\frac{\left(2R - \frac{u^2}{a^2}\frac{Wd^2R}{3w_m^2}\right)_2}{\left(2R - \frac{u^2}{a^2}\frac{Wd^2R}{3w_m^2}\right)_1} \qquad (6.2)$$

where the subscript distinguishes between tests at different crosshead rates, $\dot{u}_1$, $\dot{u}_2$. In this case the dependence of crack velocity on the ratio of R_2/R_1 is not so clear cut, the load is inversely proportional to the square of the crack length during each crack jump event, contributing the complicating second term within the bracket in Eq 6.2. Further complicating this is the relationship between P and R, which also involves the rate sensitive modulus.

Although it seems intuitively obvious that ice toughness is less at higher crack growth rates where creep has less time to be activated, there is no definitive evidence of this. The wedge loaded double cantilever beam geometry of Selby and Miller (1975) has been tried by Bentley et al (1988), but they were unable to obtain arrest.

Dempsey et al (1989b) did obtain arrest, but not stable growth, and crack growth rate versus displacement rate was not given. It seems to be a tautology, the negative dR/dA of ice is unmeasurable, due to the unstable crack growth it causes.

d) Blunt Starter Crack

Selby and Miller (1975) noted that the slip stick crack growth in PMMA could be attributed to crack tips that were not initially sharp. In the tests on ice, starter cracks were initiated by pressing a sharp blade into the ice, nucleating a micro crack. The question of whether this crack remains sharp was addressed in Chapter 2. Also Lui and Miller (1979) found no difference in toughness between pre-cracked samples, and those with crack tips prepared with razor blade, avoiding any micro crack creation.

The experimental observations of Cole (1986), indicate cracks open to the air are stable for many hours. This was explained by the thermodynamic analysis of healing (blunting) supplied by Colbeck (1986), which revealed that at $0^{\circ}C$ a crack in ice of 1 cm length, aspect ratio of 10^{3}will not change its diameter, ie its radius of curvature at the crack tip, appreciably, for a day if open to the air. This is further supported by Eq 2.23, which shows that ice should be energetically stable against spontaneous blunting

mediated through dislocation emission by the formation of a three dimensional kink pair. There is no evidence to suggest the instability is due to blunt crack tips in ice. If cracks in ice could blunt, they could also grow slowly by stable sub-critical creep crack growth, and this has not been observed.

e) Ice Has an Intermediate Yield Stress

Yamini and Young (1980) found in a study of various amorphous epoxy resins that those with low yield strength displayed ductile tearing (ie stable growth), those with high yield strength exhibit only dynamic crack growth, and those intermediate to this slip/stick crack growth. Once crack growth was arrested, it was argued, it had to restart by first growing slowly through a plastic zone before growing rapidly in the slip stage of growth.

The size of this slow growth zone was argued to be approximately the Dugdale plastic zone radius;

$$r_p = \frac{\pi}{8} \left(\frac{K_{Ic}}{\sigma_y}\right)^2, \qquad (6.3)$$

similar to Eq 2.22. The argument for the amorphous epoxys is essentially that the crack tip blunts, the extent calculable from the Dugdale plastic zone radius, and the instability in crack growth is attributable to this

blunting. They find the fracture criterion is that a critical stress three times the yield stress of the resin is achieved a critical distance ahead of the crack. This is really the same explanation of crack instability as blunt crack tips, and slow crack growth is a consequence of the same processes that blunt the crack.

This interpretation has been challenged by Troung (1989), who pointed out that the relationship between the toughness of sharp and blunt crack tips, and the corresponding yield strengths is solely controlled by the constant n. A change in n can be said to be the true reason why crack growth switched from ductile, to slip/stick to brittle as yield strength increased and toughness decreased. There are two curves, one with $n \cong 200$ corresponding to the brittle branch; and the other with $n \cong -25$ for the ductile tearing branch. The slip/stick region is the intermediate of these two, with a mix of the two types of crack growth.

These values of n are very high in the context of Hui and Riedel (1981), and opposite in sense. Troung (1989) concludes that if blunting is the main mechanism to increase toughness, n has to be a negative quantity, ie toughness has to decrease with increasing crack velocity, or displacement rate.

The fracture surfaces of the ice were not examined

with a scanning electron microscope with the necessary resolution to determine if there was a period of slow crack growth before the slip stage of crack growth. It is not clear though that the findings on amorphous epoxy are relevant to ice, even though they also display slip/stick growth. Epoxies appear to behave as a pure continuum material - the failure stress is three times the yield stress some distance ahead of the crack, see Broek (1984) for example. In amorphous materials it would appear that discrete crystal considerations such as dislocations and screening need not be considered as complicating factors.

It is not known what the yield stress of ice is, as failure at elevated stress is accompanied by fracture. Gandhi and Ashby (1979), in their fracture mechanism maps for materials that cleave, suggest that it may be as high as 100 MPa. This gives a plastic zone size of approximately 2.0 μm, smaller than the smallest observed brittle growth region of Yamini and Young (1980) of approximately 10 μm for toughness of approximately 600 $kNm^{-3/2}$. By this measure ice should display only brittle crack growth.

If on the other hand the yield strength of ice is lower than 100 MPa, then the size of a plastic zone would correspond more closely to those in epoxies that also display slip/stick growth. Depending on what the yield

stress of ice is, this theory either predicts purely brittle growth with no preceding slow growth; or predicts ice crack tips blunt and cause the slip/stick crack growth behavior observed.

It has already been noted that experimental evidence indicates crack tips in ice do not blunt, and it has been argued that crack tip blunting in ice is energetically unfavourable, if there is no crystal lock-in in ice. It can be also argued that the yield strength of ice is high, Gandhi and Ashby (1977). A yield strength of 100 MPa would be commensurate with the smallest observed ice piece size, Kendall (1978), Parsons (1989). A high yield strength would suggest that only brittle crack growth is possible, according the results on epoxies. Yet ice crack growth appears as if the crack tips blunt.

This paradox may be resolved if the screening or shielding effect of dislocations are considered. It is possible though this mechanism for the crack tip in ice to remain atomically sharp (high yield strength) and yet display the same instability that a blunt crack does.

4) Discussion

Of the five previously reported material mechanisms responsible for unstable crack growth, only two cannot be ruled out for ice; that ice has a power creep exponent n <

3, and that it has a fracture energy that decreases with increasing crack growth velocity. Also, ice crack growth is the same as that of other materials that have crack tips that blunt. We shall attempt to reconcile these views with the creep properties of ice, as mediated through the mechanisms of dislocation movement and shielding that Thomson (1978), Weertman (1978) proposed. To do this a detailed restatement of the assumptions and conclusions of Hui and Riedel (1981) will first be given.

The work of Hui and Riedel (1981) is essentially mathematical, dealing with the strength of the singularities of the stress and strain field at the tip of a growing crack tip;

$$(\sigma,\varepsilon) \alpha r^{-1/(n-1)} \tag{2.30}$$

This is to be distinguished from the fields at a stationary crack tip, the HRR field;

$$\begin{aligned} \sigma &\alpha r^{-1/(n+1)} \\ \varepsilon &\alpha r^{-n/(n+1)} \end{aligned} \tag{2.32}$$

The failure criterion is that at some distance ahead of the crack tip, some critical strain is exceeded.

It is essential to emphasize that there is no universally accepted fracture criterion. For example, in the work of Yamini and Young (1980) on epoxy resins mentioned above, they found a critical stress fracture

criterion applicable. By comparison Sinha (1982) has shown a critical (delayed elastic) strain criteria is satisfactory for crack nucleation in ice. In this aspect, the theory of Hui and Riedel (1981) appears applicable to ice.

Hui and Riedel (1981) argue that for for $n \leq 3$ steady state crack growth is not possible. For a stationary crack creep strains dominate the HRR field near the crack tip, but they claim that for a moving crack in a $n \leq 3$ material, the elastic strain must dominate and has an inverse square root singularity, $\sigma \propto r^{-1/2}$, where r is the distance from the crack tip. Their solution is for the anti-plane shear deformation (Mode III), which is mathematically tractable, and is believed to be representative of Mode I behaviour. By manipulating Eq 2.24;

$$\dot{\varepsilon} = \dot{\sigma}/E + B\sigma^n \tag{2.24}$$

into an equation for the stress function Ψ;

$$\tau_r = \frac{1}{r}\left(-\frac{\partial\Psi}{\partial\theta}\right);\ \tau_\theta = -\frac{\partial\Psi}{\partial r}, \tag{6.3}$$

they obtain;

$$-\frac{\dot{a}}{G}\nabla^2\frac{\partial\Psi}{\partial x} + \bar{B}\nabla_i(\tau_e^{n-1}\nabla_i\Psi) = 0 \tag{6.4}$$

where $\bar{B} = (3^{n+1})^{1/2} B$, G is shear modulus, and $\tau_e = |\nabla_i\Psi|$ is equivalent shear stress.

Assuming the non-linear (creep) term dominates the linear term as $r \to 0$ necessarily implies that an HRR-type singularity prevails at the crack tip. Inserting $\sigma \propto r^{-1/(n+1)}$, (ie $\Psi \propto r^{-n/(n+1)}$), the linear term is of higher

singularity, a contradiction of the original assumption. The HRR field cannot be valid at the growing crack tip.

If one assumes that the linear term dominates the asymptotic field, there is no contradiction for $n < 3$ only. Thus for $n > 3$ the linear and non-linear terms must together govern the asymptotic field.

The solution of 6.2, with the non-linear terms deleted contains an unspecified factor A such that;

$$\Psi = Ar^{1/2}\cos \theta/2 \ . \qquad (6.5)$$

Steady state growth is not possible, as A would be infinite unless the material law Eq (2.24) is modified such that as $\sigma \rightarrow 0$, the creep exponent changes to a value $n > 3$.

For $n > 3$, a new type of singular field develops at a growing crack tip, new with respect to the HRR field at a stationary crack tip. The stress and the strain have the same radial dependence, $(\sigma,\varepsilon) \alpha r^{-1/(n-1)}$. The amplitude of the near tip field depends on the current crack growth rate but not on prior history nor on applied load. As a consequence of the properties of the asymptotic field for $n > 3$, no steady state creep growth is possible below a certain minimum crack growth rate. For large growth rates a power law relation $\dot{a} \alpha K_I^n$ is predicted, as has been observed experimentally by Evans (1972) and others.

In the context of this theory, ice, with no observed creep crack growth, and n in the vicinity of 3, fits the first case. The implication is that in ice $n \leq 3$.

Despite the easy activation of creep in ice, the creep strains at the growing crack tip do not cause small scale yield - a plastic yield phenomena. The crack tip behaviour is dominated by elastic strain. This is intuitively acceptable if the very high strain rates in the vicinity of the crack tip are considered. The low value of n does not enable sufficient creep strain to accompany crack growth, only critical crack growth is possible.

Rice (1987) provided a state of the art review of the literature on the control exerted by the plastic response of a material on brittle cracking. There is as yet no comprehensive analysis of crack propagation in the presence of extensive nearby plastic flow. The mechanisms of stress relaxation at the crack tip may be either dislocation emission from the tip, or the activation of internal sources of dislocations that impinge into the crack tip along slip systems. The first case is considered to be fundamental as to whether or not a crystal is cleavable. It has already been shown, Eq 2.22, that spontaneous dislocation emission is prevented in ice by an energy barrier. The implication is that the crack tip stays atomically sharp, and thus will

cleave.

Dislocation interactions with the crack tip controls whether brittle fracture actually occurs, and if it does not, the dislocation plasticity provides the mechanism by which fracture can ultimately occur through void growth to coalescence, or localized shear, or a combination of both.

For those materials that fracture through cleavage the Griffith criteria is still essential, that is, the after-shielding k proposed by Thomson (1977, 1986, 1987) is a valid criteria, though it is said to be "screened" by the dislocation plasticity in its vicinity.

Once cracking has been initiated, if the creep strain rate increases less rapidly than σ^3, the stress field singularity at the crack tip is linear elastic.

In short, ice is brittle because it is stable against the blunting mechanism of dislocation mechanism. The K_{Ic} fracture criteria is slightly rate dependent because ice will creep at any load, increasing the shielding effect of dislocation density around the crack tip.

The macroscopic slip/stick crack growth mode of ice is indistinguishable from the amorphous materials that display crack blunting, where a continuum analysis is sufficient. In ice however consideration need be given to crystal lattice mechanisms influence on crack growth.

Despite the creep behaviour of ice, the linear elastic fracture criterion nonetheless holds, and this must be exceeded by a further increase of the remote stress to overcome the shielding. This leads to an instability.

The creep power exponent of ice to be consistent with Hui and Riedel (1981), it must then be concluded, is less than or exactly equal to three, for the brittle propagating crack to continue through the normally ductile crystal lattice.

Though the creep strain is insufficient for sub-critical crack growth, it may be that the macroscopic fracture energy is influenced by creep during crack growth, as it is when it is stationary. It is consistent with the rate sensitive creep contribution to fracture energy that at high crack velocities its contribution would be less. This would be consistent with the energy criterion for crack growth instability of Eq (3.24);

$$\frac{1}{r}\frac{dR}{dA} > -\frac{2}{ad} \qquad (3.24)$$

5) Conclusions

Slow stable sub-critical crack growth was not observed in either of the two types of ice tested. Fine grained freshwater columnar ice and first year sea ice with its much larger grains and more complicated microstructure both

required that a threshold be exceeded in every crack growth event,for crack growth to occur. In all cases the crack growth was fast and abrupt. This has been corroborated for the laboratory ice by tests with a wedge loaded compact tension specimen, which has a more stable geometric stability factor than the double torsion tests reported here, Dempsey et al (1989b). This instability was argued to be a consequence of the stability of the ice crystal against dislocation emission. The rate dependence of ice toughness is due to the screening of the crack by creep.

The other possible cause of sub-critical crack growth, a corrosive environment, did not appear to be active. The humidity difference between the field and the laboratory was insufficient to promote stable crack growth.

The arrest stress intensity factor for fine grained freshwater columnar ice and first year sea ice at -20°C tested in the same orientation are the same. There was no influence from an order of magnitude difference in grain size between the two types of ice. Variation in loading rate similarly had no effect on the arrest stress intensity factor.

Crack length was not rate dependent. There was no significant correlation between load rate and resulting crack length. Though this can be said to be statistically

true, it was at the same time impossible to obtain arrest in 1.4 m of freshwater ice sample if crack initiation took longer than 72 seconds. Arrest was observed in sea ice even after initiation that took 70 minutes, due perhaps to the coarser microstructure, and presence of brine drainage channels.

Both lab grown and naturally occurring field ice displayed significant spatial variation in toughness over distances as short as a few centimeters.

CHAPTER 7

APPLICATIONS

1) Risk Analysis

Paluzny (1977), Paluzny and Wu (1977) first presented a methodology for assessing the probability of failure of brittle materials that creep fracture. He supplied a formulation for the time to failure at various levels of probability P;

$$t = t_o(\ln (1 - P)^{-1}]^{1/m} \qquad (7.1)$$

where $m = \beta/(n-2)$

β is the Weibull modulus and

n is exponent in the kinetic law of creep crack growth;

$$v = AK_I^n$$

In ceramics β is generally less than n which means that $m < 1$. This means that in ceramics failures from creep crack growth occur over several orders of magnitude in time. The longer a given load is supported, the greater the probability that it will continue to be supported.

If $m > 1$, the probability of failure at a given load level increases with time.

The value of n for ice is in the vicinity of 3, the theory of Hui and Riedel (1981) used to explain the lack of sub-critical crack growth in ice requires it to be no

greater than 3.

Tozawa and Taguchi (1986), Parsons and Lal (1989) report the Weibull modulus of sea ice and laboratory ice to also be in the vicinity of 3, the highest value they report is 5.8 for lab grown ice.

This yields a value for m of grater than one, implying, according to the theory of Paluzny (1976) that the probability of failure of ice under a constant load increases with time. This does not agree with the experimental results reported here, that for crack growth to occur load in every case must be increased.

Since sub-critical crack growth does not occur in ice, this method of evaluating time to failure under load, worked out for creep brittle materials that do exhibit fatigue crack growth, is not applicable to ice. The experimental results contradict the predictions of the theory, for the values of β and n obtained from ice. Risk analysis for ice-structure interaction must be based on the probability distribution for ice strength alone.

2) The Radial Crack Problem

There are a number of mathematical models in the literature for predicting the length of a radial crack resulting from various loading geometries of ice, Smith (1976), Palmer et al (1983), Hamza and Muggeridge (1984),

Evans et al (1984), Bhat (1988), Bhat et al (1989). With the exception of the last two references, these models all assume that the arrest criteria for cracks in ice is the same as the initiation criteria. Hamza and Muggeridge (1984a, 1984b) also assume the ice may creep crack.

The results of this study show that subcritical crack growth is not possible in ice, and the arrest criteria is lower than the initiation criterion for crack growth in ice, except at very high load rates. This is particularly relevant when considering crack growth into the decreasing K_I field beneath an indenter. Because there is no sub-critical crack growth the radial crack will not grow unless the load increases. No stress relief may be expected from slow crack growth.

Smith (1976) calculated the maximum depth of a crevasse in a glacier by considering the effect on an edge crack of an opening tensile stress of 200 kPa due to gravity driven slide of the glacier, and a closing hydrostatic stress due to ice overburden. Field measurements report a maximum depth of approximately 35 m. Smith (1976) calculated the maximum depth to be 36 m if ice fracture toughness is zero, and 33 m if it is 200 $kNm^{-3/2}$. If the arrest stress intensity factor value of 90 $kNm^{-3/2}$ is used, a 35 m depth is obtained.

Evans et al (1984) in their analysis of edge indentation of an ice sheet used a damage zone radius of seven times the contact radius, obtained from an algorithm of Hill (1950). This calculation assumed that the zone of irreversible deformation is entirely plastic, and neglects any effects from ice fracture.

Parsons (1989) addressed the influence of ice fracture on damage zone size. Experimental results were obtained for macroscopic crack length due to indenter load, for loads up to 1200 N. It was assumed that K_{Ia} obtained at the tip of the resulting crack, and that the radial stress field due to a point contact, the Boussinesq field, was the crack opening stress outside the damage zone. This was a modification of the indentation model presented by Lawn and Swain (1975), which assumed K_{Ic} obtained at the crack tip. The size of the damaged zone radius beneath the indenter calculated in this way was only 1.4 times the contact radius, significantly smaller than the value of 7 predicted by the elastic/plastic cavity analysis of Hill (1950). This was due partly to the use of arrest fracture toughness instead of critical fracture toughness at the crack tip, but also points out the significantly greater stress relief caused by micro crack damage in ice than that by purely plastic damage in other materials.

3) Ice Sheet Failure Dynamics

Palmer et al (1983) postulated theoretically that in the aspect ratio range 4 to 20 the failure mechanism of the ice sheet is determined only by the indentation velocity. This was found to be true in fine grained columnar freshwater ice tests done in the laboratory Timco (1987a).

The experiments reported here show that there is no dependence of resulting crack length on loading rate. The switch from a failure mode of local crushing accompanied by radial cracks, to one of purely local crushing, or local crushing accompanied by both radial and circumferential cracks cannot be explained by the different radial crack lengths that might result from varying indentation velocity. The switch in dominance between the failure modes must then be a consequence of some other rate sensitive material property of ice, probably the effective global modulus.

CHAPTER 8

SUMMARY

The Double Torsion fracture toughness test geometry was used on ice samples 0.05 x 0.50 x 1.50 m prepared from large grained columnar first year sea ice, and fine grained columnar freshwater ice. No subcritical crack growth was observed in either ice, under deadweight loading of five days duration, or for $0.7 < \dot{K}_I < 85$ $kNm^{-3/2}s^{-1}$ in the freshwater ice and $0.06 < \dot{K}_I < 44$ $kNm^{-3/2}s^{-1}$ in the sea ice. All crack growth was abrupt and a consequence of the ice material properties. The length of the resulting crack was not found to depend on the load rate. Ten percent of the crack length was a consequence of the test frame compliance, and in engineering structures the relative stiffness of structure and ice is relevant to crack length prediction.

The arrest stress intensity factor was the same for the two ices, approximately 90 $kNm^{-3/2}$ at -20°C. The different grain size of the two ices was not as relevant as the brine drainage channels found in the sea ice, which supplied stress relief in both arrest and initiation.

The material instability responsible for the abrupt crack growth was explained to be a consequence of

anatomically sharp crack shielded by dislocations. Previous workers have shown experimentally that cracks in ice are stable over hours, days. Theoretical work predicts that an atomically sharp crack in the ice crystal lattice is stable against spontaneous blunting because the activation energy for the formation of dislocation loops out of the crack tip is greater than zero. Dislocations in the vicinity of the crack shield or screen the crack tip, thus requiring an increase in applied stress intensity factor to initiate fracture. Dislocation movement is responsible for the rate dependent creep of ice and the rate dependence of ice toughness reported by previous workers and found here. This is consistent with the energy criterion for unstable crack growth, that the fracture energy decreases with increasing crack velocity. This is also consistent with the current model of creep fracture, if the creep power exponent of ice is less than three.

The arrest stress intensity factor was used as a crack length criterion in previous crack length prediction models. The indentation model was shown to require modification to accommodate both the arrest criterion and the effects of contact micro cracking.

A reliability/risk analysis, previously developed for brittle materials that creep fracture, was shown to be

inapplicable to ice, as it does not creep fracture.

Finally it is suggested that the switch in failure modes in indentation of ice is not a consequence of radial crack length dependence on indentation rate, but rather some other rate dependent ice material property such as the modulus.

BIBLIOGRAPHY

ADAMS, T.E., LANDINI, B.J., SCHUMACHER, C.A., BRANDT, D.C., (1981), Micro and Macrocrack Growth in Alumina Refractories, Am. Cer. Soc. Bull. 60.

ANDERSON, W.E., (1969), Some Designer Oriented Views on Brittle Fracture, 1969 Gulf Coast Metals Conference, Houston Texas, Feb. 1969, Battele Northwest Laboratory rep. No. 2290, 43 pages.

ANDREWS, R.M., MCGREGOR, A.R. and MILLER, K.J. (1984). Fracture Toughness of Glacier Ice. In: The International Karakorum Project, K.J. Miller ed.. Vol 1, Proc of the Int. Conf. (Cambridge University Press, 1984) pp 147-159.

ANDREWS, E.H., LOCKINGTON, N.A., (1983), The Cohesive and Adhesive Strength of Ice, Jnl. Mat. Sci. 18 (1983) pp 1455-1465.

ASHBY, M.F., PALMER, A.C., THOULESS, M., GOODMAN, D.J., HOWARD, M., HALLAM, S.D., MURREL, S.A.F., JONES, N., SANDERSON, T.J.O., PONTER, A.R.S., (1986). Nonsimultaneous Failure and Ice Loads on Arctic Structures, 18th Annual Offshore Technology Conference, Houston, Texas, May 5-8 1986, Vol 1, pp 399-404.

ATKINS, A.G., MAI, Y-W, (1985). Elastic and Plastic Fracture, Ellis Horwood Ltd., Chichester England,

ATKINS, A.G., (1975). Icebreaking Modeling. Jnl. of Ship Research Vol 19, No. 1, pp 40 - 43.

AZADEH-TEHRANY, A.R., (1983), M. Eng. Thesis, Memorial University of Newfoundland.

BARKER, D.B., CHONA, R., CORWIN, W.R., FOURNEY, W.L., IRWIN, G.R., MARSCHALL, C.W., ROSENFIELD, A.R., WESSEL, E.T., (1988), A Method For Determining the Crack Arrest Toughness of Ferritic Materials, Fracture Mechanics: Nineteenth Symposium, ASTM STP 969, T.A. Cruse, Ed., pp 569-593.

BENTLEY, D.L., DEMPSEY, J.P., SODHI, D.S., WEI, Y., (1988), Fracture of S2 Columnar Freshwater Ice: Floating Double Cantilever Beam Tests, IAHR, Proc. 9th Int. Symp. on Ice, Aug. 23-27, 1988, Sapporo Japan, Vol. 1, pp 152-161.

BEVINGTON, P.R., (1969), Data Reduction and Error Analysis for the Physical Sciences, McGraw Hill.

BHAT, S.U., (1988), Analysis for Splitting of Floes During Summer Impact, Cold Regions Science and Technology, 15 (1988), pp 53-63.

BHAT, S.U., CHOI, S.K., WIERZBICKI, T., KARR, D.G., (1989), Failure Analysis of Impacting Ice Floes, Proc. 8th Int. Conf. OMAE, The Hague, Vol. IV, pp 275-285.

BROEK, D. (1984). Elementary Engineering Fracture Mechanics Noordhoff Int. Publ.

BROEK, D., (1989), The Practical Use of Fracture Mechanics, Kluver Academic Publications.

BOND, T.L., YESKE, R.A., PUGH, E.N., (1984), Studies of Stress Corrosion Crack Growth in Al-Zn-Mg Alloys by the Double Torsion Method, ASTM STP 821, S.W. Dean Ed., American Society for Testing and Materials, Philadelphia, 1984, pp. 128-149.

CANNON, W.R., LANGDON, T.G., (1983), Review; Creep of Ceramics, Part 1, Mechanical Characteristics, Jnl. Mat . Sci. 18 (1983) pp 1-50.

CANNON, W.R., LANGDON, T.G., (1988), Creep of Ceramics, Part 2, An Examination of Flow Mechanisms, Jnl. Mat. Sci. 23 (1988), pp 1-20.

CHAMPOMIER, F.P., (1979). Crack Propagation Measurements on Glass: A Comparison Between Double Torsion and Double Cantilever Beam Specimens. Fracture Mechanics Applied to

Brittle Materials. ASTM STP 678 S.W. FREIMAN Ed pp 60-72

CHIANG, S.S.; Marshall, D.B., EVANS, A.G., (1982). The Response of Solids to Elastic Plastic Indentation, J. Appl. Phy.,53CD Jan 1982, pp 298-317

COLBECK, S.C., (1986), Theory of Microfracture Healing in Ice, Acta. Metal., Vol. 34, No. 1, pp 89-95.

COLE, D.M., (1986), Effect of Grain Size on the Internal Fracturing of Polycrystalline Ice, CRREL Report 86-5.

COOK, F.R., LAWN, B.R., (1984), Controlled Indentation Flaws for Construction of Toughness and Fatigue Maps, in ASTM STP 844, Methods for Assessing the Structural Reliability of Brittle Materials, Eds S.W. Frieman, C.M. Hudson, pp 22-42.

CROASDALE, K.R., METGE, M., VERITY, P.H., (1978), Factors Governing Ice Ride-Up on Sloping Beaches, Proc. IAHR Ice Symp., Pt. 1, Lulea, pp 405-420.

CROASDALE, K.R., (1988), Ice Forces: Current Practices, Proc. Int. Conf. Offshore Mechanics and Arctic Engineering, Houston, Feb. 7-12, 1988, Vol. 4, pp 133-151.

DANILENKO, V.I., (1985), Determination of Crack Resistance (K_{Ic}) of Freshwater Ice, Mechanics of Solids, Vol. 20, No.

5 ,pp 131-136.

DEMPSEY, J.P., NIGAM, D., COLE, D.M., (1988), The Flexure and Fracture of Macrocrystalline S1 Type Freshwater Ice, Proc. 7th Int. Conf. Offshore Mechanics and Arctic Engineering (OMAE) Houston, Vol. 4, pp 39-47.

DEMPSEY, J.P., WEI, Y., DEFRANCO, S., RUBEN, R., FRACHETTI, R., (1989a), Fracture Toughness of S2 Columnar Freshwater Ice; Crack Length and Specimen Size Effects - Part1, Proc. 8th Int. Conf. on Offshore Mechanics and Arctic Engineering, Vol. IV, pp 83-91.

DEMPSEY, J.P., WEI, Y., DEFRANCO, S., RUBEN, R., FRACHETTI, R., (1989b), Fracture Toughness of S2 Columnar Freshwater Ice: Crack Length and Specimen Size Effects - Part II, POAC 89 , in press.

EVANS, A.G., (1972). A Method for Evaluating the Time Dependent Failure Characteristics of Brittle Materials-and its Application to Polycrystalline Alumina. Jnl. of Mat. Sci. 7. pp 1137-1146.

EVANS, A.G., (1973), Fracture Mechanics Determinations, in Fracture Mechanics of Ceramics, Ed. Bradt, Vol. 1, pp 17-48.

EVANS, A.G., (1974). Slow Crack Growth in Brittle Materials under Dynamic Loading Conditions. Int. Jnl. of Fract Vol. 10, No. 2, June 1974, pp 251-259.

EVANS, A.G., PALMER, A.C., GOODMAN, D.J, ASHBY, M.F., HUTCHINSON, J.W, PONTER, A.R.S., WILLIAMS, G.S.(1984). Interaction Spalling of Edge Loaded Ice Sheets IAHR Symposium, Hamburg, pp 113-121.

EWALDS, H.L., WANHILL, R.J.H., (1984), Fracture Mechanics, Edward Arnold, London.

FREDERKING, R.M.W., and TIMCO, G.W., (1985). Quantitative Analysis of Ice Sheet Failure Against an Inclined Plane. Jnl. of Energy Resources Technology, Sept Vol 107. pp 381-387.

FROST, H.J., ASHBY, M.F., (1982), Deformation Mechanism Maps; The Plasticity and Creep of Metals and Ceramics, Pergamon Press.

FULLER, E.R.Jr., (1979). An Evaluation of Double Torsion Testing-Analysis. Fracture Mechanics Applied to Brittle Materials, ASTM STP 678, S.W. FREIMAN Ed., pp 3-18.

GOLD, L.W. (1963). Crack Formation in Ice Plates by Thermal Shock. Cdn. Jnl. of Phys., Vol 41, pp 1712-1728.

GOLD, L.W., (1965). The Initial Creep of Columnar-Grained Ice, Cdn. Jnl. Phys., Vol 43, No. 8, pp 1414-1434.

GOLD, L.W., (1967). Time to Formation of First Cracks in Ice in Physics of Snow and Ice, Ed. H. Oura, Inst. of Low Temp. Sci., Hokkaido University, Sapporo.

GOLD, L.W., (1977). Engineering Properties of Freshwater Ice Jnl. of Glaciology, Vol 19,No 81.

GOODMAN, D.J. (1980). Physics & Mechanics of Ice; Symposium Copenhagen August 1977. New York: Springer Verlag

GOODMAN, D.J., TABOR, D., (1978). Fracture Toughness of Ice. Journal of Glaciology, Vol. 21, No. 85, 1978, pp 651-660.

GRIFFITH, A.A., (1921). The Phenomena of Rupture and Flow in Solids. Phil. Trans. Roy. Soc. A221, pp 163-198.

GURNEY, C. and HUNT, J., (1967). Quasi-Static Crack Propagation. Proc. Roy. Soc. A299 508-524.

GURNEY, C., MAI, Y.W., (1972), Stability of Cracking, Eng. Fract. Mech., Vol 4, pp 853-863.

GURNEY, C., NGAN, K.M., (1971), Quasistatic Crack

Propagation in Nonlinear Structures, Proc. R. Soc. Lond. A, 325, pp 207-222.

HART, E.W., (1980), A Theory for Stable Crack Extension Rates in Ductile Materials, Int. J. Solids Structures, Vol. 16, pp 807-823.

HART, E.W., (1981), Stable Crack Extension Rates in Ductile Materials: Characterization by a Local Stress Intensity Factor, in Elastic-Plastic Fracture: Second Symposium, Volume 1-Inelastic Crack Analysis, ASTM STP 803, C.F. Smith and J.P. Gudas, Eds, 1983, pp I-521 - I531.

HAZMA, H., and MUGGERIDGE D.B., (1979). Plane Strain Fracture Toughness (K_{Ic}) of Freshwater Ice, In Proc. POAC 79. Norwegian Institute of Technology, Trondheim, Norway, Vol 1, pp. 697-707.

HAMZA, H., MUGGERIDGE, D.B., (1984a), A Theoretical Fracture Analysis of the Impact of a Large Ice Flow with a Large Offshore Structure. Proc. of 3rd Int. Symp. OMAE, New Orleans, Vol. III, pp 291-297.

HAMZA, H., MUGGERIDGE, D.B., (1984b). An Analysis of the Viscoelastic Fracture Toughness and Crack Growth in Ice. Cold Region Science & Tech., 9, pp 249-258.

HILL, R., (1950). The Mathmatical Theory of Plasticity. Oxford Press.

HIRAYAMA, K., SCHWARZ, J., WU, H.C., (1975), Ice Forces on Vertical Piles: Indentation and Penetration, Proc. IAHR Ice Symp. Hanover N.H., pp 429-446.

HIRTH, J.P., LOTHE, J., (1982), Theory of Dislocations, John Wiley and Sons.

HOBBS, P.V., (1974). Ice Physics. Clarendon Press, Oxford.

HSIEH, C., THOMSON, R., (1973). Lattice Theory of Fracture and Crack Creep, J. Appl. Phys., Vol., 44, No. 5, May 1973, pp 2051-2063.

HUI, C.Y., RIEDEL, H., (1981). The Asymptotic Stress and Strain Field Near the Tip of a Growing Crack under Creep Conditions. Int. Jnl. of Fract., Vol. 17, No. 4, Aug 1981 pp 409-425.

HUI, C.Y., (1983), Steady-State Crack Growth in Elastic Power-Law Creeping Materials, In, Elastic Plastic Fracture:2nd Symp., Vol 1 - Inelastic Crack Analysis, ASTM STP 803, C.F. Shih, J.P. Gudas eds, pp I-573 - I-593.

HUI, C.Y., (1986). The Mechanics of Self-Similar Crack

Growth in an Elastic Power-Law Creeping Material, Int. J. Solid Structures Vol. 22, No. 4, pp 357-372.

HUTCHINSON, J.W., (1968), Singular Behaviour at the End of a Tensile Crack in a Hardening Material, J. Mech. Phy. Solids, 1968, Vol. 16, pp 13-31.

INGLIS, G.R., (C.E., (1913), Stresses in a Plate Due to the Presence of Cracks and Sharp Corners, Trans. Inst. Naval Architects, Vol. 53, 1913, pp 219-241.

IRWIN, G.R., (1957), Analysis of Stresses and Strains Near the End of a Crack Traversing a Plate, Jnl. App. Mech., Vol 24, 1957, pp 361-364.

IRWIN, G.R., KIES, J.A., (1952), Fracturing and Fracture Dynamics, Welding Research Supplement, 1952, Vol. 17, pp 95s-100s.

IRWIN, G.R., KIES, J.A., (1954), Critical Energy Rate Analysis of Fracture Strength, Welding Research Supplement, 1954, pp 193s-198s.

KALIFA, P., DUVAL, P., RICARD, M., (1989), Crack Nucleation in Polycrystalline Ice Under Compressive Stress States, OMAE 89, Vol. IV, pp 13-21.

KETCHAM, W.M., and HOBBS, P.V., (1969). An Experimental Determination of the Surface Energies of Ice., Phil. Mag., 19, pp 1161-73.

KOLLE, J.J., (1981), Fracture Toughness of Ice, Crystallographic Anisotropy, Proc. 6th Int. Conf. on Psrt and Ocean Eng. under Arctic Conditions, Vol. 1, pp 366-374.

KUMAR, V, GERMAN, M.D., SHIH, C.F., 1981, An Engineering Approach for Elasto-Plastic Fracture Analysis, Electric Power Research Institute, Topical Report, Research Project 1237-1.

KUSUMOTO, S., TAKASE, T., UCHIDA, T., KIDERA, T., KAJI, S., (1986). Fracture Toughness of Single Ice Crystal Ice and Columnar Grained Ice. Reports- Faculty of Engineering Nagasaki University. V. 15 No. 25, 19-27.

LANDES, J. D., BEGLEY, J. A., (1976), A Fracture Mechanics Approach to Creep Crack Growth, in Mechanics of Crack Growth, ASTM STP 590, pp 128-148.

LAWN, B.R., HOCKEY, B.J., WEIDERHORN, S.M., (1980), Atomically Sharp Cracks in Brittle Solids: an Electron Microscopy Study, Jnl. Mat. Sci. 15(1980), pp 1207-1223.

LAWN, B.R., ROACH, D.H., THOMSON, R.M., (1987), Thresholds

and Reversibility in Brittle cracks, Jnl. Mat. Sci. 22, pp 4036-50.

LAWN, B.R., and SWAIN, M.V., (1975). Microfracture Beneath Point Indentors in Brittle Solids, Jnl. of Mat. Sci. 10 pp 1049-1081.

LEWIS, M.H., KARUNARATNE, B.S.B., (1981), Determination of High Temperature K_I-V Data for Si-Al-O-N Ceramics, ASTM STP 745, S.W. FRIEMAN, Ed.,American Society for Testing and Materials, 1981, pp 13-32.

LIN, I.-H., HIRTH, J.P., (1982), On Brittle Crack Advance by Double Kink Nucleation, Jnl. Mat. Sci., 17 (1982), pp 447-460.

LIN, I-H., THOMSON, R. (1986). Cleavage, Dislocation and Emmision, Shielding for Cracks under General Loading. Acta. Vol. 34, No. 2, pp 187-206, 1986.

LIU, H.W., and MILLER, E.S., (1978). Fracture Toughness of Freshwater Ice. J. Glac., Vol 22, No. 86, pp 135-142.

LIU, H.W., LOOP, L.W., (1972), Fracture Toughness of Freshwater Ice, CRREL Technical Note, Cold Regions Research and Engineering Lab, Hanover N.H.

MAI, Y.W., ATKINS, A.G., (1975), On the Velocity Dependent Fracture Toughness of Epoxy Resins, Jnl. Mat Sci. 10 (1975), pp 2000-2003.

MAI, Y.W., ATKINS, A.G., (1980). Crack Stability on Fracture Toughness Testing. Jnl. of Strain Anal., Vol. 15, No. 15 pp 63-74, 1980.

MARSHALL, G.P., COUTTS, L.H., WILLIAMS, J.G., (1974), Temperature Effects in the Fracture of PMMA, Jnl. Mat. Sci. 9(1974), pp 1409-1419.

MCKINNEY, K.R., SMITH, H.L., (1973), A Method for Studying Sub-critical Crack Growth of Opaque Materials, Am. Cer. Soc. 56, pp 30.

MICHALSKE , T.A., FRIEMAN, S.W., (1987), A Molecular Interpretation of Stress Corrosion in Silica, Nature V 295, pp 511-513.

MICHEL, B., (1978), Ice Mechanics, Les Presses de l'Univerité Laval

MICHEL, B., BLANCHET, D., (1983), Indentation of S2 Floating Icesheet in the Brittle Range, Annals of Glac. 4, 1983, pp 180-187.

MICHEL, B. and TOUSSAINT, N. (1977). Mechanism and Theory of Indentation of Ice Plates. Jnl. of Glaciology, Vol 19 No. 81 pp 285-300.

NIXON, W.A., (1988), The Effect of Notch Depth on the Fracture Toughness of Freshwater Ice, Cold Reg. Sci. and Tech., Vol. 15, No. 1, pp 75-78.

NIXON, W.A., SCHULSON, E.M., (1986a), The Fracture Toughness of Ice Over a Range of Grain Sizes, Proc. 5th Int. OMAE Symp., Tokyo, Japan, pp 349-352.

NIXON, W.A., SCHULSON, E.M., (1986b), Fracture Topughness of Freshwater Ice as a Function of Loading Rate, in Ice Technology; Proc. of 1st Int. Conf., Cambridge, Mass. pp 287-296.

NIXON, W.A., TURBELL, S.L., BENNETT, K.A., SMITH, T.R., (1989), Preliminary Results Concerning the Effects of Notch Accuity and Pre-Strain on the Fracture Toughness of Equiaxed Ice, Proc. 8th Int. Conf. on Offshore Mechanics and Arctic Engineering, Vol IV, pp 23-31.

OROWAN, E., (1945), Energy Criteria of Fracture, Weld. J. Res. Suppl., March, 1955, pp

OUTWATER, J.O., MURPHY, M.C., KUMBLE, R.G., BERRY, J.T.,

(1974). Double Torsion Technique as a Universal Fracture Toughness Test Method, Fracture Toughness and Slow Stable Cracking, ASTM STP 559, pp 127-138.

PALMER, A.C., GOODMAN, D.J., ASHBY, M.F., EVANS, A.G.,HUTCHINSON, J.W., PONTER, A.R.S., (1983). Fracture and its Role in Determining Ice Forces on Offshore Structures. Annals of Glaciology 4, pp 216-221.

PALUZNY, A., (1977), Lifetime Prediction Methodology for Ceramic Structures, Workshop on Ceramics for Advanced Heat Engines, Orlando Fla., Jan. 24, 1977.

PALUZNY, A., WU, W., (1977), Probabilistic Aspects of Designing with Ceramics, Gas Turbine Conf., Am. Soc. of Mech. Eng., Paper No. 77-gt-41, Trans of ASME. Jnl. of Eng. for Power, Oct. 1977, pp 617-630.

PARSONS, B.L., (1989), An Estimate of the Size of the Damage Zone Beneath an Indenter on Ice, OMAE89, Proc. Eighth (1989) Int. Conf. & Ex. on Offshore Mechanics and Arctic Engineering, The Haugue, The Netherlands, Mar 19-23, 1989, Vol IV, pp 411-417.

PARSONS, B.L., LAL, M., (1989), Ice Strength Dependence on Volume, Cold Regions Science and Technology, submitted.

PARSONS, B.L., SNELLEN,J.B. (1985). Fracture Toughness of Fresh Water Prototype ice and Carbimide Model Ice. Proc. 8th Int. Conf. on Ports and Ocean Engineering under Arctic Conditions POAC 85,pp 128-137.

PARSONS, B.L., SNELLEN, J.B., HILL, B., (1986). Physical Modeling and the Fracture Toughness of Sea Ice, Proc. of the Fifth (1986) International Offshore Mechanics and Arctic Engineering Symposium, Vol. IV, pp 358 - 362.

PARSONS, B.L., SNELLEN, J.B., HILL, B., (1987). Preliminary Measurements of Terminal Crack Velocity in Ice, Cold Regions Science and Technology, 13(1987), pp 233-238.

PARSONS, B.L., SNELLEN, J.B., MUGGERIDGE, D.B., (1988), The Initiation and Arrest Stress Intensity Factors Of First Year Sea Ice, IAHR, Proc. 9th Int. Symp. on Ice, Aug. 23-27, 1988, Sapporo, Japan, Vol. 1, pp 502-512.

PARSONS, B.L., SNELLEN J.B., MUGGERIDGE, D.B., (1989), The Double Torsion Test Applied to Fine Grained Freshwater Columnar Ice, and Sea Ice, European Mechanics Colloquium 239, The Mechanics of Creep Brittle Materials, 15-17 Aug. 1988, U. Of Leicester, England, in press.

PLETKA,B.J., FULLER,E.R.Jr., KOEPKE,B.G., (1979). An Evaluation of Double Torsion Testing-Experimental, in

Fracture Mechanics Applied to Brittle Materials, ASTM STP 678, S.W.FREIMAN Ed., pp 19-37.

POPELAR, C.H., KANNANIN, M.F., (1987), Advanced Fracture Mechanics, Oxford Engineering Science Series 15, Oxford University Press.

RICE, J.R. (1966), An Examination of the Fracture Mechanics Energy Balance from the Point of View of Continuum Mechanics, in Proc. 1st Int. Conf. on Fracture (Sendar 1965), Ed. T. Yokobori et al, Japanese Soc. fro Strength and Fracture, Tokyo, Vol. 1 pp 309-340.

RICE, J.R., (1968), A Path Independent Integral and the Approximate Analysis of Strain Concentrations by Notchs and Cracks, Jnl. Appl. Mech., 35, pp 379-386.

RICE, J.R., (1976), Elastic-Plastic Fracture Mechanics, in The Mechanics of Fracture, Mech. Fract. ASME Winter Annu. Meet., 1976, AMD 19, 33(1976)

RICE, J.R., (1987), Mechanics of Brittle Cracking of Crystal Lattices and Interfaces, in Chemistry and Physics of Fracture, Eds R.M. Latanision, R.H. Jones, NATO ASI Series, Series E: Applied Sciences - No. 130, pp 23-43.

RICE, J.R., ROSENGREN, G.F., (1968), Plane Strain Deformation Near a Crack Tip in a Power Hardening Material, J. Mech. Phy. Solids, Vol. 16(1968), pp 1-12.

RICE, J.R., THOMSON, R, (1974), Ductile Versus Brittle Behavior of Crystals, Phil. Mag., Vol. 29 (1974), pp 73-96.

RIEDEL, H., (1987), Fracture at High Temperatures, Springer-Verlag, Berlin.

RIEDEL, H., RICE, J.R., (1980). Tensile Cracks in Creeping Solids. ASTM STP 700, pp 112-130.

RITTER, J.E. JR. CAVANAUGH, M.S., (1976), Fatigue Resistance of a Lithium Aluminosilicate Glass-Ceramic, Jnl. Am. Cer. Soc., Vol. 59, pp 57-59.

SANDERSON, T.J.O., CHILD, A.J., (1986), Ice Loads on Offshore Structures: The Transition from Creep to Fracture, Cold Regions Sci. and Tech., 12(1986), pp 157-161.

SANO, O., (1988), A Reveision of the Double-Torsion Technique for Brittle Materials, Jnl. Mat. Sci. 23(1988), pp 2505-2511.

SELBY, K., MILLER, L.E., (1975), Fracture Toughness and the Mechanicla Behaviour of an Epoxy Resin, Jnl. Mat. Sci. 10

(1975), pp 12-24.

SHEN, W., LIN, S.-Z., (1986), Fracture Toughness of Bohai Bay Sea Ice, Proc. 5th Int. Symp. OMAE, Vol. 4, pp 354-357.

SIH,G.C. (1973). Hydrodynamics Handbook of Stress Intensity Factors, Lehigh University, 6th Ed. Dover

SINHA, N.K., (1978). Short Term Rheology of Polycrystalline Ice, Jnl. of Glac., Vol. 21, No. 85,1978, pp 457-473.

SINHA, N.K., (1979). Grain Boundary Sliding in Polycrystalline Materials. Phil. Mag. Vol.40,No. 6, 825-842.

SINHA, N.K., (1981), Rate Sensitivity of Compressive Strength of Columnar-Grained Ice, Exper. Mech., 21(6), pp 209-218.

SINHA, N.K., (1982a). Delayed Elastic Strain Criterion for First Cracks in Ice., Int. Union of Theoretical and Applied Mechanics, Symp. on Deformation and Failure of Granular Materials., Aug 31, pp 323-330.

SINHA, N.K., (1982b), Acoustics Emission and Microcracking in Ice, Proc. 1982 Society of Experimental Stress Analysis (SESA) and Japan Society for Mechanical Engineers (JSME),

Hawaii, Part II, pp 767-772.

SMITH, R.A., (1976). The Application of Fracture Mechanics to the Problem of Crevasse Penetration, Jnl. of Glac., Vol. 17, No. 76, 1976, pp 223-228.

SODHI, D.S., HAMZA, H.E., (1978), Buckling Analysis of Semi-Infinite Ice Sheet, Proc. Int. Conf. POAC, Vol. 1, Trondheim, pp 797-810.

SUNDER, S.S., Ting, S.-K., (1985), Ductile To Brittle Transition in Sea Ice Under Uni-Axial Loading, 8th Int. Conf. POAC, Narssarssuaq Greenland, Sept. 7-14, 1985, Vol. 2, pp 656-666.

TADA, H., PARIS, P., IRWIN, G.R., (1973), The Stess Analysis of Cracks Handbook, Hellertown, Penna: Del Reseach Corp.

THOMSON, R., (1978), Brittle Fracture in a Ductile Material with Application to Hydrogen Embrittlement, Jnl. Mat. Sci. 13 (1978), pp 128-142.

THOMSON, R., (1986), Physics of Fracture, Solid State Physics, Vol. 39, H. Ehrenreich, D. Turnbull Eds., Academic Press, pp 1 - 129.

THOMSON, R., (1987), Physics of Fracture, J. Phys. Chem.

Solids, Vol. 48, No. 11, pp 965-983.

THOMSON, R., FULLER, E.R. Jr., (1982), A Crack as a Crystal Defect, in Fracture Mechanics in Ceramics (R. Bradt et al eds.), Plenum, pp 253-276.

THOMSON, R., HSIEH, C., RANA, V., (1971). Lattice Trapping of Fracture Cracks, J. Appl. Phys., Vol. 42, No. 8, July 1971, pp 3154-3160.

TIMCO, G.W., (1987a). Indentation and Penetration of Edge Loaded Freshwater Ice Sheets in the Brittle Range. Jnl. Offshore Mechanics and Arctic Engineering, Aug. 1987, pp 287-294.

TIMCO, G.W., (1987b), Ice/Structure Interaction Tests With Ice Containing Flaws, Jnl. Glac., Vol 33, No. 114, pp 186-194.

TIMCO, G.W. and FREDERKING, R.M.W. (1983). Flexural Strength and Fracture Toughness of Sea Ice. Cold Regions Science and Technology 8 (1983) pp. 35-41.

TIMCO, G.W., FREDERKING, R.M.W., (1986), The Effects of Anisotropy and Microcracks on the Fracture Toughness of Freshwater Ice, Proc. 5th Int. Conf. Offshore Mechanics and

Arctic Engineering, Tokyo, Japan, 13-17 Apr. Vol. 4, pp 341-348.

TIMOSHENKO, S.P., GOODIER, J.N., (1970), Theory of Elasticity, McGraw-Hill, Toronto.

TOZAWA, S, TAGUCHI, Y., (1986), A Preliminary Study of Scale Effect on Flexural Strength of Ice Specimens, Proc. 5th Int. Symp. OMAE Vol. IV, pp 336-341.

TRANTINA, G.G., (1977), Stress Analysis of the Double Torsion Specimen, Jnl. of Amer. Cer. Soc., Vol. 60, No.7-8,July-Aug. 1977, pp 338-341.

TROUNG, V.-T., (1989), Relationship Between the Micromechanics of the Crack Tip and the Fracture Toughness of Crosslinked Epoxy, Jnl. Mat. Sci. Letters, 8(1989), pp 442-444.

TSENG, A.A., and BERRY, J.T., (1979), A Three-Dimensional Finite Element Analysis of the Double-Torsion Test, Jnl. of Press. Ves. Tech., Vol 101, 1979, p 328.

TUHKURI, J., (1987), The Applicability of LEFM and the Fracture Toughness (K_{Ic}) to Sea Ice, POAC 87, pp 21-32.

URABE, N, IWASAKI, T. and YOSHITAKE, A. (1980). Fracture Toughness of Sea Ice, Cold Regions Science and Technology, 2 (1980) pp. 29-37.

URABE, N., YOSKITAKE, A. (1981a). Fracture Toughness of Sea Ice. Proceedings of POAC (1981) p. 356.

URABE, N., YOSHITAKE, A. (1981b). Strain Rate Dependent Fracture Toughness of Pure Ice and Sea Ice. International Symposium of Ice, Quebec, (1981) pp 551-564.

VAUDREY, K.D., (1977), Ice Engineering - Study of Related Properties of Floating Sea-Ice Sheets and Summary of Elastic and Viscoelastic Analyses, Tech. Rep. R 860, Civil Eng. Lab., Naval Const. Battalion Center, Port Hueneme, California.

VIRKAR, A.V., JOHNSON, D.L., (1976), Some Kinetic Considerations Regarding the Double-Torsion Specimen, Jnl. Am. Cer. Soc., Vol. 59, No. 5-6, pp 197-200.

WEERTMAN, J., (1978), Fracture Mechanics: A Unified View for Griffith-Irwin-Orowan Cracks, Acta. Metall., Vol 26, pp 1731-1738.

WEERTMAN, J., (1983), Creep Deformation of Ice, Ann. Rev. Earth Planet Sci. 1983, 11, pp 215-240.

WESTERGAARD, H.M., (1939). Bearing Pressures and Cracks, Jnl. of Appl. Mech., Vol. 6, No. A, 1939, pp 49-53.

WILLIAMS, D.P., and EVANS, A.G., (1973), A Simple Method for Studying Slow Crack Growth., Jnl. of Testing and Evaluation., Vol. 1, No. 4, pp 264-270.

WU, K.-C., HART, E.W., (1987), Steady State Crack Growth in Elasto-Viscoelastic Materials, Int. Jnl. Fract. 33, pp 175-194.

YAMINI, S. Young, R.J. (1980), Stability of Crack Propagation in Epoxy Resins, Polymer, 1977, Vol. 18, pp 1075-1080.

SUMMARY OF FRACTURE-TOUGHNESS DATA FOR FRESH WATER, GLACIER AND SEA ICE

Glacier Ice

Andrews et al (1984), K_{Ic} = 125 $kNm^{-3/2}$, grain size = 18 mm, prepared crack length = 7 - 30 mm. Fracture measured from samples prepared from ice cores, a radially cracked ring was was fractured with internal pressure. Ice collected from Roslin Gletscher, lat 71°N, long 24°W, Ice temp -1 °C, air temp +6° C, 194 results, 20 outside range of validity for geometry, due to crack length to grain size ratio, 30 more invalid, no statistical correlation between rate and toughness.

Andrews (1985) K_{Ic} = 58 $kNm^{-3/2}$, grain size = 9.6 - 3.2 mm, crack length = 10 mm. Lat 72°N, long 24°W, Bersaerkerbrae,Greenland; samples were radially cracked ring fractured by internal pressure, results half that of other workers. Outside diameter 79 mm, inside 40mm, thickness 29mm, crack sharpened by drawing fine wire across notch cut with hacksaw. Nineteen lab tests at -12° C gave 120 ± 12 $kNm^{-3/2}$. Great difficulty preparing samples, broke while drilling centre hole, air temperature +4°C. Time to failure 10 s, rate 6 $kNm^{-3/2}s^{-1}$, twenty samples. No trend in

fracture toughness with specimen thickness, crack length, or depth of sample Results held to be valid plane strain test, but are corrected by formula of Urabe & Yoshitake (1981) for longer effective crack length, due to bubbles, grain size.Conclude results not affected by crack tip plasticity, but sample size too small for grain size.

Freshwater Laboratory Grown Ice

Gold (1963), thermal shock, K_{Ic} = 50-160 $kNm^{-3/2}$, grain size = 1.5 - 6 mm, crack length = 2.4 - 9 mm. K_{IC} at arrest of propagation, resulting from two pieces of ice at least 6°C apart in temperature being brought together. Results not particular to crystal orientation, calculated from thermal stress gradient calculations. There was a preference for cracks to form parallel to the basal and prismatic planes.

Liu & Loop (1972), compact tension specimen (CTS), K_{IC} = 90 - 160 $kNm^{-3/2}$, grain size = 2.5 - 6 mm, crack length = 50 mm. Compact tension specimen with 25.4 mm thickness used. The crack was prepared at the root of a band saw cut by forcing a razor slowly into the ice to avoid actual cracking. Tip radius was less than 0.08 mm. This was then covered with silicon grease to avoid sublimation, placed in

plastic bags and stored at test temperature for twenty-four hours. A precooled tank was seeded with 6 mm thick layer of fine grained ice, precooled water added, and ice formed by freezing from bottom up, while air above tank was kept above freezing. The tank was mechanically vibrated to obtain bubble free ice. Polycrystalline columnar ice with grain size 2.5 to 5 mm was obtained. Toughness decreases from 160 $kNm^{-3/2}$ at -40° C to 90 $kNm^{-3/2}$at -2°C. Two rates 46 $kNm^{-3/2}s^{-1}$, and 4.6 $kNm^{-3/2}s^{-1}$, highest toughness for slowest rate.

Liu & Miller, (1979), CTS, K_{Ic} = 124 $kNm^{-3/2}$, grain size = 5 mm, crack length = 50 mm. Used the compact tension specimen, approximately 125 mm square. The crack tip was prepared with a razor, with notch tip radius less than 0.0025 mm, and then covered with silicon grease to prevent sublimation. Some specimens were precracked, it is not said how, and these give results no different than the notched samples. The 25.4 mm thickness was considered adequate to ensure plane strain conditions at the crack tip. The ice was polycrystalline, columnar, bubble free, formed by spraying fine mist on bottom of tank, then adding precooled water, and freezing from the bottom up. The four fastest loading rates were displacement controlled; 580 mm/min, 50mm/min, 10 mm/min, and 1 mm/min. The two slowest rates ,

0.6mm/min and 0.05 mm/min were load controlled. All results showed temperature dependence, toughness increasing with decreasing temperature. The fastest rate, greater than 1000 $kNm^{-3/2}s^{-1}$ provided the lowest toughness, approximately 110 $kNm^{-3/2}$. The slowest rate supplied toughness of approximately 400 $kNm^{-3/2}$. The rate dependence is explained as a consequence of stress relaxation in the vicinity of the crack tip, requiring a higher applied K to reach the same level of fracture stress at the crack tip. Toughness tests done in water at low rate, approximately 2 $kNm^{-3/2}s^{-1}$are approximately half that in air, 240 and 180 $kNm^{-3/2}$ compared to 420 and 480 $kNm^{-3/2}$, following an ice-water surface energy that is half ice-air surface energy. Five arrest values obtained from wedge opening compact tension specimen, 134, 152 $kNm^{-3/2}$ at -12°C, 142 $kNm^{-3/2}$at -9°C, and 138, 152 $kNm^{-3/2}$ at -4°C; slightly lower than static fracture toughness. Unable to obtain arrest at temperatures lower than -12°C.

Goodman and Tabor (1978), SEN 3 pt, K_{IC} = 116 $kNm^{-3/2}$,grain size = 1mm to single crystal, crack length = 10 mm, temperature = -13°C. Also used pyramid indenter, K_{IC} = 170-290 $kNm^{-3/2}$ on single crystal, and conical indenter, K_{IC} = 300 $kNm^{-3/2}$ on single crystal. Distilled water was used and bubble free ice obtained, grain size varied from 1 mm to

single crystal. Three and four point tests were done, and indentation with Vickers indenter. The crack was prepared by pushing a razor into the ice while avoiding cracking. In the Vickers indenter tests cracks 1 to 10 mm long were obtained as load was varied, at -28°C and -20°C. Three point bending tests at -13°C, unspecified rate , gave toughness of 116 ± 13 $kNm^{-3/2}$. Loading time was 10 seconds approximately. The Vickers indenter (half angle 68°) results were found to be lower by about a third than those obtained with a sharper cone (half angle 30°). These were adjusted by assuming an effective half angle of 45° due to the plastic zone beneath the indenter, supplying an increase of 2.5 from the algorithm for calculating the toughness. The results for the pyramid adjusted in this was were 70 ±15 $kNm^{-3/2}$ at -38°C, 210 ± 40 $kNm^{-3/2}$ at -20°C; and for the cone, 240 ± 50 $kNm^{-3/2}$ at -20°C, and > 300 $kNm^{-3/2}$ at -16°C.

Hamza and Muggeridge (1979), SEN 3 pt, K_{Ic}= 40-190 $kNm^{-3/2}$ grain size = 8,12 mm, crack length = 10 mm. Bubble free freshwater ice was made from boiled tap water at -23.°C, both by seeding with snow and with no seeding, resulting in grain size of 8 mm and 12 mm. Only columnar grained ice was tested. Prepared notch was sharpened with a razor blade, and left for twenty four hours before testing. Four temperatures and four crosshead rates were used, showing

toughness decreased from average 142 $kNm^{-3/2}$, to 40 $kNm^{-3/2}$ as temperature went from -40°C and 0.1 mm/min to -4°C and 50.0 mm/min. The larger grain size ice had higher toughness in all conditions.

Goodman (1980) SEN 4 pt, K_{IC}= 118 $kNm^{-3/2}$, grain size = 10 mm, crack length = 5-10 mm, $\dot{K}_{IC}$ = 10^3 $kNm^{-3/2}s^{-1}$. Polycrystalline ice, four point bend geometry. To meet restriction of LEFM assumes the strain rate at the crack tip to be $10^{-1}s^{-1}$, to provide conservative estimate of ice yield strength and thus plastic zone size of approximately 0.6 mm. High load rates, 500 N/s, are used to avoid plastic zone at the crack tip becoming significant. The fracture toughness at -4°C from 44 samples, 118 ± 32 $kNm^{-3/2}$; at -11°C from 40 samples, 119 ± 34 $kNm^{-3/2}$; and at -24°C from 44 samples, 108 ± 21 $kNm^{-3/2}$. Preliminary results at -38°C indicate that at the load rates used the toughness does not vary with temperature. The ice was columnar with grain size 5 - 10 mm, and the crack prepared with a scalpel. Recommends that COD measurements be used to observe any contribution of plasticity at crack tip.

Kollé (1981), SEN 3 pt, K_{IC} = 240, 186 $kNm^{-3/2}$, grain size = 10 mm, prepared crack = 8 mm. Ice was freshwater,columnar, tested in three point bending, crack oriented across and

along basal plane. Across basal plane toughness was 240 ± 79 $kNm^{-3/2}$, and along were 186 ± 82 $kNm^{-3/2}$, explained by the anisotropy of creep of ice. Samples were .22 x .025 x .05 m, and load rate was 4.8 N/s. Strain rate was estimated to be 3 x $10^{-6}s^{-1}$, in the equivalent un-notched beam. Crack tip was sharpened by running a razor along a saw cut, and a small (1 to 2 mm) micro crack was observed to form. Grain size was approximately 1 cm. Test temperature was -17°C. Discrepancies with other, earlier work explained by slower loading rate used .

Azadeh-Tehrany, (1983), 78 < K_{Ic} < 182 $kNm^{-3/2}$ for -4 < T < -20°C, 50 mm/min > displacement rate > 2.5 mm/min, 8 < grain size < 17 mm. Three point bend specimen used, LEFM shown to be applicable. Crack Opening Displacement measurements were used in a LEFM calculation to calculate the energy release rate, found to be 0.79 J/m^2 minimum, and 3.27 J/m^2 maximum. The toughness increased with decreasing temperature and increasing rate of loading, and decreased with increasing brine volume and decreasing grain size, and agreed well with previous work. Yield strength was calculated to be 0.24 < σ < 1.80 MPa, using the LEFM relationship between COD, G and K_{Ic}. K_{Ic} for freshwater ice was 62 $kNm^{-3/2}$ for crosshead speed 0.1mm/min , 0.4 mm/min, and 3.6 mm/min for temperatures of-4°C, and -21°C. Average grain sizes varied

from 9mm in one experiment to 12 mm in another. The average toughness for artificial saline ice varied from 78 $kNm^{-3/2}$ to 182 $kNm^{-3/2}$ for average grain size 144 mm, salinity 6.8 ‰ at temperatures of -4°C, -7°C,-11°C and -20°C, for crosshead speeds 2.5 mm/min, 5 mm/min and 50 mm/min.

Andrews and Lockington (1983), Pressurized crack, K_{Ic} = 105 $kNm^{-3/2}$, grain size = 2-5 mm, crack length = 50 mm, failure time = .02-.9 s. The fracture energy was measured with a unique specimen geometry, for ice, ice frozen to steel and titanium substrates. The fracture energy was 1 J/m^2 for relatively high loading rates, and never higher than 3 J/m^2. Adhesion energies differences were attributed to layer of bubble ice that is prone to time-dependent micro-cracking. The presence of interfacial melting and thus a layer of disorder as temperature approaches 0°C, or one containing high concentration of a eutectic phase in the presence of salt solutions, controls the transition from cohesive failure.

Andrews (1985) see above.

Danilenko (1985), Double Cantilever Beam (DCB), K_{Ic}= 180 -440 $kNm^{-3/2}$, grain size = 1 mm to single crystal, crack length = 7.5 mm. Large (.1 x .1 x .1 m) mono-crystals and

multigrain columnar with grain size 1-2 mm on upper and 8-10 mm on lower surface. Prepared cracks were sharpened with a scalpel, and loaded to failure in 0.1 to 1.0 seconds. Temperature from 0°C to -20°C. Load increased linearly, the dropped abruptly at fracture, fracture surface was similar to that of silicate glass. Fracture toughness depended weakly on rate. Fracture toughness of monocrystal depends only weakly on crystal anisotropy, notch in basal plane was 202 ± 34 $kNm^{-3/2}$ at 0°C, 336± 94 $kNm^{-3/2}$at -10°C, and 111 ± 85 $kNm^{-3/2}$at -15°C; notch coincident with c-axis was 147 ± 28 $kNm^{-3/2}$ at 0°C, 335 ± 50 $kNm^{-3/2}$at −10°C, and 439 ± 72 $kNm^{-3/2}$ at −15°C; and for notch parallel to c-axis 184 ± 31 $kNm^{-3/2}$ at 0°C, 318 ± 40 $kNm^{-3/2}$at -10°C and 460 ± 150 $kNm^{-3/2}$at −15°C. Similarly the results for columnar grained ice increased at lower temperatures, from 200 $kNm^{-3/2}$ at 0°C to 300 $kNm^{-3/2}$ at -15°C, with a slight increase as average grain size increases from 3 to 8 mm .

Kusumoto et al (1985), SEN 3 pt, K_{Ic} = 80-150 $kNm^{-3/2}$single and bi-crystal, crack length = 15 mm. Original paper in Japanese, with no translation available, though figures are captioned in English. Single edge notched beams tested at -10°C at rate between 1 to 3800 $kNm^{-3/2}s^{-1}$. The crack was sharpened by pressing razor into the root of a saw cut.

Toughness was not dependent on rate above 30 $kNm^{-1/2}s^{-1}$, and was approximately 100 $kNm^{-3/2}$. Cracks 45° to the C-axis had slightly lower toughness than cracks oriented 0° and 90° to c-axis, but variation was small.

Parsons and Snellen (1985), DCB, K_{IC} = 90-250 $kNm^{-3/2}$, grain size = 10-100 mm, crack length = 150-250 mm, 70°N,134°W cold freshwater ice with large grain size, 5-10 cm tested at the mouth of McKenzie River. Large samples were used ranging in size from .45 x .45 x .90m to .90 x .90 x 2.0 m, to meet demands of LEFM. Air temperature -15°C to-20°C. Anisotropy of the columnar ice was investigated, and the spalling crack found to be the toughest. The large grains may have been responsible for the large scatter in the results, and for the higher toughness. The rate dependence appeared opposite from that of fine grained freshwater ice, increasing from 150 to 400 $kNm^{-3/2}$, for load rate increasing from 4 to 130 $kNm^{-3/2}s^{-1}$. Results are too few to be compelling. This was, however, very unusual ice. The authors expected sea ice at this site, forty miles offshore, and the grain size was large as in sea ice, but the water was fresh, due to presence of the McKenzie River. There were no brine drainage channels, which have been associated with effective flaw size by Urabe et al (1981b). No other results for large grained freshwater columnar ice are in the literature.

Nixon and Schulson (1986a), Notched Right Circular Cylinder, K_{Ic} = 60-140 $kNm^{-3/2}$, grain size = 1.6 - 9.3 mm, notch depth 8 mm, all tests at -10°C on circumferentially notched right circular cylinders of randomly oriented polycrystalline freshwater ice. Grain size was varied from 1.6 mm to 9.3 mm, and toughness observed to decrease by 25 % at 10 $kNm^{-3/2}s^{-1}$, as grain size increased. Notch depth was 8 mm, reducing section to 75 mm, and then further sharpened by machine held razor, further reducing diameter by 0.5 mm. The machining was done with new blade, 16-20 hours prior to testing, to avoid notch tip blunting due to sublimation. Two load rates, 10 and 0.01 $kNm^{-3/2}s^{-1}$ were used, twelve results at the higher rate and four at the lower. A regression analysis of the data to the equation $K_{Ic} = K_0 + Kd^n$, but no value of n between -2 and +2 had a clearly better fit, so n = 1 was chosen, K_0 = 92.8 and K = 2.5, with $r^2 = 0.62$. By choosing n = -0.5 to fit the Hall Petch relationship, they obtain $K_{Ic} = 42.4 + 58.3d^{-0.5}$ with r^2 = .60. At the lower rate, they conclude plane strain is not achieved, as the creep zone size calculated from Riedel and Rice (1980) exceeds 1/50 the notch depth after 53 seconds. They conclude the large scatter in reported toughness values of ice cannot be accounted for by grain size effects alone, and suggest notch acuity, specimen size effects, and method

of sample preparation may contribute.

Nixon & Schulson, (1986b), Notched Right Circular Cylinder,K K_{Ic} = 67 - 140 $kNm^{-3/2}$, grain size 2.2 and 8.2 mm, notch depth 8mm, temperature = -10°C, rate 0.01 - 10^5 $kNm^{-3/2}s^{-1}$. Circumferentially notched right circular cylinders were made from randomly oriented polycrystalline freshwater ice, to determine influence of loading rate on ice fracture toughness, from 0.01 to 10^5 $kNm^{-3/2}s^{-1}$. Grain size was held constant within 10%, and all tests were done at -10°C. Above 10 $kNm^{-3/2}s^{-1}$, ice toughness is constant, 75.5 ± 3.0 $kNm^{-3/2}$ for grain size 8.2 ± 0.3 mm; and 89.6 ± 3.4 $kNm^{-3/2}$ for grain size of 2.2 ± 0.2 mm. As the loading rate decreases to 0.01 $kNm^{-3/2}s^{-1}$ the toughness increases monotonically to 117.3 ± 0.8 $kNm^{-3/2}$ for grain size 8.2 ± 0.3 mm, and to 137.5 ± 0.5 $kNm^{-3/2}$ for grain size of 2.2 ± 0.2 mm. Using the algorithm of Riedel and Rice (1980) good agreement between a calculated time for plain strain conditions to switch to plane stress, and the observed increase in toughness with decreasing rate was found, at about K_{Ic} = 1.9 $kNm^{-3/2}s^{-1}$ for this specimen geometry. This was calculated with n = 3, then recalculated with n = 8.2, to obtain a transition rate of 4.9 $kNm^{-3/2}s^{-1}$, indicating the calculation is not very sensitive to n. These calculations are for -10°C, and the critical rate will

need to be higher at higher temperatures to ensure plane strain, and may lower at colder temperatures.

Timco and Frederking (1986), SEN, K_{Ic} = 70 - 190 $kNm^{-3/2}$grain size = 1 - 4 mm, crack length = 12 mm. Tested ice that had first been loaded in compression until microcracking appeared in ice. For vertical crack propagating horizontally in columnar ice with c-axis in horizontal, $K_{Ic} = 188\ \dot{K}_I^{-.13}$, for $6 < \dot{K}_I < 90$ $kNm^{-3/2}s^{-1}$, compared to $K_{Ic} = 216\ \dot{K}_I^{-.11}$ from Urabe and Yoshitake (1981b). Reported $K_{Ic} = 87 \pm 10$ $kNm^{-3/2}$ for vertical crack propagating vertically into the same ice, and no rate dependence over the same load rate range. Higher fracture toughness results of 240 $kNm^{-3/2}$ obtained at rate of 2 $kNm^{-3/2}s^{-1}$ were not included, as it was felt that the requirements of LEFM were not met, in particular that the creep zone calculated from Riedel and Rice (1980) was too large. In order to meet the requirements of LEFM, it was calculated tests must be done within 45 seconds of sharpening the crack tip. For horizontally propagating cracks fracture toughness dependence on time to failure was found to be $K_{Ic} = 97t^{0.16}$, due to the contribution of plastic work involved in advancing the crack. At time to failure of 0.01 second, this predicts pure brittle ice fracture. As a function of crack density, $K_{Ic} = 127$ $kNm^{-3/2}$

- $4.2C_p$, $0 < C_p < 7$ cracks/cm^2, all tests done at the same nominal loading rate, and time to failure of approximately 5 seconds.

Nixon (1988), Notched Right Circular Cylinder, K_{Ic} = 60 to 120 kNm$^{-3/2}$, grain size 3.4 and 7.3 mm, notch depth varied from 2.54 to 17.8 mm. Polycrystalline freshwater ice, for the smallest notch, none of the samples broke at the notch. Results were in the range 60 to 120 kNm$^{-3/2}$, with no significant variation for notch depths greater than 5.1 mm. For notch depth less than 2.5 mm,dislocation build-up elsewhere in the sample would appear to supply greater stress concentration.

Bentley et al (1988), Tapered Double Cantilevered Beam(TDCB), K_{Ic} = 126 - 165 kNm$^{-3/2}$, grain size = 2.4 - 3.4 mm, crack length = 88-190 mm, temperature = -2°C. Floating Tapered Double Cantilever beam was wedge loaded. Thirty tests at -2° to 0°C were done. Grain size was 2.4 mm at top and 3.4 mm at bottom. The effective modulus was measured during the loading to failure of the specimen. Load rates were $215 < \dot{K}_I < 1010$ kNm$^{-3/2}$s^{-1}, with little influence on fracture toughness, $126 < \dot{K}_I < 165$ kNm$^{-3/2}$. Crack Mouth Opening Displacement was measured, and crack velocity for 5 milliseconds was calculated at 240 to 390m/s.

Unable to obtain crack arrest, due to loading system compliance, blunt crack tips, and high loading rates.

Parsons, Snellen and Muggeridge, (1989), Double Torsion (DT), K_{Ic} = 124 ± 38 $kNm^{-3/2}$, K_{Ia} = 91 ± 28 $kNm^{-3/2}$, grain size 1-5 mm, crack length 200 - 350 mm, temperature = -20°C. Double torsion geometry used on lab grown fine grain columnar ice, no stable sub-critical crack growth was observed. Two samples were deadweight loaded at 25 and 40 $kNm^{-3/2}$ for five days each, with no crack growth observed. Crack growth was abrupt and proceeded in slip/stick mode, the resulting crack length was not load rate dependent. The creep of ice delays initiation to higher loads at slow load rates, but longer cracks do not necessarily result.

Dempsey et al (1989), S2 columnar grained freshwater ice was tested in three and four point bend specimens, in one crack orientation and grain size, while the crack lengths were varied from very short to very long to study crack size effects. The crack was oriented with respect to columnar grains as a radial crack. Aim of the study was to determine minimum crack length with respect to grain size for valid tests. Average grain size was 3mm, and tests were done at -10°C. The crack tip was sharpened with a teflon coated razor, care being taken to avoid micro-cracking, and the

razor left in place until testing. Fracture tests done on identical samples with crack tips sharpened with 0.2 mm diameter diamond coated wire, provided consistently higher results. CMOD was measured with MTS clip gauge. Crosshead rate was 7.62 mm/min, and failure occurred within 6 seconds, load rate between 10 and 100 $kNm^{-3/2}s^{-1}$. A small K_Q was observed for crack length to grain size ratio between 6.5 and 10, for depth to grain size ratio = 17. For depth to grain size ratio of 25 the K_Q plateau ranges from 7 to 13 the crack length to grain size ratio. The largest plateau was established for sample depth to grain size ratio of 34, the toughness being approximately constant for crack length to grain size ratio greater than 10.

Nixon et al (1989), circumferentially notched samples (diameter 91 mm, length 231 mm, notch depth 9.156 mm) of equiaxed freshwater ice were tested at 10 $kNm^{-3/2}s^{-1}$, and $-10^{\circ}C$. Grain size was 7.5 ± 0.5 mm. The sharpness of the notch was varied from 2×10^{-3} mm to 4 mm, six toughness tests at six different radii indicate toughness increases from 70 to 110 $kNm^{-3/2}$. To measure effects of precracks on toughness, samples of grain size 2.8 ± 0.3 mm were loaded in compression at strain rate $10^{-5}s^{-1}$ to pre-strains between 0% and 2%. Toughness decreased from 90 $kNm^{-3/2}$ at zero prestrain, density 916 kg/m^3, to 65 $kNm^{-3/2}$ at 2% prestrain

and density of 850 kg/m^3, for six experimental results.

Dempsey and Wei (1989), macrocrystalline type S1 freshwater ice was tested at -10°C. Used four point bending geometry. Fractographic analysis was carried out on the fracture surfaces. Fracture toughness from 116 to 675 $kNm^{-3/2}$ were reported, loading rates from 45 to 240 $kNm^{-3/2}s^{-1}$. Specimens with larger (up to 10 cm) grain sizes had higher toughness, associated with cleavage. Specimens with smaller grain sizes had lower toughness, associated with decohesive rupture. It was postulated that ice has an equicohesive temperature for certain types of ice, above this the toughness increases with grain size, below it it decreases with decreasing grain size.

Sea Ice

Vaudrey, (1977), SEN 4pt, K_{Ic} = 28-100 $kNm^{-3/2}$, grain size = 10 mm, crack length = 12 mm, temperature = -10°C, -20°C. Sea ice specimen size .05 x .05 x .5m with crack length 12 mm,support span .5m, load span 15 cm, regression yields toughness dependence of $K_{Ic} = 144\ kNm^{-3/2} - 12.4\sqrt{\nu}$, $4 \leq \sqrt{\nu} \leq 7$, and $28 \leq K_{Ic} \leq 130\ kNm^{-3/2}$, where ν is brine volume in ppt.

Urabe et al (1980), SEN 3 pt, K_{Ic} = 98 $kNm^{-3/2}$, grain size = 5-10 mm, crack length = 50 mm, temperature = -2°C. Fracture toughness was constant for strain rate less than 10^{-1} s^{-1}, decreases with increasing strain rate above $10^{-1}s^{-1}$, for cracks prepared in bottom of ice sheet, no data at higher rates for other crack orientations. Large specimens (.2 x .3 x 1.6m), were tested, sea water and air temperature -2°C, with in situ tests of 45 cm thick Saroma ice. The load record was linear, with abrupt load drop and minimal deformation, suggesting LEFM was applicable. Cracks on bottom of ice gave higher toughness than those on top, on side are intermediate. Conclude flaw size, the distance from brine channel to brine channel, is 2.5 mm for top surface, 1.9 cm for bottom surface.

Urabe et al (1981a), SEN, K_{Ic}< 135 $kNm^{-3/2}$, grain size 3 - 22 mm, crack length = 80 mm, temperature = -2°C. Calculated flaw sizes agree well with subgrain sizes, and are independent of $\dot{K}_I$. $K_{Ic} = 135\ e^{-1.9/\sqrt{d}}$, where d is subgrain size in mm. Specimen size is large, 20 x 40 x 160 cm. Fracture toughness constant with rate for rate less than 100 $kNm^{-3/2}s^{-1}$, and decreases for rate greater than this.

Urabe et al (1981b), Notched Cantilever Beam, and SEN, K_{Ic} = 50 $kNm^{-3/2}$, grain size not specified, crack length = 80 mm, temperature = -2°C. Fracture toughness was measured with the usual SEN specimen,and with a notched cantilever beam, which is not an ASTM standard geometry, but is convenient for in situ testing of ice. Results were identical, within small scatter. Notched cantilever 40 x 40 x 200 cm.

Timco and Frederking (1982), SEN 3&4 pt, K_{Ic} = 110 $kNm^{-3/2}$, grain size = 2 mm, crack length = 12 mm. All reported results corrected with algorithm of Urabe et al (1981b) to account for prepared crack lengths that were not significantly longer than the large grain size of the ice. The correction increased K_{Ic} by 9 - 43 %. Load-time curves were linear, and load drop abrupt, with failure time 9 -15 seconds. Fracture toughness was constant 110 $kNm^{-3/2}$ in granular region of ice, increasing with increasing depth and grain size. As depth into ice increased from 10 to 60 cm fracture toughness increased to 145 $kNm^{-3/2}$. Results dependent on brine volume, decreasing from 145 to 85 $kNm^{-3/2}$ as brine volume increased from 15 ‰ to 55 ‰, and suggest grain size, not subgrain is effective flaw size.

Parsons, Snellen and Hill (1986), DCB, K_{Ic} = 55-875 $kNm^{-3/2}$, grain size = 10-100 mm, crack length = 150-250 mm,

temperature = -25°C to -8°C, 74°N, 95°W, Allen Bay, NWT (near Resolute NWT); cold sea ice. Preferred c-axis orientation in ice has influence on temperature dependence of fracture toughness, below -8°C the spalling crack is toughest, K_{Ic} = 291 ± 187 $kNm^{-3/2}$for 34 results, with maximum obtained of 875 $kNm^{-3/2}$, for 7.7 < $\dot{K}_I$ < 395 $kNm^{-3/2}s^{-1}$, for all orientations to preferred c-axis, -25°C< -10.7°C. The least tough was the crack propagating along the basal plane, 98 ± 45 $kNm^{-3/2}$, for six results, 10°C < $\dot{K}_I$ < 51 $kNm^{-3/2}s^{-1}$, -12°C< temperature < -7.9°C. The other seven orientations of crack to columnar grains are intermediate. Fracture toughness increases with decreasing temperature, and the rate of change is dependent on orientation, $K_{Ic} = K_{Ico}e^{At}$, where A = -.077, for spalling crack, -0.051 for vertical crack 45° to preferred c-axis, -0.044 parallel to it, and -.137 perpendicular to it. No regression was done for radial type cracks, as there was a temperature gradient along the crack front, ie through thickness.

Shen and Lin (1986), SEN 3 pt, K_{Ic} = 60-100 $kNm^{-3/2}$, grain size unspecified, crack length = 64 to 96 mm, temperature= -20°C, sea ice from Bohai Bay was tested. Samples were 68 x 38 x (40-50) cm columnar sea ice, that were then transported in "adiabatic wood cases" to cold storage, at -20°C. The

ice was divided into an upper and lower layer, the later less dense; .8725 versus .8905 for Bayui Harbour ice, and .9068 versus .9130 for Lithe River mouth ice. Fracture specimens were 60 x 8 x 16 cm, three point bend, plane strain, with cracks along basal plane. Prepared crack sharpened with shaving blade, crack opening displacement was measured. For rate from 0.1 to 20 $kNm^{-3/2}s^{-1}$ load and crack opening displacement rate have linear relationship. The toughness was found to not depend on rate in this range, and was 80 $kNm^{-3/2}$. The K_{IIc} measurement was obtained with an eccentric four point loading apparatus, with one load point outside supports pan, and the prepared crack between the load and support points that were closest together. Sample dimension was 40 x 8 x 14 cm, with cracks along the basal plane of the columnar grains. K_{IIc} was found to be 80 $kNm^{-3/2}$, and rate independent for rate 0.03 to 2 $kNm^{-3/2}$. Mixed mode tests were done with eccentricly cracked three point specimen. Experimental results for mixed mode fracture of sea ice coincide with curve determined from strain energy density factor theorem. Also the angle of crack growth was calculated from strain energy density theorem, but there was poor agreement with experimental results, in general a twenty degree discrepancy.

Tuhkuri (1987), SEN 3 pt., K_{Ic} = 136 & 119 $kNm^{-3/2}$, grain

size not specified, crack length = 200 mm. Tests on beam 200 x 200 x 3600 mm, two rates, 7 & 323 $kNm^{-3/2}s^{-1}$, yield 136 & 119 $kNm^{-3/2}$ respectively. K_{Ic} and CTOD decrease with increased loading rate, no influence on K_{Ic} or CTOD from blunt crack tips noted, blunt being chain saw cut. Possibly microcracks were formed at root of chain saw cut from the action of the saw.

Parsons, Snellen, and Muggeridge (1988), DT, K_{Ic} = 35-250 $kNm^{-3/2}$, (113 ± 38 $kNm^{-3/2}$), K_{Ic} = 91 ± 28 $kNm^{-3/2}$, grain size = 10-100 mm, crack length = 250-350 mm, $0.06 < \dot{K}_I < 44$ $kNm^{-3/2}s^{-1}$, $-23^{\circ}C <$ temperature $< -14^{\circ}C$. Double Torsion geometry, sample .05 x .5 x 1.5 m long. All cracks oriented perpendicular to surface, running parallel, samples prepared from depth of .45-1.5 m, initiation times to cracking as high as 72 minutes, load increasing monotonically. Arrest fracture toughness appears to be creep free initiation fracture toughness, independent of load rate. Resulting crack length independent of load rate, but correlated with $\Delta K = (K_{Ic} - K_{Ia})$. No stable slow crack growth observed, all cracks grow in abrupt jumps. The amount of kinetic energy emparted to ice as a result of instability is less than 2% of the fracture surface energy, for crack velocity of 20 m/s.